NUREG/CR-6584, Vol. 3

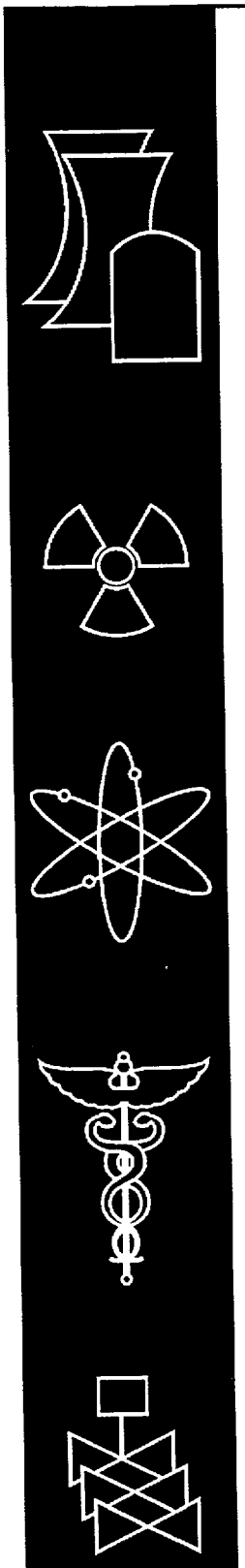

Evaluation of the Hualien Quarter Scale Model Seismic Experiment

Results of the Forced Vibration Tests

City College of New York

U.S. Nuclear Regulatory Commission
Office of Nuclear Regulatory Research
Washington, DC 20555-0001

AVAILABILITY OF REFERENCE MATERIALS IN NRC PUBLICATIONS

NRC Reference Material

As of November 1999, you may electronically access NUREG-series publications and other NRC records at NRC's Public Electronic Reading Room at www.nrc.gov/NRC/ADAMS/index.html. Publicly released records include, to name a few, NUREG-series publications; *Federal Register* notices; applicant, licensee, and vendor documents and correspondence; NRC correspondence and internal memoranda; bulletins and information notices; inspection and investigative reports; licensee event reports; and Commission papers and their attachments.

NRC publications in the NUREG series, NRC regulations, and *Title 10, Energy*, in the Code of *Federal Regulations* may also be purchased from one of these two sources.

1. The Superintendent of Documents
   U.S. Government Printing Office
   Mail Stop SSOP
   Washington, DC 20402–0001
   Internet: bookstore.gpo.gov
   Telephone: 202-512-1800
   Fax: 202-512-2250
2. The National Technical Information Service
   Springfield, VA 22161–0002
   www.ntis.gov
   1–800–553–6847 or, locally, 703–605–6000

A single copy of each NRC draft report for comment is available free, to the extent of supply, upon written request as follows:

Address: Office of the Chief Information Officer,
Reproduction and Distribution
Services Section
U.S. Nuclear Regulatory Commission
Washington, DC 20555-0001
E-mail: DISTRIBUTION@nrc.gov
Facsimile: 301–415–2289

Some publications in the NUREG series that are posted at NRC's Web site address www.nrc.gov/NRC/NUREGS/indexnum.html are updated periodically and may differ from the last printed version. Although references to material found on a Web site bear the date the material was accessed, the material available on the date cited may subsequently be removed from the site.

Non-NRC Reference Material

Documents available from public and special technical libraries include all open literature items, such as books, journal articles, and transactions, *Federal Register* notices, Federal and State legislation, and congressional reports. Such documents as theses, dissertations, foreign reports and translations, and non-NRC conference proceedings may be purchased from their sponsoring organization.

Copies of industry codes and standards used in a substantive manner in the NRC regulatory process are maintained at—

The NRC Technical Library
Two White Flint North
11545 Rockville Pike
Rockville, MD 20852–2738

These standards are available in the library for reference use by the public. Codes and standards are usually copyrighted and may be purchased from the originating organization or, if they are American National Standards, from—

American National Standards Institute
11 West 42nd Street
New York, NY 10036–8002
www.ansi.org
212–642–4900

Legally binding regulatory requirements are stated only in laws; NRC regulations; licenses, including technical specifications; or orders, not in NUREG-series publications. The views expressed in contractor-prepared publications in this series are not necessarily those of the NRC.

The NUREG series comprises (1) technical and administrative reports and books prepared by the staff (NUREG–XXXX) or agency contractors (NUREG/CR–XXXX), (2) proceedings of conferences (NUREG/CP–XXXX), (3) reports resulting from international agreements (NUREG/IA–XXXX), (4) brochures (NUREG/BR–XXXX), and (5) compilations of legal decisions and orders of the Commission and Atomic and Safety Licensing Boards and of Directors' decisions under Section 2.206 of NRC's regulations (NUREG–0750).

NUREG/CR-6584, Vol. 3

Evaluation of the Hualien Quarter Scale Model Seismic Experiment

Results of the Forced Vibration Tests

Manuscript Completed: October 2000
Date Published: March 2001

Prepared by
C. A. Miller, C. J. Costantino

City College of New York
Earthquake Research Center
Department of Civil Engineering
New York, NY 10031

H. L. Graves, NRC Project Manager

Prepared for
Division of Engineering Technology
Office of Nuclear Regulatory Research
U.S. Nuclear Regulatory Commission
Washington, DC 20555-0001
NRC Job Code W6769

ABSTRACT

This report is the third volume of a four volume set describing the work performed in evaluating the results obtained from the Hualien quarter scale model seismic experiments. The results discussed in this volume are the response of the structure to the forced vibration tests.

Five forced vibration tests were performed in this series. The shaker was placed on the roof for the first two tests and the excitation was in the two horizontal directions. The shaker was placed on the basemat for the last three tests and the excitation was in the two horizontal and vertical directions. Two sets of tests were performed; one before placement of the backfill and a second after placement of the backfill. Responses were measured throughout the structure and in the free field for input force frequencies ranging from 2 - 25 cps.

The measured data were studied to evaluate the structural system characteristics and the measured data were compared with predicted values using the CARES computer code.

The volumes contained in this report ("Evaluation of the Hualien Quarter Scale Model Seismic Experiment" are:

Vol. 1	Description of Experiment and Summary of Results
Vol. 2	Geotechnical Site Characterization Review
Vol. 3	Results of the Forced Vibration Tests
Vol. 4	Response of the Model to Seismic Events

TABLE OF CONTENTS

LIST OF FIGURES

LIST OF TABLES

ACKNOWLEDGEMENT

The authors wish to acknowledge the contributions to this project made by Applied Research Associates (ARA) who are subcontractors to CCNY on the study. Drs. C.N. Higgins and J. Pires of ARA made significant contributions to this report. Research Associates at CCNY who participated in the work reported here are: E. Heymsfield, S. Jaysena, J. McClean, A. Mousa, A. Yang, and Y. Zhu.

A special acknowledgement is given to the NRC Project Manager Mr. Herman Graves. He actively participated in all aspects of the program. Recognition is also due to Dr. H.Tang of the Electric Power Research Institute who is directing the consortium of researchers conducting the Hualien project.

1.0 Introduction

This report is submitted on Contract No. NRC-04-92-049, "Hualien SSI Experiment." It covers a portion of the work performed on a review of the results obtained from the forced vibration tests conducted both before and after backfill was placed. The work was performed from November 1992 through April 1994. This is the third volume of four volumes comprising the final report on the program. A listing of the title for each of the volumes is given in the Abstract.

A soil structure interaction (SSI) experiment is being conducted in Hualien, Taiwan. A quarter scale model reactor containment building model has been constructed at a seismically active site in Hualien. The structure and free field are instrumented so that response data within the structure and in the free field can be obtained for seismic events occurring at the site. Forced vibration tests have been performed to evaluate vibration characteristics of the combined soil-structure system. Two such tests were performed, one before the backfill was placed and the second after the backfill was placed. This experiment is similar to the recently completed experiment at Lotung (Ref. 1). The soil at the Lotung site was rather soft (having a shear wave velocity of about 350 fps) while the Hualien soil is relatively stiff (having a shear wave velocity of about 1000 fps). The objective of the City College of New York (CCNY) contract is to provide support to NRC in planning the experiment and in evaluating the results. Applied Research Associates (ARA) is a subcontractor to CCNY on the project.

The objective of the work reported in this volume is to review the results obtained from the forced vibration tests performed during October and November 1992 before the backfill was placed (FVT-1) and during February 1993 after backfill was placed (FVT-2). These reviews include two tasks. The first task is to interpret the likely characteristics of the soil/structure system from the measured response data. The second task is to correlate the measured data with predicted responses using standard soil-structure-interaction methodologies.

Predictions of response were made for FVT-1 (Ref. 2) before the measured data became available, and these were presented at a meeting in Taiwan on April 22, 1993. The measured FVT-1 data was made available at this meeting in Taiwan. Correlation studies were then performed using the measured data. The FVT-2 predictions (Ref. 3) were made prior to receiving the measured results which were obtained during a meeting in Korea on November 2-3 1993.

A general description of the tests are given in Section 2. The FVT-1 and FVT-2 results are discussed in Section 3 and 4 respectively. Correlation studies for both tests are presented in Section 5 and the work is summarized in Section 6. The FVT-1 and FVT-2 measured results are shown in Appendices A and B respectively.

2.0 Description of FVT Tests

The characteristics of the site and structure, and the parameters of the FVT tests are discussed in this section of the report. A complete description of the site properties are discussed in Volume 2. Structural data and instrumentation characteristics are discussed in Volume 1. These data are summarized here for convenience. The parameters of the FVT-1 and FVT-2 tests are taken from Ref. 4 and 5 respectively.

2.1 Site Description

A sketch of the site configuration at the time of the FVT tests is shown on Fig. 2.1. The two dark shaded areas against the wall of the model are backfill areas which were not in place during the FVT-1 tests. The differences in soil properties between the two tests are largely due to the change in overburden pressure when the backfill was place. CRIEPI provided a "Unified Model of the Ground for the FVT-1 Analysis" (January 1993), and a "Unified Model of the Ground for the FVT-2 Analysis" (July 1993). The recommended soil property data (shear wave velocity - V_S; density - γ; Poisson's ratio - μ; and soil hysteretic damping - β) are shown on the figure. Soils data are not available below a depth of 65.6 feet. The water table was located immediately beneath the bottom of the basemat during the FVT-1 tests and at 8.2 feet below the ground surface for the FVT-2 tests.

2.2 Structural Model

The structural model used for the test is also shown on Fig. 2.1. The cylindrical shell walls are about 1 foot thick and both the roof and basemat are relatively thick (4.92 feet and 9.84 feet thick respectively). Brackets are placed on the inside of the shell and around the circumference at midheight (22.37 feet above the top of the basemat) to support accelerometers. The concrete has a Young's Modulus of 4093 ksi, density of 150 pcf, and Poisson's ratio of 0.2 (Ref. 6). The cross sectional properties of the cylindrical shell are:

Cross Sectional Area	= 105.2 square feet
Shear Area	= 52.6 square feet
Moment of Inertia	= 14,764 feet^4

The reinforcing steel characteristics are not used in the model since the concrete is not cracked. These properties result in a fixed base cantilever frequency of about 10.7 cps for the structure.

The structural model used for the analyses is shown on Fig. 2.2. A shear beam is used to

model the cylindrical shell portion of the structure and it spans from nodes 2 through 7. Rigid links connecting nodes 7-8 and 1-2 are used to model the roof and basemat slabs both of which are considered to be rigid. Nodes 9 and 10 are included in the model to represent the cg of the shaker on the roof and first floor respectively. These nodes are connected with rigid links to nodes 8 and 2. The remaining nodes (11 through 30) are used to replicate accelerometer locations in the structure. All of these nodes are connected with rigid links to the nodes 2 through 8 on the structural model. Accelerometers are also placed at nodes 2 and 8. The "north" arrow on Fig. 2.2 corresponds to the "north" definition used in the test. This is about 41.25^{o} west of magnetic north at the site. Table 2.1 lists all of the nodal coordinates. The origin is located at the center of the bottom of the basemat, the x-axis points east, the y-axis points north, and the z-axis points up. All dimensions are in feet.

2.3 Test Parameters

References 4 and 5 contain descriptions of the FVT-1 and FVT-2 tests respectively. Five forced vibration tests were run for each FVT. Two had the shaker placed at the roof (node 9) with the excitation in the E-W and N-S directions. Three had the shaker placed at the first floor (node 10) with the excitation in the E-W, N-S, and U-D (up down) directions. Measurements were taken from 2 - 20 cps for the horizontal tests and from 2 - 25 cps for the vertical tests. The frequency increment was 0.2 cps except around the fundamental system frequency where the increment was reduced to 0.1 cps. The exciting force varied depending on the frequency of the excitation but all of the data was normalized to 1 metric ton. At the fundamental horizontal frequencies the applied force was about 400 kg (882 pounds). The shaker weighed 2.5 metric tons (5.51 k) for the vertical tests and 3.7 metric tons (8.16 k) for the horizontal tests.

The location at which structural response measurements were taken for each of the tests is shown on Table 2.2 keyed to the nodal locations shown on Fig. 2.2. There are some differences between the FVT-1 and FVT-2 locations. These are marked with an asterisk on the table with the FVT-2 locations shown in ( ). No measurements were made at the locations of nodes 11, 15, 23, and 28 for the FVT tests.

The free field accelerometers were located along two lines, one running north from the center of the structure and the other running east from the center. Three stations were established along each line as shown on Fig. 2.1. The gages for FVT-1 were located on the steps of the excavation while the gages for FVT-2 were located on the surface. The gages closest to the model wall (designated BS) were located 4.92 feet from the wall of the structure, the MS gages were located 19.68 feet from the wall, and the TS gages were located 31.17 feet from the wall. Table 2.3 lists the measurements that were made in the soil for each of the five FVT-1 tests. Once again there are

small differences between the FVT-1 and FVT-2 placement of these gages. These are marked with an asterisk with the FVT-2 location shown in ( ).

Pressure gages were also placed at the structure/soil interface. The responses of these gages was not of sufficient amplitude, however, to obtain any useful information and are therefore not discussed in this report.

Table 2.1

Definition of Nodal Coordinates (feet)

Node #	X-Coord	Y-Coord	Z-Coord
1	0.	0.	0.
2	0.	0.	9.84
3	0.	0.	16.40
4	0.	0.	22.66
5	0.	0.	32.21
6	0.	0.	39.36
7	0.	0.	47.80
8	0.	0.	52.92
9	0.	0.	55.14
10	0.	0.	12.06
11	0.	4.74	52.92
12	0.	15.76	52.92
13	0.	-15.76	52.92
14	15.81	0.	52.92
15	-4.64	0.	52.92
16	-15.81	0.	52.92
17	-4.21	15.23	32.21
18	4.21	15.23	32.21
19	-15.23	-4.21	32.21
20	-15.23	4.21	32.21
21	0.	15.58	9.84
22	0.	8.14	9.84
23	0.	2.62	9.84
24	0.	-2.62	9.84
25	0.	-15.52	9.84
26	15.58	0.	9.84
27	8.14	0.	9.84
28	-2.62	0.	9.84
29	-8.14	0.	9.84
30	-15.58	0.	9.84

Table 2.2

Locations / Directions of In-Structure Measurements

Node	Roof N-S	Roof E-W	Test 1st Flr N-S	1st Flr E-W	1st Flr U-D
2	UD	UD	UD	UD	UD
8	NS, UD	EW,UD			UD
12	EW, UD	EW, UD	EW, UD	EW, UD	EW, UD
13	EW, UD	EW, UD	EW, UD	EW, UD	EW, UD
14	NS,UD	NS, UD	NS, UD	NS, UD	NS, UD
16	NS, UD	NS, UD	NS, UD	NS, UD	NS, UD
17	NS	NS	NS	EW	
18	UD	EW	UD	*(NS)	UD*( )
19	EW	EW	EW	EW, UD	*(UD)
20	NS	UD	NS	NS*( )	
21	EW, UD	EW, UD	EW, UD	EW, UD	EW, UD
22	UD		UD		
24	UD		UD		
25	EW, UD	EW, UD	EW, UD	EW, UD	EW, UD
26	NS, UD	NS, UD	NS, UD	NS, UD	UD*(NS,UD)
27		UD			
29		UD		*(UD)	
30	NS, UD	NS, UD	NS, UD	NS, UD	NS, UD

* FVT-1 and 2 locations are different. FVT-1 location given before asterisk and FVT-2 location is given after asterisk in brackets.

** No measurements were taken for either FVT-1 or FVT-2 for those locations that are blank.

Table 2.3

Locations / Directions of Soil Measurements

Node	Test				
	Roof N-S	Roof E-W	1st Flr N-S	1st Flr E-W	1st Flr U-D
N-BS	NS, EW, UD		EW, UD		EW*( )
N-MS	NS, EW, UD	NS, EW	NS, EW, UD	NS, EW	NS, UD*(add EW)
N-TS	NS		*(NS)		
E-BS		NS, EW, UD	NS*( )	NS, EW, UD	NS, UD*(add EW)
E-MS	NS, EW	NS, EW, UD	NS, EW	NS, EW, UD	NS, EW, UD*( )
E-TS		EW	NS*( )	EW	

* FVT-1 and 2 locations are different. FVT-1 location given before asterisk and FVT-2 location is given after asterisk in brackets.

** No measurements were taken for either FVT-1 or FVT-2 for those locations that are blank.

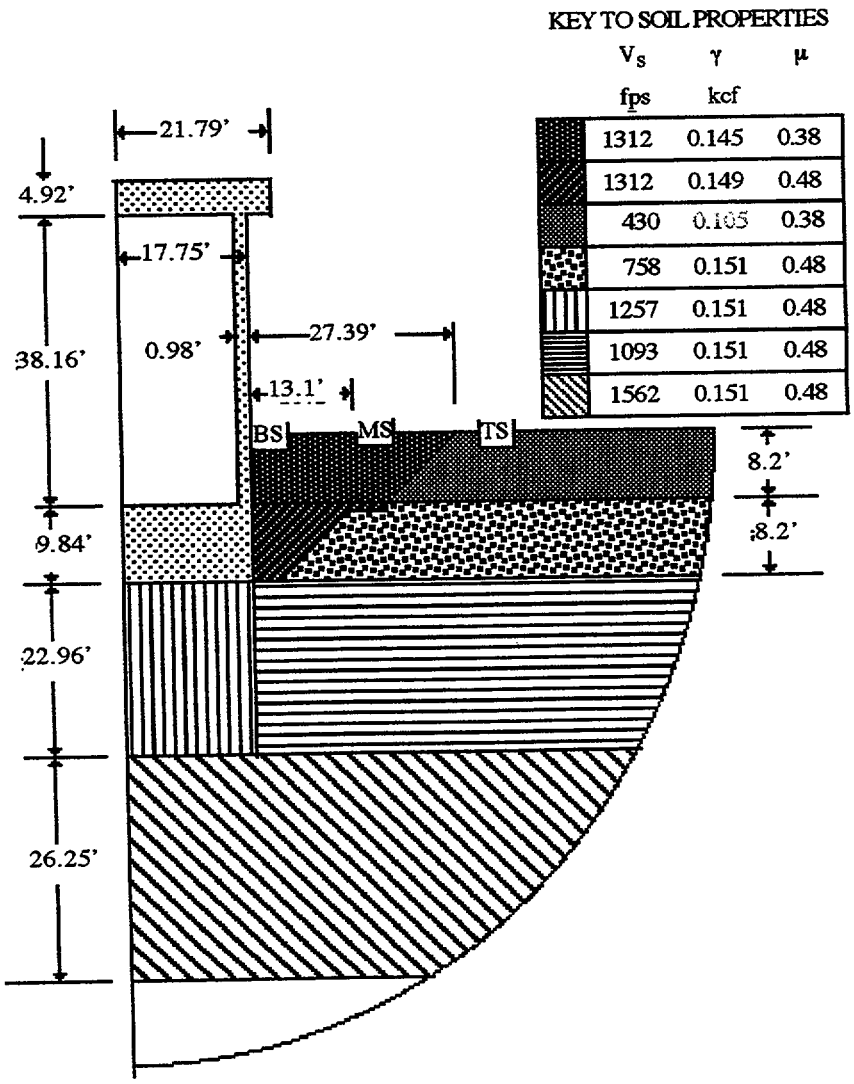

Fig. 2.1 FVT Test Description

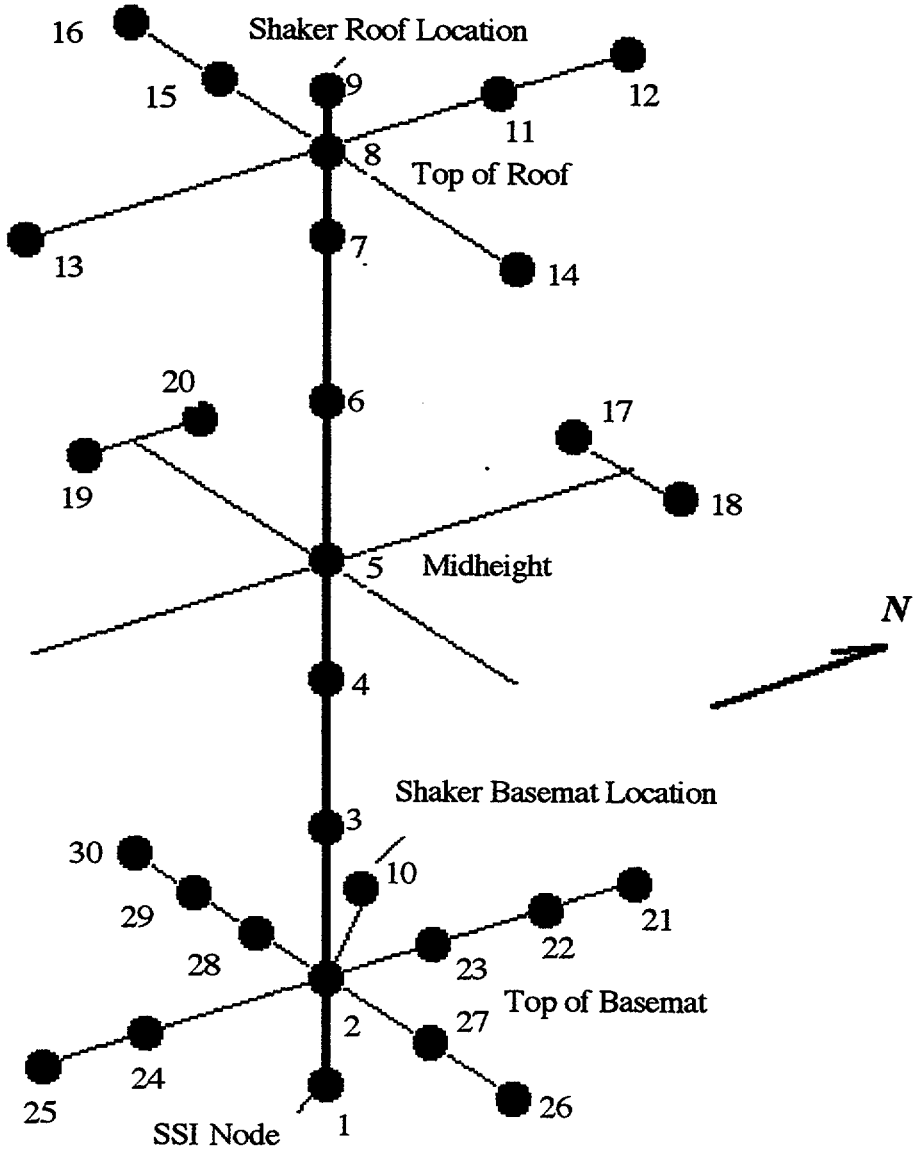

Fig. 2.2 Description of Structural Model

3.0 FVT-1 Tests

The characteristics of the measured data are first discussed. This is followed with comparisons between the measured and predicted results.

3.1 Evaluation of FVT-1 Measured Data

The response of the structure to each of the five FVT-1 tests is discussed in this Section based upon a review of the measured data. The measured data is plotted in Appendix A for all of the structural and soil gages. The structural data is plotted so that all of the measurements in one direction (NS, EW, or UD) on one elevation (roof, midheight, or 1st floor) for one of the five tests are plotted on the same figure. The gage location is keyed to the node numbers defined in Fig. 2.2 with the nodal coordinates given in Table 2.1. The soil data is plotted so that all of the measurements in one direction for one of the five tests are plotted on the same figure. The soil gage locations are keyed to elevation (bottom of basemat - BS, step in excavation - MS, and surface of soil - TS) and gage line (north from structure - N, and east from structure - E). An index of the data contained in Appendix A is shown on the cover page to the Appendix.

The structural measurements are first discussed followed with a discussion of the soil measurements.

3.1.1 Structural Measurements

The measured results for the first FVT-1 test (shaker mounted on the roof with the excitation acting in the N-S direction) are shown on pages A.1, A.2, and A.3 for the roof, midheight, and 1st floor elevations respectively.

The major N-S response can be seen to occur at 4.1 cps and the roof, midheight, and 1st floor displacements are 213 μm/t, 145 μm/t, and 48 μm/t respectively. The basemat rotation can be determined from the vertical deformations of the base measured at opposite ends of a N-S diameter (about 40 μm/t at each end of the basemat with the measurements separated by 9.48 m) to be:

$$\theta = 2^* 40 / \text{Diameter} = 80\ \mu\text{m/t} / 9.48 = 8.44\ \mu\ \text{rad} / \text{t}$$

The N-S motion at the base of the basemat (Δ_b) is therefore:

$$\Delta_b = 48 - 8.44 * 3 = 22.7 \ \mu m/t$$

The displacement (Δ_r) at the elevation of the roof gages (16.63 m above bottom of basemat) is:

$$\Delta_r = 8.44 * 16.63 = 140.4 \ \mu m/t$$

Therefore the roof displacement of 213 μm/t is divided into 11% rigid body translation (22.7/213), 66 % rigid body rotation (140.4/213) and 23 % flexure (100-11-66). It may also be seen (Fig. A.1, A.4, and A.5) that the N-S displacements are the same at diametrically opposite ends of each of the floors. This indicates that there is no rotation of the floor about a vertical axis. A second peak in the N-S response occurs at about 4.6 cps (the primary frequency for the E-W excitation) and has a magnitude of about 136 μm/t.

Examination of the vertical displacements indicate that the only vertical displacement are due to rigid body rotations of the floor. The vertical displacement at diametrically opposite points are equal to each other and 180° out of phase. Vertical displacements at the center of the roof and 1st floor are also equal to zero.

The surprising result is that the N-S excitation causes a significant E-W response, which is not expected in a symmetric structure. This response occurs at a frequency of 4.6 cps which is equal to the primary frequency resulting from E-W shaking. This out-of plane response is discussed in the following section of the report.

The measured results for the second FVT-1 test (shaker mounted on the roof with the excitation acting in the E-W direction) are shown on pages A.4, A.5, and A.6 for the roof, midheight, and 1st floor elevations respectively. The response characteristics are very similar to that of the first shaker test. The peak in-plane (E-W) response occurs at about 4.6 cps and has amplitudes of 175 μm/t, 107 μm/t, and 42 μm/t at the roof, midheight, and 1st floor respectively. There is no rotation of the structure about a vertical axis or vertical deformation other than that caused by the rotation of a floor about a horizontal axis. The base rotation about the N-S axis can be determined as above to be 7.25 μ rad / t , and this results in 12 % of the roof deformation caused by rigid body translation of the base, 69 % caused by rigid body rocking, and the remaining 19 % caused by flexural deformations.

The same out-of-plane effects are observed with this test as with the first test. The E-W roof response has a second peak at the N-S primary frequency of 4.1 cps and an amplitude of about 130 μm/t. The E-W excitation also causes a N-S deformation at the roof elevation with an amplitude of 52 μm/t at a frequency of 4.1 cps. These non symmetric effects are most likely caused by non isotropic characteristics in the underlying soil since any nonsymmetry in the structure would result in a torsional response of the structure. The data clearly indicates that no such torsional response occurs because the measured horizontal response on opposite sides of a diameter are identical (see for example Fig. A.1 where the response of nodes 14 and 16 are identical, and Fig. A.2 where the measured horizontal response at nodes 12 and 13 are identical).

Heavy rains during construction of the facility caused a partial collapse of the embankment in the northeast quadrant. There was some discussion that this may have caused the "softer" response in the N-S direction than in the E-W direction. If this were the case however one would have expected that the horizontal excitation would cause some vertical rigid body response. This is not seen in the data.

The measured results for the third FVT-1 test (shaker mounted on the first floor with the excitation acting in the N-S direction) are shown on pages A.7, A.8, and A.9 for the roof, midheight, and 1st floor elevations respectively. The peak in-plane (N-S) response occurs at about 4.1 cps (the same as the first test with the shaker placed at the roof and the excitation applied in the N-S direction) and has amplitudes of 60 μm/t, 37 μm/t, and 16 μm/t at the roof, midheight, and 1st floor respectively. There is no rotation of the structure about a vertical axis or vertical deformation other than that caused by the rotation of a floor about a horizontal axis. The base rotation about the E-W axis can be determined as above to be 2.17 μ rad / t , and this results in 13 % of the roof deformation caused by rigid body translation of the base, 60 % caused by rigid body rocking, and the 27 % caused by flexural deformations.

The same out-of-plane effects are observed with this test as with the first test. The N-S roof response has a second peak at the E-W primary frequency of 4.6 cps and an amplitude of about 32 μm/t. The N-S excitation also causes an E-W response at the roof elevation with an amplitude of 34 μm/t at a frequency of 4.1 cps.

The measured results for the fourth FVT-1 test (shaker mounted on the first floor with the excitation acting in the E-W direction) are shown on pages A.10, A.11, and A.12 for the roof, midheight, and 1st floor elevations respectively. The peak in-plane (E-W) response occurs at about

4.6 cps (the same as the second test with the shaker placed at the roof and the excitation applied in the E-W direction) and has amplitudes of 47.5 μm/t, 29.4 μm/t, and 10.8 μm/t at the roof, midheight, and 1st floor respectively. There is no rotation of the structure about a vertical axis or vertical deformation other than that caused by the rotation of a floor about a horizontal axis. The base rotation about the N-S axis can be determined as above to be 1.81 μ rad / t , and this results in 11 % of the roof deformation caused by rigid body translation of the base, 63 % caused by rigid body rocking, and the 26 % caused by flexural deformations.

The same out-of-plane effects are observed with this test as with the first test. The E-W roof response has a second peak at the N-S primary frequency of 4.1 cps and an amplitude of about 35 μm/t. The E-W excitation also causes a N-S response at the roof elevation with an amplitude of 36 μm/t at a frequency of 4.6 cps.

The measured vertical deformation results for the fifth FVT-1 test (shaker mounted on the first floor with the excitation acting in the U-D direction) are shown on page A.13. There was no significant horizontal deformation measured for this test. This result also supports the interpretation that there was not a soft spot in the soil under one quadrant of the structure which would be expected to introduce some rocking response thereby giving rise to horizontal deformations. The peak vertical displacements at the roof, midheight, and 1st floor are 1.45 μm/t, 1.33 μm/t, and 1.27 μm/t for the roof, midheight, and roof elevations respectively. This indicates that 88 % of the deformation results from the rigid body vertical deformation and 12 % from the axial shortening of the cylindrical portion of the structure. Amplification curves for all points on the roof (see Fig. A.37) are identical indicating that the roof deforms as a rigid body. However, the amplification curves shown on Fig. A.39 indicate that the vertical deformation near the center of the basemat (Node 2) is somewhat larger (1.33 μm/t at the center as compared with 1.27 at the periphery of the mat) than that recorded for other nodes on the basemat. Therefore the basemat does not quite behave as a rigid mat.

It is also interesting to note that the deformation of the lower half of the the structure is (1.33 - 1.27 = 0.06 μm/t) while the deformation over the upper half of the cylinder is (1.45 - 1.33 = 0.12 μm/t). This indicates that the upper portion of the cylinder is more flexible than the lower half. There is some evidence that the construction procedure resulted in this characteristic. Holes were cut in the upper portion of the cylinder to support the formwork for the roof construction. These holes were then grouted, but there is evidence that the grouting was not of the quality

required to restore the stiffness of the upper portion of the structure. Consideration should be given to reducing the stiffness (by changing the concrete's elastic modulus) of the upper half of the cylinder.

The frequencies at which the maximum amplification occurs range from 9.5 cps to 11 cps, and the amplification curves generally contain a double peak. The fundamental frequency defined at the 90^{o} phase angle is 11 cps.

3.1.2 Soil Measurements

The soil measurements are shown on pages A.14 through A.18 with the results for each of the tests contained on one page. These results are consistent with the in-structure results. For example, the N-S excitation at the roof results in a N-S response of 14.6 μm/t at the BS N location, 5.3 μm/t at the MS N location, and 4.0 μm/t at the TS N location. The deformation at the bottom of the basemat is 22.7 μm/t. These measurements were taken at 6.91 m, 11.41 m, and 14.91 m respectively from the center of the basemat, and indicate that the peak amplitude attenuates as 1/radius as anticipated (the product of amplification times radius represents the slope of an amplification vs. 1/radius curve). These peaks occur at the same frequency (4.1 cps) as that found for the in-structure measurements.

Non symmetric results are also found for the soil data. A symmetric response for the N-S excitation would result in zero E-W response along a N-S line. However, Fig. A.41 indicates a significant E-W response. The vertical excitation would only result in radial horizontal displacements in the soil. The data shown on Figs. A.53 and A.54 indicate significant tangential responses.

3.2 Comparison of Measured Data with Predictions

The pre test predictions and post test correlations with the experimental data are discussed in this section. In all cases the work is performed using the CARES computer code (Ref. 7). The CARES code and the data used for the prediction and correlation models are first discussed. The results obtained for each are then discussed.

3.2.1 Description of Prediction and Correlation Models

FVT-1 predictions are made with the CARES computer code (Ref. 7). This is a computer code that was developed for the U.S. NRC and contains several packages (generation of

waveforms to fit specified response spectra, convolution/deconvolution calculations to determine free field motions consistent with a specified motion at one location and site soil properties, calculation of structural response to these free field motions including SSI effects, and utility routines) required to perform seismic response calculations.

The structural response portion of the code is used for the FVT-1 predictions. It models the structure as a lumped mass shear beam and connects the beam to the free field with lumped parameter SSI spring/damper models. Four SSI models are included in that computer code:

- ASCE 4-86 (Ref.8)
- Kausel (Ref.9)
- Beredugo and Novak (Ref.10)
- Veletsos (Ref.11)

Predictions are made with the third model but parametric studies are performed to evaluate the sensitivity of the predictions to the model.

Solutions in the structural response portion of CARES are carried out in the frequency domain. A shaker load of (1 kip sin ωt) was used as input. The frequency of the input was varied from 1 - 20 cps at the following values (0.5, 0.75, 1, 1.5, 2, 2.2, 2.4, 2.6, 2.8, 3, 3.1 , 3.2, 3.3, 3.4, 3.5, 3.6, 3.7, 3.8, 3.9, 4, 4.1, 4.2, 4.3, 4.4, 4.5, 4.6 , 4.7, 4.8, 4.9 , 5, 5.2, 5.4 , 5.6, 5.8, 6, 6.25, 6.5, 6.75, 7, 7.5, 8, 8.5, 9, 10, 11, 12, 13, 14, 15, 16, 17, 18, 19, and 20 cps). The solution for the deformation at a given degree of freedom (D_i) was obtained in the form:

$$D_i = A_{in} \text{ Cos } \omega_n t + B_{in} \text{ Sin } \omega_n t$$

The amplitude of the response at the degree of freedom is:

$$\text{Amplitude} = [A_{in}^2 + B_{in}^2]^{1/2}$$

The phase angle is:

$$\text{Phase Angle} = \tan^{-1} [A_{in} / B_{in}]$$

The response is determined in the units of feet for the one kip input and then converted to micro

meters per metric ton (μ m / t).

The structure is modeled for the correlation study with the lumped mass shear beam shown on Fig. 2.2. The same model is used for the pre test prediction study except that nodes 9 and 10 are not included and the shaker load is applied to either node 2 or node 8. The SSI model is attached to node 1. The parameters used for the prediction and correlation studies are shown on Table 3.1. As may be seen the soil shear wave velocity is changed from 333 m/s for the predictions to 317 m/s for the correlation study. This change results in a better fit of the experimental data and is in agreement with the final unified soil model as defined by CRIEPI. Several small changes were also made in the structural characteristics to better represent the data. The most significant change is made to the representation of the structural damping. A damping matrix proportional to the mass and stiffness matrices is used in CARES. The two proportionality constants were determined in the original prediction model so that the 2 % structural damping was achieved at frequencies of 10.7 cps (the fixed base frequency of the structure) and 25 cps. The result is that the damping at the fundamental frequency of the system (4-5 cps) is significantly higher than 2 %. The proportionality constants are selected for the correlation study so that the 2 % damping is achieved at 4 cps and 10 cps. This is a better representation of the structural damping than was used for the prediction study.

3.2.2 Prediction of FVT-1 Results

The pre test predictions are shown on Figs. 3.1 through 3.3. The results on Fig. 3.1 indicate that there is little difference in the results for the four SSI models contained in the CARES code. The Beredugo-Novak model is therefore used for the remainder of the study. The predicted horizontal response at the roof, midheight, and first floor for the horizontal shaker load at the roof is shown on Fig.3.2 and indicates peak amplitudes of 120 μm/t, 65 μm/t, and 24 μm/t at the three elevations and the fundamental frequency of the response is 4.9 cps. The measured data for the N-S test indicate deformations of 213 μm/t, 145 μm/t, and 48 μm/t at a frequency of 4.1 cps, and the results for the E-W test indicate deformations of 175 μm/t, 107 μm/t, and 42 μm/t at a frequency of 4.6 cps. The frequency of the predicted results is reduced from 4.9 cps to the range of the measured frequency (4.1-4.6 cps) when the soil shear wave velocity of the CRIEPI unified model is used. The peak deformations are increased when the structural damping is modified as discussed in Section 3.2.1 so that 2 % structural damping is used at the frequencies of interest.

The predicted vertical response is shown on Fig. 3.3. As may be seen the SSI damping is very high in the vertical direction with very little amplification so that the peak vertical displacement

at the roof due to the vertical shaker load at the basemat is 1.1 μm/t and the frequency (determined at the 90° phase angle) is about 14 cps. The measured data is 1.4 μm/t at a frequency of 11 cps.

3.2.3 Correlation of Predictions with Measured Data

The changes to the structural model as described in the second part of Table 3.1 were made and comparisons were made between computed and measured responses for a range of soil shear wave velocities. The horizontal roof excitation tests are used as the bases for the correlations. The results of these studies are summarized in Table 3.2. As may be seen the best fit shear wave velocity to obtain the average frequency of 4.35 cps is 320 m/s and the best fit velocity to obtain the average peak displacement of 194 μm/t is 328 m/s. The CRIEPI soils exploration work indicates that a shear wave velocity of 317 m/s should be used. This is close to the values required for a best fit of the data and is therefore used.

A comparison of the computed and measured results are shown on Figs. 3.4 through 3.12. The results of the comparisons are summarized on Table 3.3. With the exception of the last two rows the data is organized in groups of three rows each. The first row is the computed value and the following two rows (marked with an *) are the experimental data for the NS and EW tests. The last two rows are for the computed and measured data respectively. As may be seen the agreement between the computed and measured data is excellent.

Predicted contributions (rigid body rocking, rigid body translation, and flexural) to the total roof displacements are compared with the measured data on Table 3.4. It may be seen that the predicted rigid body rocking contribution is a larger percentage of the total, the rigid body translation is a slightly smaller percentage, and the flexural contribution is smaller than the contributions computed from the measured results. A lower stiffness assigned to the structure (as discussed above) would place the predicted values in closer agreement with the measured data.

Table 3.1

Structural and Soil Parameters Used in Prediction and Correlation Studies

Parameter	Pre Test	Post Test
Soil:		
Shear Velocity (m/s)	333	317
Density (gm/cc)	2.40	2.40
Poisson's Ratio	0.47	0.47
Damping	2 %	2 %
Structure:		
Young's Modulus (ksi)	3,600	4,093
Poisson's ratio	0.20	0.20
Damping (see discussion)	2 %	2 %
Wall Thickness (ft)	1	0.98
Foundation Radius (ft)	17.25	17.75
Basemat Thickness (ft)	9.84	9.84
Roof Thickness (ft)	4.92	4.92
Length of Cylinder (ft)	38.16	38.16
Location of Roof Shaker - Node	8	9
Location of Basemat Shaker - Node	2	10
Include Weight of Shaker ?	No	Yes
Roof Weight (k)	1100.8	1084.4
Basemat Weight (k)	1379.8	1460.9

Table 3.2

Effect of Soil Shear Wave Velocity on Peak Roof Horizontal Response Resulting From the Horizontal Shaker Load Applied at the Roof

Shear Velocity (m/s)	Frequency of Peak Response (cps)	Amplitude of Peak Response (μm/t)
	Computed	
280	3.99	232
317	4.29	207
333	4.62	188
383	5.24	166
400	5.40	159
	Measured NS Test	
---	4.1	213
---	4.6	175

Table 3.3

Comparison of Predicted and Measured Results

Shaker Location	Shaker Direction	Displacement Location	Displacement Direction	Frequency of Pk Amplitude (cps)	Amplitude of Peak (μm/t)
Roof	Horizontal	Roof	Horizontal	4.3	207
*	NS	Roof	NS	4.1	213
*	EW	Roof	EW	4.6	175
Roof	Horizontal	FF	Horizontal	4.3	42
*	NS	FF	NS	4.1	48
*	EW	FF	EW	4.6	42
Roof	Horizontal	Roof	UD	4.3	57
*	NS	Roof	UD	4.1	54
*	EW	Roof	UD	4.6	51
Roof	Horizontal	FF	UD	4.3	45
*	NS	FF	UD	4.1	37
*	EW	FF	UD	4.6	34
FF	Horizontal	Roof	Horizontal	4.3	47
*	NS	Roof	NS	4.1	60
*	EW	Roof	EW	4.6	48
FF	Horizontal	FF	Horizontal	4.3	10
*	NS	FF	NS	4.1	16
*	EW	FF	EW	4.6	11
FF	Horizontal	Roof	UD	4.3	12
*	NS	Roof	UD	4.1	12
*	EW	Roof	UD	4.6	13
FF	Horizontal	FF	UD	4.3	10
*	NS	FF	UD	4.1	10
*	EW	FF	UD	4.6	8
FF	UD	FF	UD	13	1.0
*	UD	FF	UD	11	1.3

Table 3.4

Components of Roof Deformation

Source	Shaker	% Rocking	% Horizontal	% Elastic
Computed	Roof Hor	76	7	17
Measured	Roof NS	66	11	23
Measured	Roof EW	69	12	19
Computed	FF Hor	75	8	17
Measured	FF NS	60	13	27
Measured	FF EW	63	11	26
Computed	FF UD	--	92	8
Measured	FF UD	--	88	12

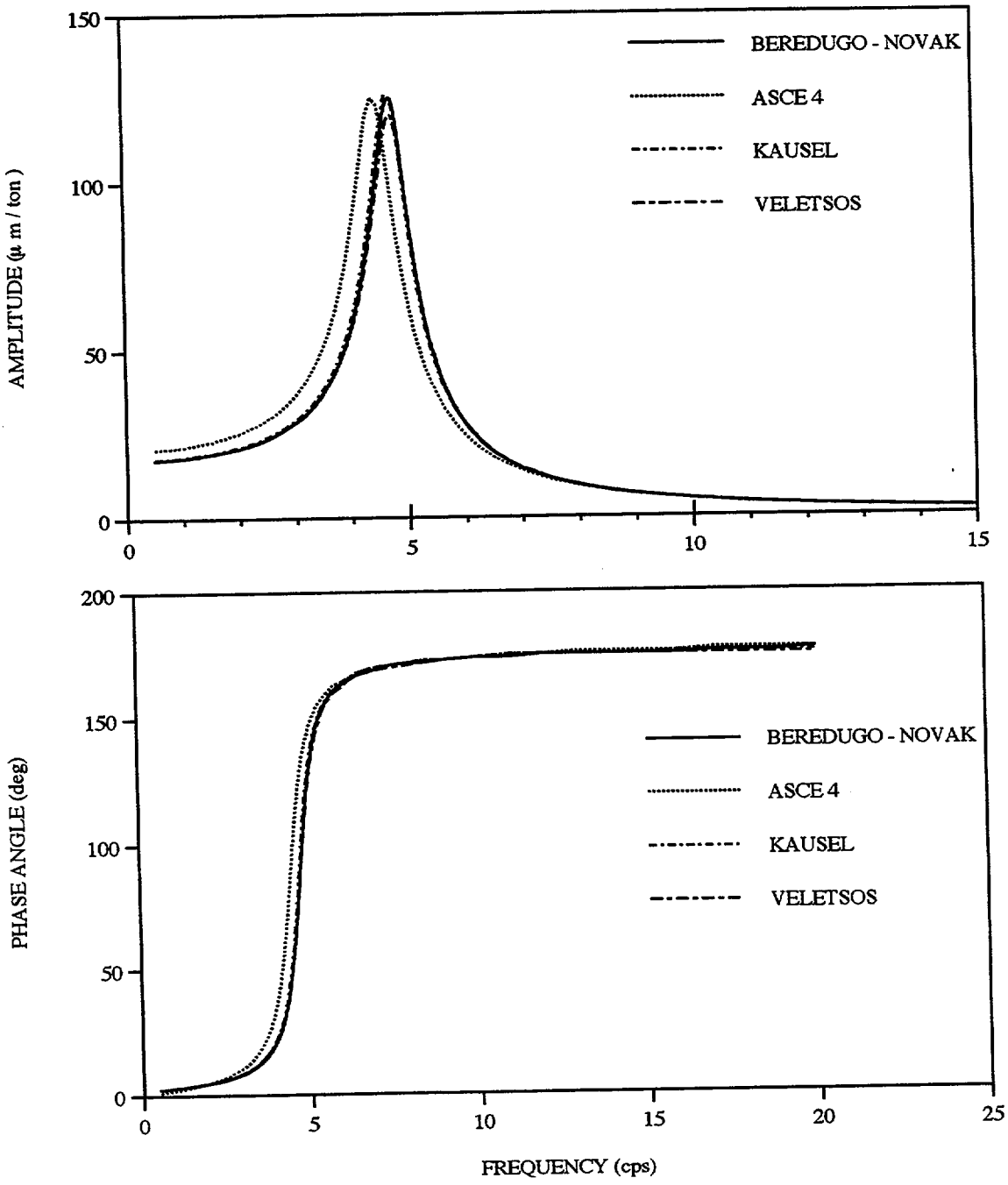

Fig. 3.1 Comparison Of Predictions For Different SSI Models
Shaker At Roof - Horizontal Roof Response (FVT-1)

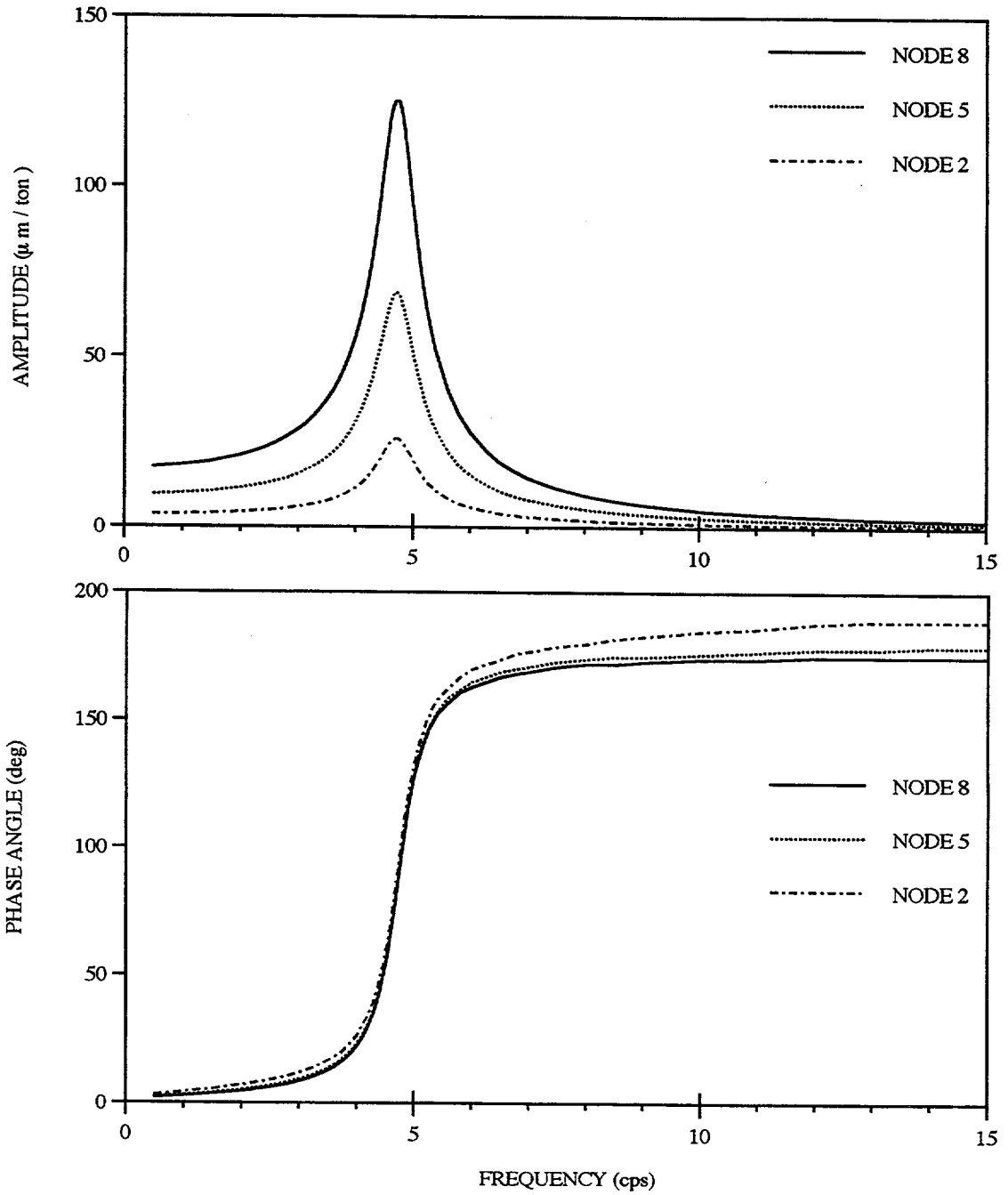

Fig. 3.2 Horizontal Response Due To Horizontal Shaker Load At Roof (FVT-1)

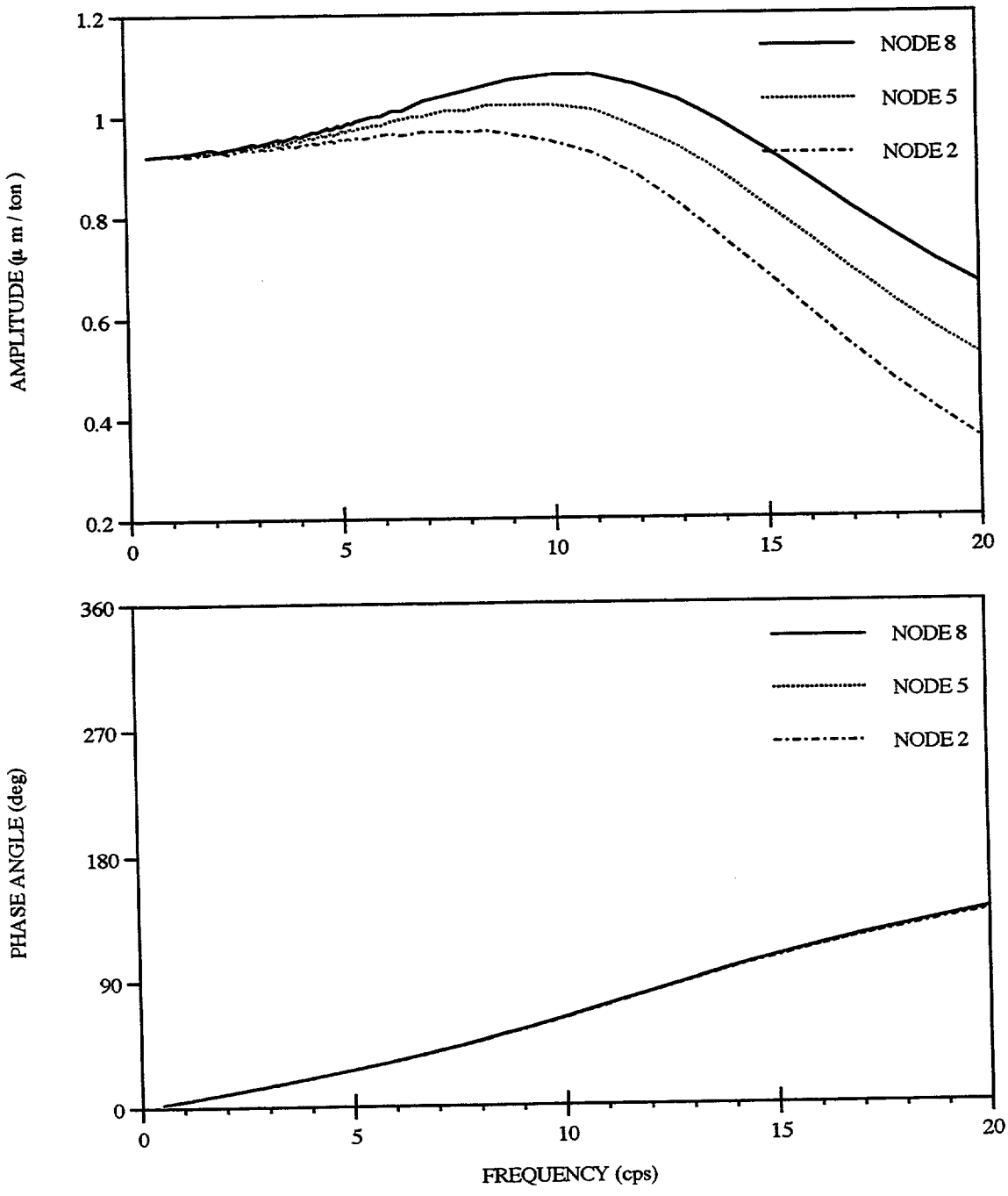

Fig. 3.3 Vertical Response Due To Vertical Shaker Load At Basemat (FVT-1)

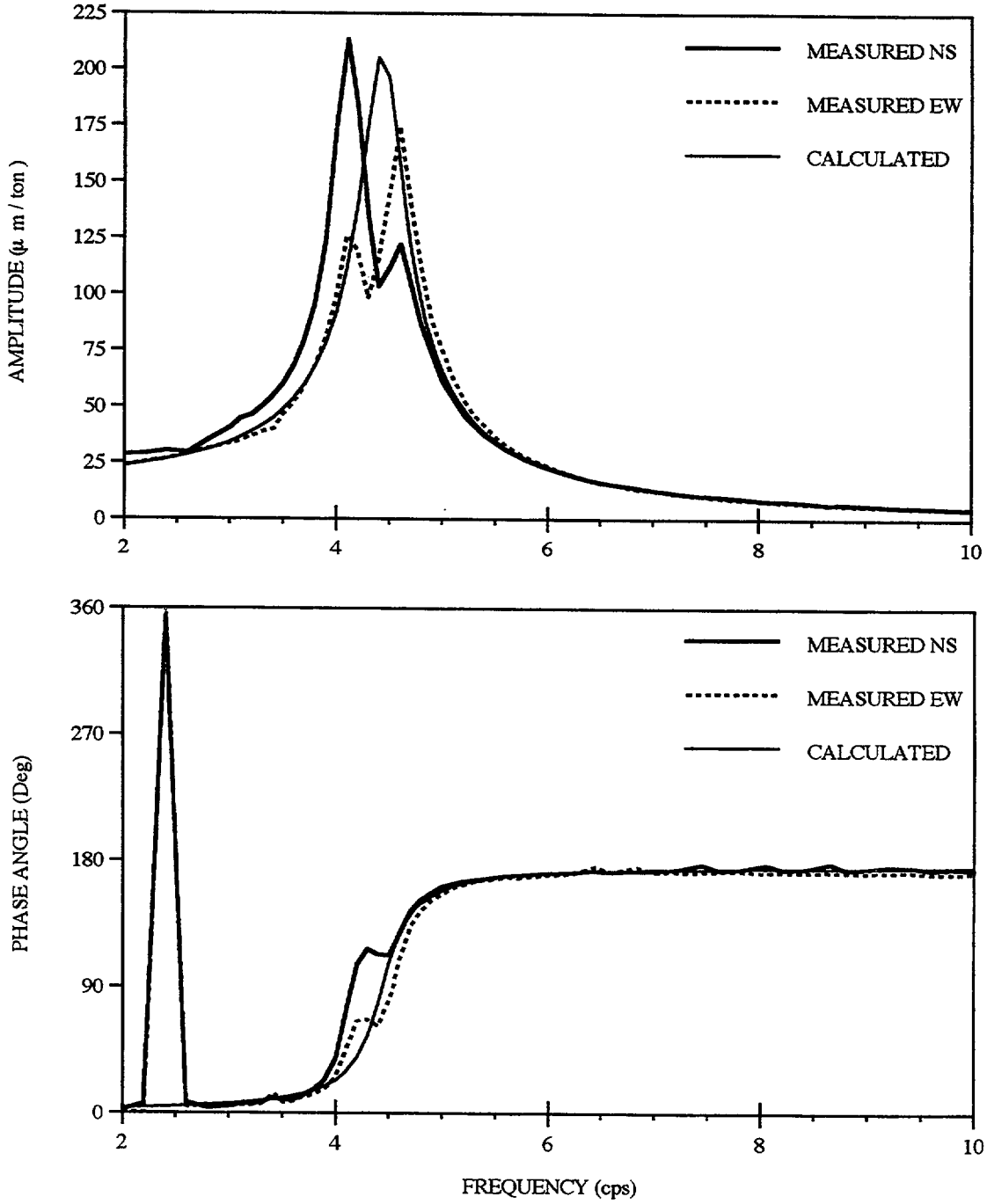

Fig. 3.4 Comparison of Predicted and Measured Horizontal Response at Roof Caused by Horizontal Shaker Load at Roof (FVT-1)

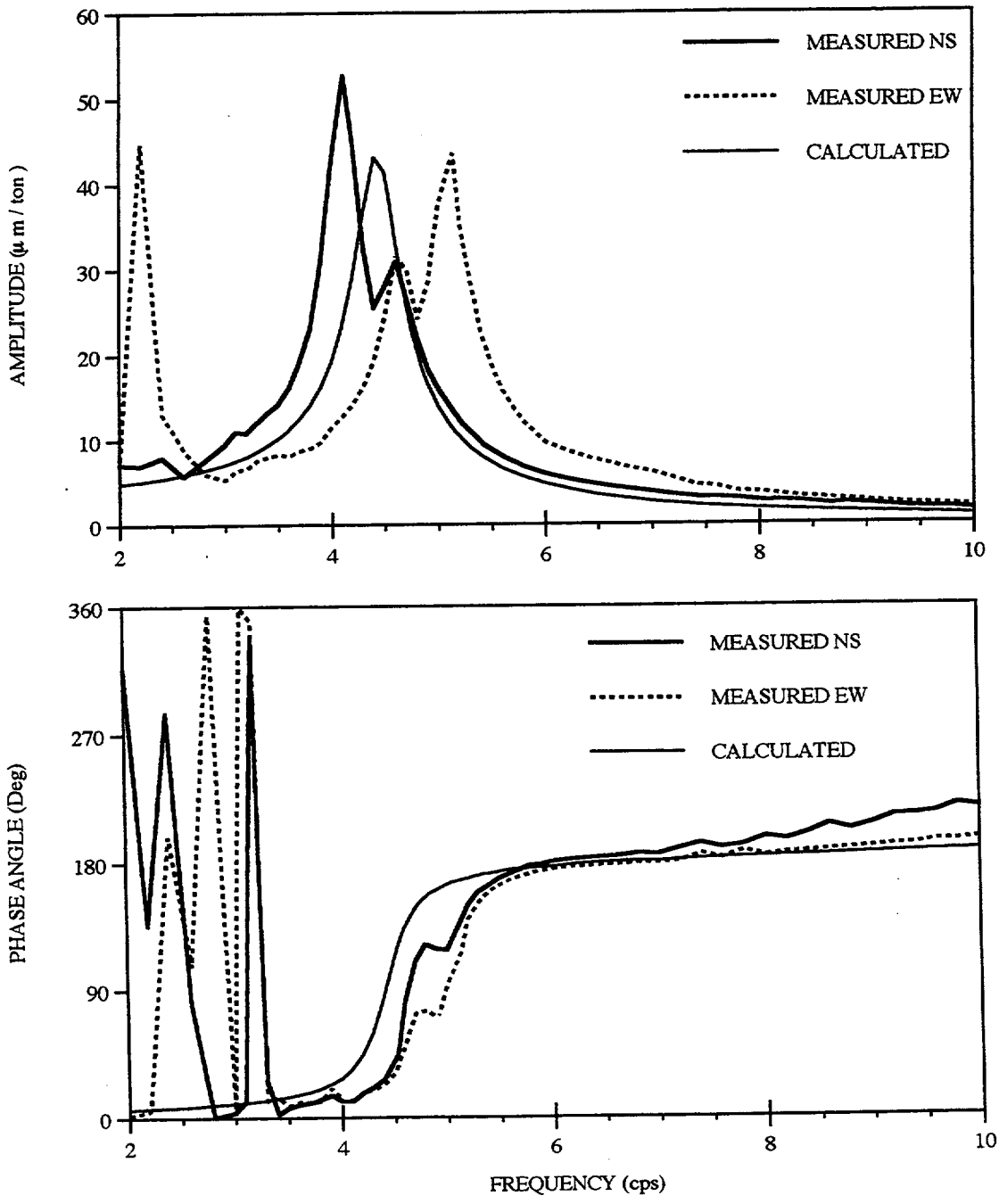

Fig. 3.5 Comparison of Predicted and Measured Horizontal Response at First Floor Caused by Horizontal Shaker Load at Roof (FVT-1)

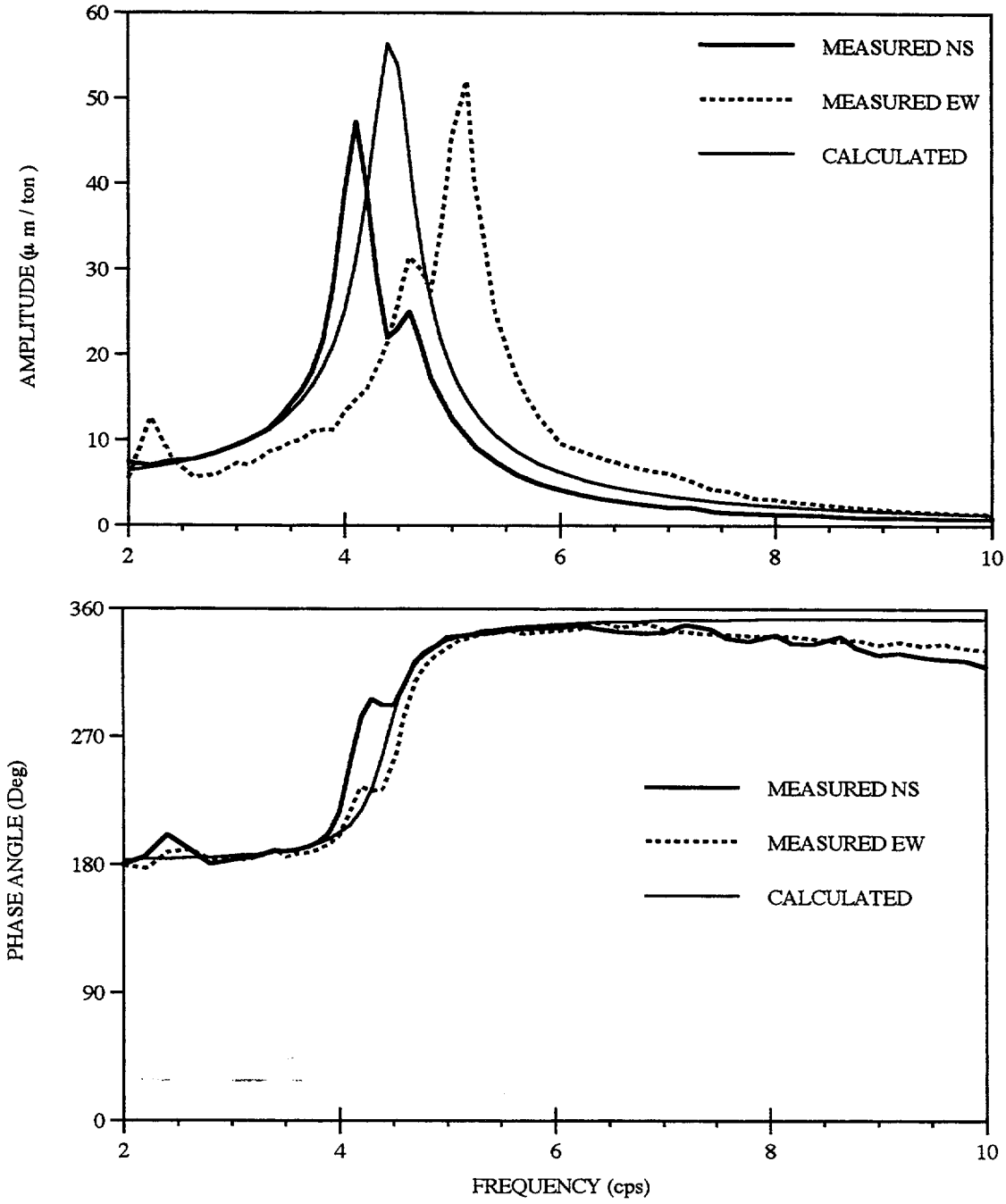

Fig. 3.6 Comparison of Predicted and Measured Vertical Response at Roof Caused by Horizontal Shaker Load at Roof (FVT-1)

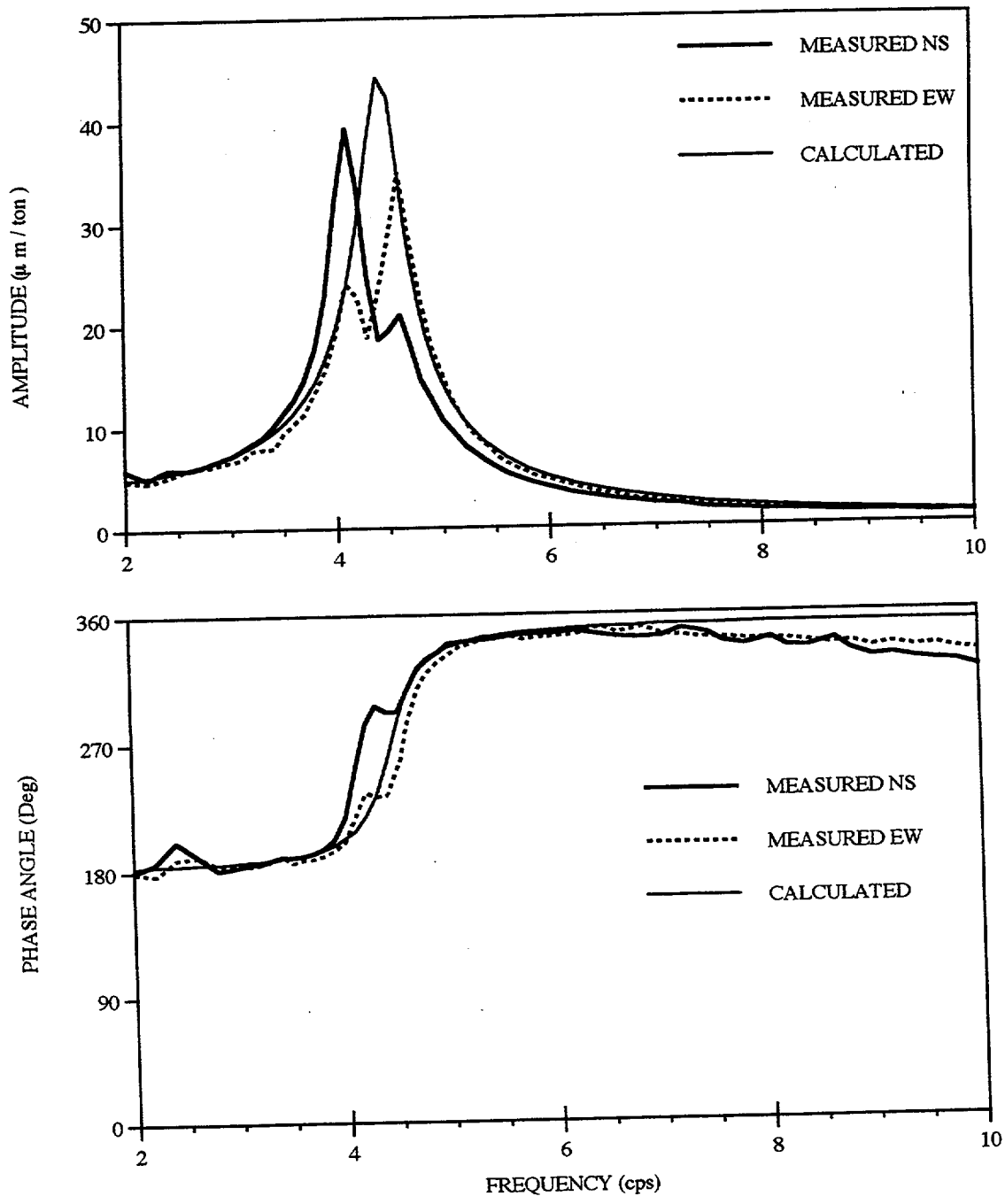

Fig. 3.7 Comparison of Predicted and Measured Vertical Response at First Floor Caused by Horizontal Shaker Load at Roof (FVT-1)

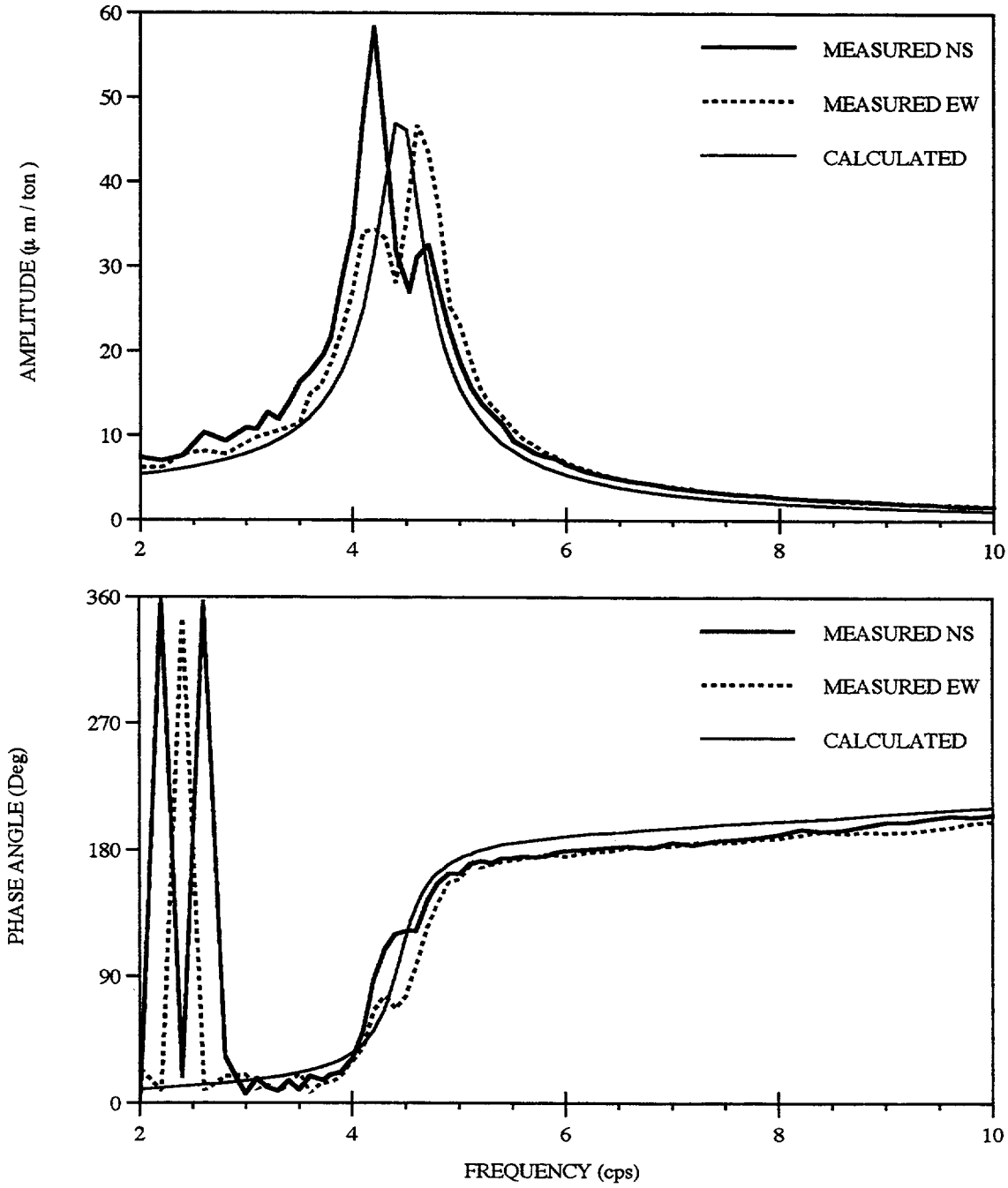

Fig. 3.8 Comparison of Predicted and Measured Horizonatl Response at Roof Caused by Horizontal Shaker Load at First Floor (FVT-1)

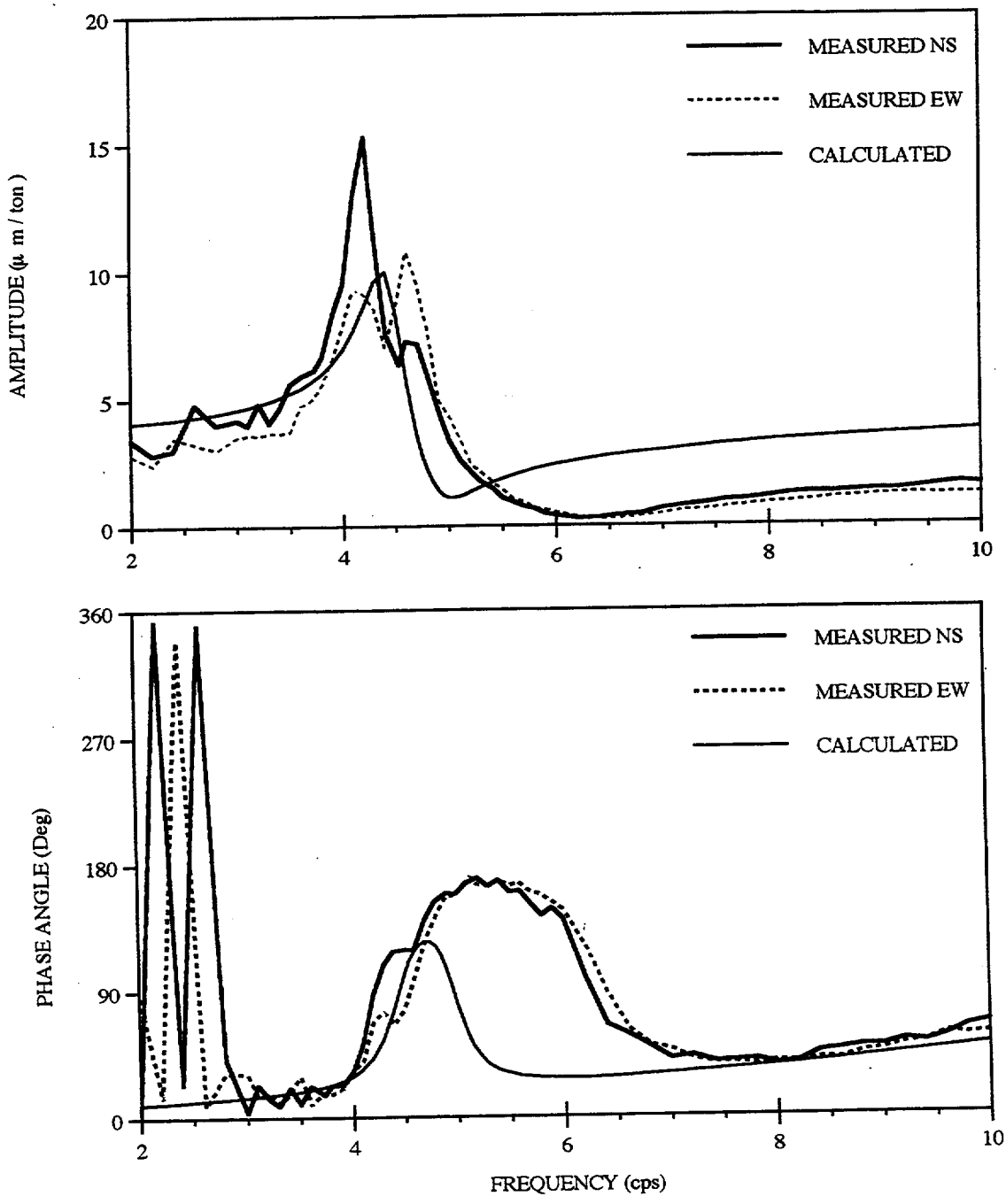

Fig. 3.9 Comparison of Predicted and Measured Horizontal Response at First Floor Caused by Horizontal Shaker Load at First Floor (FVT-1)

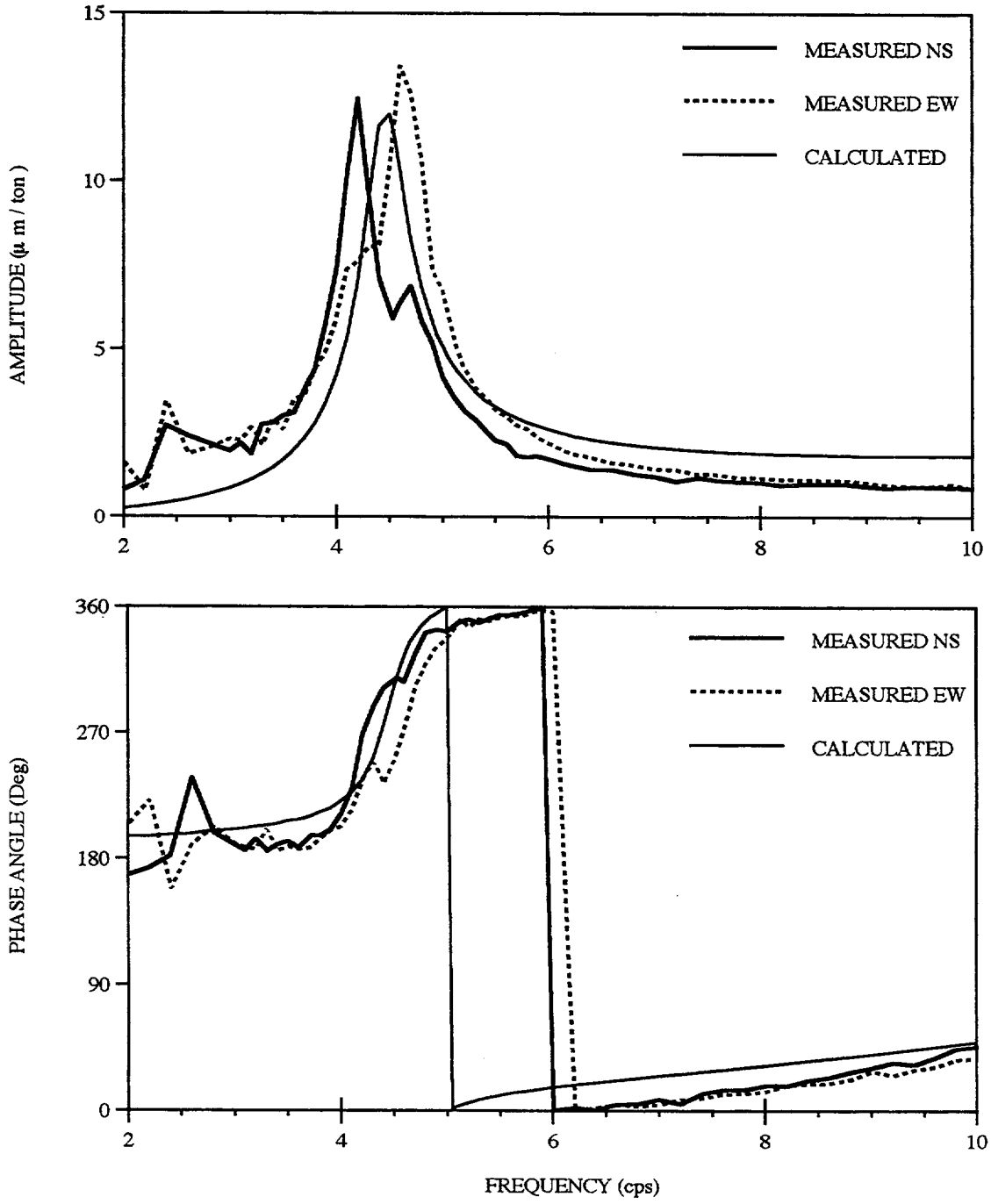

Fig. 3.10 Comparison of Predicted and Measured Vertical Response at Roof Caused by Horizontal Shaker Load at First Floor (FVT-1)

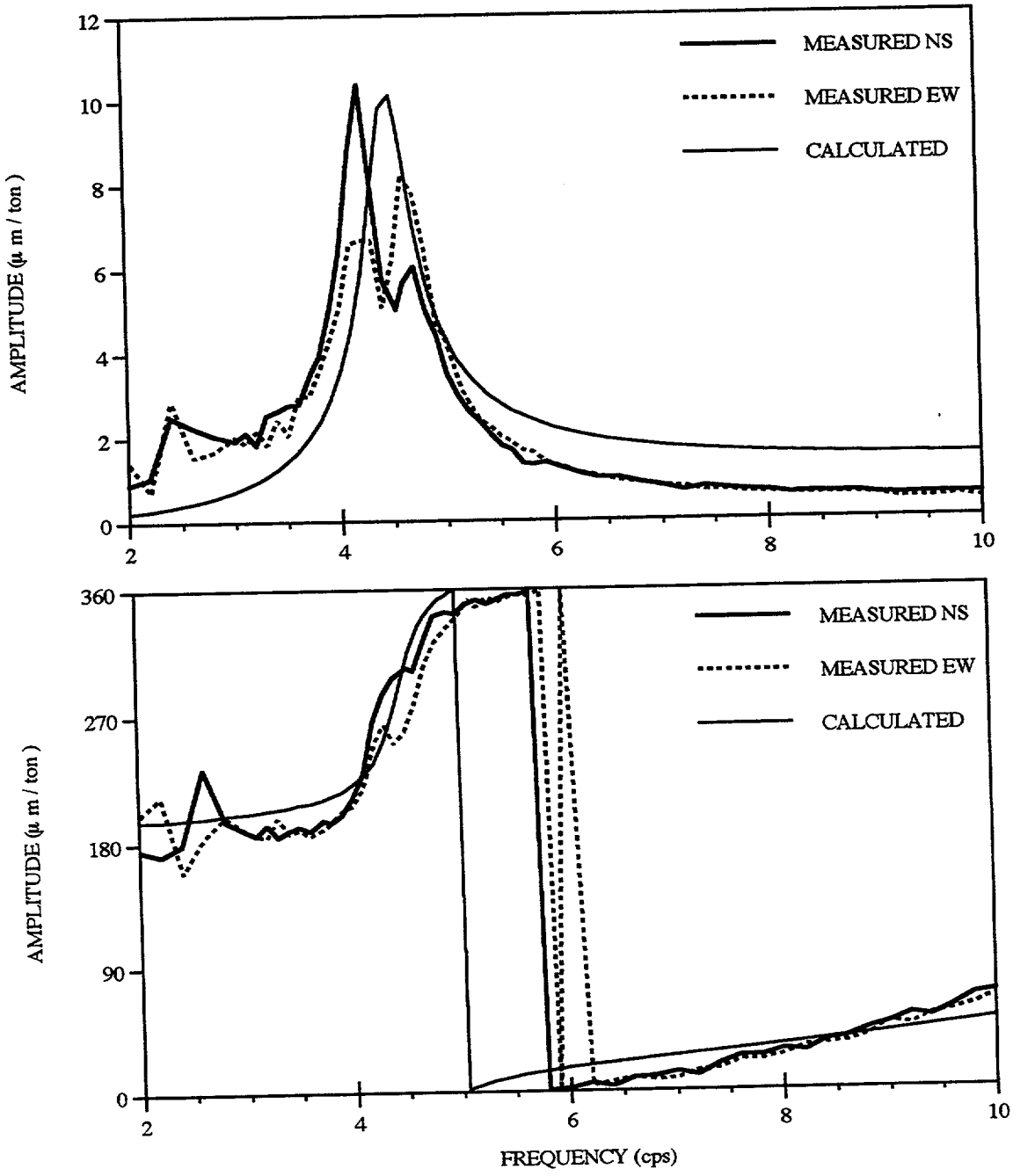

Fig. 3.11 Comparison of Predicted and Measured Vertical Response at First Floor Caused by Horizontal Shaker Load at First Floor (FVT-1)

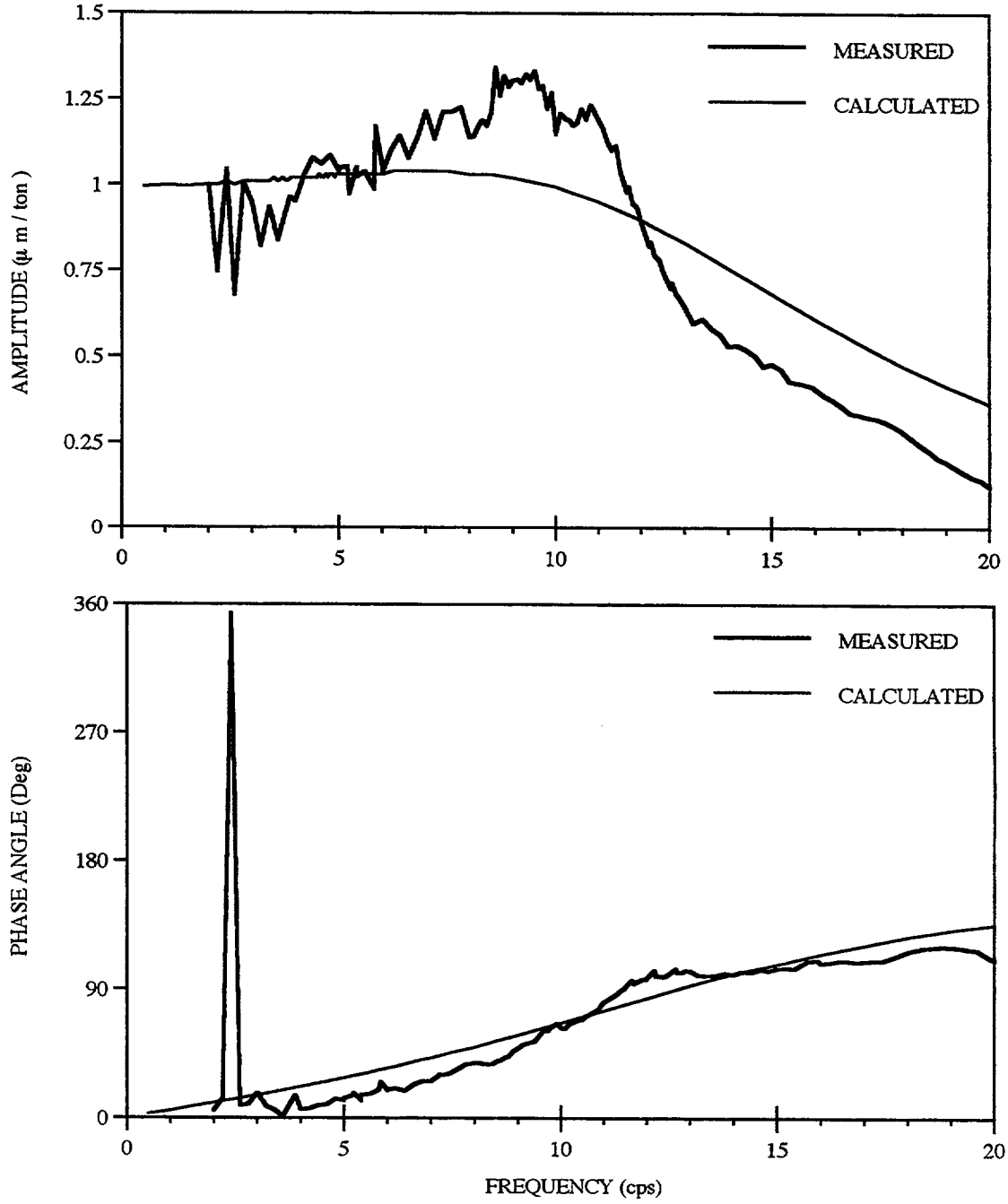

Fig. 3.12 Comparison of Predicted and Measured Vertical Response at First Floor Caused by Vertical Shaker Load at First Floor (FVT-1)

4.0 FVT-2 Tests

The characteristics of the measured data are first discussed. This is followed with comparisons between the measured and predicted results.

4.1 Evaluation of FVT-2 Measured Data

The response of the structure to each of the five FVT-2 tests is discussed in this Section based upon a review of the measured data. The measured data are plotted in Appendix B for all of the structural and soil data. The structural data is plotted so that all of the measurements in one direction (NS, EW, or UD) on one elevation (roof, midheight, or 1st floor) for one of the five tests are plotted on the same figure and the three figures for one elevation are printed on the same page. The gage location is keyed to the node numbers defined in Fig. 2.2 with the nodal coordinates given in Table 2.1. The soil data is plotted so that all of the measurements in one direction for one of the five tests are plotted on the same figure. The soil gage locations are keyed to distance from the wall of the structure (1.5 m BS; 6 m - MS; and 9.5 m - TS) and gage line (north from structure - N, and east from structure - E). An index of the data contained in Appendix B is shown on the cover page to the Appendix.

The structural measurements are first discussed followed with a discussion of the soil measurements.

4.1.1 Structural Measurements

The measured results for the first FVT-2 test (shaker mounted on the roof with the excitation acting in the N-S direction) are shown on pages B.1, B.2, and B.3 for the roof, midheight, and 1st floor elevations respectively.

The major N-S response can be seen to occur at 6.1 cps and the roof, midheight, and 1st floor displacements are 64 μm/t, 34 μm/t, and 9 μm/t respectively. A comparison of these data with the FVT-1 results indicate that the embedment increases the frequency by about 50 % from 4.1 cps and decreases the deformations by a factor of about 3.3 at the roof (from 213 μm/t) and a factor of about 5.3 at the basemat (from 48 μm/t).The basemat rotation can be determined from the vertical deformations of the base measured at opposite ends of a N-S diameter (about 10 μm/t at each end of the basemat with the measurements separated by 9.48 m) to be:

$$\theta = 2^* 10 / \text{Diameter} = 20\ \mu m/t / 9.48 = 2.10\ \mu\ rad / t$$

The N-S motion at the base of the basemat (Δ_b) is therefore:

$$\Delta_b = 9 - 2.10 * 3 = 2.55\ \mu m/t$$

The displacement (Δ_r) at the elevation of the roof gages (16.63 m above bottom of basemat) is:

$$\Delta_r = 2.10 * 16.63 = 34.9\ \mu m/t$$

Therefore the roof displacement of 64 μm/t is divided into 4 % rigid body translation (2.55/64), 55 % rigid body rotation (34.9/64) and 41 % flexure (100-4-55). As expected the addition of the backfill reduces the rigid body contributions and increases the flexural contribution as found by comparing the FVT-1 and FVT-2 results . The reduction in rigid body translation (from 11 % to 4 %) is more than the reduction in rocking (from 66 % to 55 %).

The N-S displacements at the east, center and west locations on the roof are 60, 65, and 68 μm/t respectively. This indicates that there is a small torsional rotation of the roof about a vertical axis but displacements caused by this rotation are small. Similar torsional response was not evident in the FVT-1 results. There is a small out of plane (EW) response caused by the NS excitation. The EW response at the roof is 13.5 μm/t or about 21 % of the in plane response. This is much smaller than found for the FVT-1 results. It is likely that the backfill material is isotropic and restrains the out of plane response resulting from the non isotropic characteristics of the underlying material.

Examination of the vertical displacements along a NS line on the roof indicate displacements of 14.4, 5.6, and 19.5 μm/t at the north, center and south location respectively. The same measurements taken on the basemat are 10, 0.7, and 9.9 μm/t respectively. These data indicate that there is some rigid body vertical displacement at the roof but not at the basemat. Non uniformities in the cylindrical shell properties could result in such an effect.

The measured results for the second FVT-2 test (shaker mounted on the roof with the excitation acting in the E-W direction) are shown on pages B.4, B.5, and B.6 for the roof, midheight, and 1st floor elevations respectively. The response characteristics are very similar to that of the first shaker test. The peak in-plane (E-W) response occurs at about 6.3 cps and has

slightly smaller amplitudes than measured for the NS excitation. The amplitudes of 60 μm/t, 32 μm/t, and 9 μm/t are measured at the roof, midheight, and 1st floor respectively. There is the same slight rotation of the structure about a vertical axis (the E-W displacements at the north, center and south locations on the roof are 62, 59, and 59 μm/t respectively).

The base rotation about the N-S axis can be determined as above to be 2.07 μ rad / t , and this results in 5 % of the roof deformation caused by rigid body translation of the base, 57 % caused by rigid body rocking, and the remaining 38 % caused by flexural deformations.

The same out-of-plane effects are observed with this test as with the first test. The E-W excitation causes a N-S deformation at the roof elevation with an amplitude of 13.4 μm/t which is 22 % of the in plane response. The vertical responses at the roof and first floor are very similar to those found for the NS roof excitation.

The measured results for the third FVT-2 test (shaker mounted on the first floor with the excitation acting in the N-S direction) are shown on pages B.7, B.8, and B.9 for the roof, midheight, and 1st floor elevations respectively. The peak in-plane (N-S) response occurs at about 6.5 cps (slightly higher than the first test with the shaker placed at the roof and the excitation applied in the N-S direction) and has amplitudes of 9.6 μm/t, 5.1 μm/t, and 1.6 μm/t at the roof, midheight, and 1st floor respectively. There is no rotation of the structure about a vertical axis or vertical deformation other than that caused by the rotation of a floor about a horizontal axis. The base rotation about the E-W axis can be determined as above to be 0.32 μ rad / t , and this results in 6 % of the roof deformation caused by rigid body translation of the base, 55 % caused by rigid body rocking, and the remaining 39 % caused by flexural deformations.

The same out-of-plane effects are observed with this test as with the first test. The E-W roof response is about 2.3 μm/t or 24 % of the in plane response.

The measured results for the fourth FVT-2 test (shaker mounted on the first floor with the excitation acting in the E-W direction) are shown on pages B.10, B.11, and B.12 for the roof, midheight, and 1st floor elevations respectively. The peak in-plane (E-W) response occurs at about 6.6 cps (again slightly higher than the second test with the shaker placed at the roof and the excitation applied in the E-W direction) and has amplitudes of 10.0 μm/t, 5.3 μm/t, and 1.7 μm/t at

the roof, midheight, and 1st floor respectively. There is no rotation of the structure about a vertical axis or vertical deformation other than that caused by the rotation of a floor about a horizontal axis. The base rotation about the N-S axis can be determined as above to be 0.30 μ rad / t , and this results in 8 % of the roof deformation caused by rigid body translation of the base, 52 % caused by rigid body rocking, and the remaining 40 % caused by flexural deformations.

The same out-of-plane effects are observed with this test as with the first test. The N-S roof response is 2.4 μm/t or 25 % of the in plane response.

The measured vertical deformation results for the fifth FVT-2 test (shaker mounted on the first floor with the excitation acting in the U-D direction) are shown on page B.13. There was no significant horizontal deformation measured for this test. The peak vertical displacements at the roof, midheight, and 1st floor are 0.63 μm/t, 0.56 μm/t, and 0.5 μm/t for the roof, midheight, and roof elevations respectively. The fundamental frequency (phase angle passes through 90°) is at about 10.8 cps. These displacements are about 60 % of those that were found for FVT-1 and this frequency is about the same as found from the FVT-1 results. It appears that the effect of the backfill material is to increase the effective damping of the system.

These results indicate that 79 % of the deformation results from the rigid body vertical deformation and 21% from the axial shortening of the cylindrical portion of the structure. It is also interesting to note that the deformation of the lower half of the the structure is 0.56 - 0.5 = 0.01 μm/t) while the deformation over the upper half of the cylinder is (0.63 - 0.56 = 0.07 μm/t). This indicates that the upper portion of the cylinder is more flexible than the lower half. There is some evidence that the construction procedure resulted in this characteristic. Holes were cut in the upper portion of the cylinder to support the formwork for the roof construction. These holes were then grouted, but there is evidence that the grouting was not of the quality required to restore the stiffness of the upper portion of the structure. Consideration should be given to reducing the stiffness (by changing the concrete's elastic modulus) of the upper half of the cylinder.

4.1.2 Soil Measurements

The soil measurements are shown on pages B.14 through B.18 with the results for each of the tests contained on one page. These results are consistent with the in-structure results. For example, the N-S excitation at the roof results in a N-S response of 6.7 μm/t at the BS N location, 5.4 μm/t at the MS N location, and 4.9 μm/t at the TS N location. The deformation at the bottom of

the basemat is 2.6 μm/t.These peaks occur at the same frequency (6.5 cps) as that found for the in-structure measurements. It is interesting to note that the amplitudes at the MS and TS locations are essentially the same as for the FVT-1 tests while the amplitudes at the BS location are significantly higher for the FVT-1 tests than are found for the FVT-2 test.

Non symmetric results are also found for the soil data. A symmetric response for the N-S excitation would result in zero E-W response along a N-S line. However, Fig. B.41 indicates a significant E-W response. The vertical excitation would only result in radial horizontal displacements in the soil. The data shown on Figs. B.53 and B.54 indicate significant tangential responses.

4.2 Comparison of Measured Data with Predictions

The pre test predictions and post test correlations with the experimental data are discussed in this section. In all cases the work is performed using the CARES computer code (Ref.7). The CARES code and the data used for the prediction and correlation models are first discussed. The results obtained for each are then discussed.

4.2.1 Description of Prediction Models

FVT-2 predictions are made with the CARES computer code as discussed above for FVT-1. The structure is modeled for the correlation study with the lumped mass shear beam shown on Fig. 2.2. The same model is used for the pre test prediction and post test correlation studies. The SSI model is attached to node 1. The model parameters are shown on Table 4.1. As may be seen the soil shear wave velocity to the side of the structure is modeled with the 1312 fps (400 m/s) shear wave velocity soil and the soil below the foundation is modeled with 1257 fps (383 m/s) shear wave velocity soil. The CARES program can only accommodate uniform soil properties to the side and beneath the structure. It is generally recommended that the uniform base soil properties be determined as a weighted (by distance beneath the foundation) average of the actual soil properties within one diameter of the foundation depth. If this is done for the soil properties shown on Fig. 2.1 the "average" shear wave velocity is found to be 1295 fps. The soil immediately beneath the foundation is used for the predictions, however, and variations in the soil properties considered in the correlation studies. A similar "average" soil property may be evaluated for the side soil by using a weighting function that increases in proportion to its distance above the foundation (for the rocking mode) and decreases in proportion to $1/\text{radius}^4$ (assuming that displacements vary inversely with radius). If this is done the side soil shear wave velocity would be reduced to about 90 % of the shear wave velocity of the soil adjacent to the structure.Once again the soil properties adjacent to the structure are used for the predictions and variations of these properties are

considered in the correlation studies.

4.2.2 Prediction of FVT-2 Results

A comparison of the predicted and measured results are shown on Figs. 4.1 through 4.10. The predicted response is shown with the thin solid curves and the measured data are represented with either the solid or dashed thick curves. There were two horizontal tests performed (shaker in N-S and E-W directions) for each shaker location. Of course the predictions for these two tests are identical since the problem geometry is symmetric. Both of the measured data are, therefore included on the same figure. There are often several sets of data representing a single measured response. For example, the N-S roof response caused by the N-S roof shaker excitation was measured at the east center and west locations on the roof (see Fig. B.1). Since the measured responses are very similar, only one is plotted on Figs. 4.1 through 4.10. The symmetry of the problem also results in predictions of zero out of plane response. As noted above there is a measured out of plane response and this represents a significant difference between the measured and predicted results.

The results of the comparisons are summarized on Table 4.2. With the exception of the last two rows the data is organized in groups of three rows each. The first row is the computed value and the following two rows (marked with an *)are the experimental data for the NS and EW tests. The last two rows are for the computed and measured data respectively. As may be seen the agreement between the computed and measured data is excellent.

Predicted contributions (rigid body rocking, rigid body translation, and flexural) to the total roof displacements are compared with the measured data on Table 4.3. It may be seen that the predicted contributions agree very well with the measured results.

Table 4.1

Structural and Soil Parameters Used in Prediction and Correlation Studies

Parameter	Property
Soil Beneath Foundation:	
Shear Velocity (fps)	1257
Density (kcf)	0.151
Poisson's Ratio	0.48
Damping	2 %
Soil to Side of Structure:	
Shear Velocity (fps)	1312
Density (kcf)	0.149
Poisson's Ratio	0.48
Damping	2 %
Structure:	
Young's Modulus (ksi)	4,093
Poisson's ratio	0.20
Damping	2 %
Wall Thickness (ft)	0.98
Foundation Radius (ft)	17.75
Basemat Thickness (ft)	9.84
Roof Thickness (ft)	4.92
Length of Cylinder (ft)	38.16
Location of Roof Shaker - Node	9
Location of Basemat Shaker - Node	10
Roof Weight (k)	1084.4
Basemat Weight (k)	1460.9

Table 4.2

Comparison of Predicted and Measured Results

Shaker Location	Shaker Direction	Displacement Location	Displacement Direction	Frequency of Pk Amplitude (cps)	Amplitude of Peak (μm/t)
Roof	Horizontal	Roof	Horizontal	6.0	58
*	NS	Roof	NS	6.1	64
*	EW	Roof	EW	6.3	60
Roof	Horizontal	FF	Horizontal	6.0	11
*	NS	FF	NS	6.1	9
*	EW	FF	EW	6.3	9
Roof	Horizontal	Roof	UD	6.0	15
*	NS	Roof	UD	6.1	17
*	EW	Roof	UD	6.3	17
Roof	Horizontal	FF	UD	6.0	9.6
*	NS	FF	UD	6.1	10.0
*	EW	FF	UD	6.3	9.8
FF	Horizontal	Roof	Horizontal	6.0	12
*	NS	Roof	NS	6.5	9.6
*	EW	Roof	EW	6.6	10
FF	Horizontal	FF	Horizontal	6.0	2.5
*	NS	FF	NS	6.5	1.6
*	EW	FF	EW	6.6	1.7
FF	Horizontal	Roof	UD	6.0	3.0
*	NS	Roof	UD	6.5	2.5
*	EW	Roof	UD	6.6	2.6
FF	Horizontal	FF	UD	6.0	2.0
*	NS	FF	UD	6.5	1.6
*	EW	FF	UD	6.6	1.7
FF	UD	FF	UD	15	0.7
*	UD	FF	UD	10.8	0.5

Table 4.3

Components of Roof Deformation

Source	Shaker	% Rocking	% Horizontal	% Elastic
Computed	Roof Hor	56	8	36
Measured	Roof NS	55	4	41
Measured	Roof EW	57	5	38
Computed	FF Hor	56	9	35
Measured	FF NS	55	6	39
Measured	FF EW	52	8	40
Computed	FF UD	--	89	11
Measured	FF UD	--	79	21

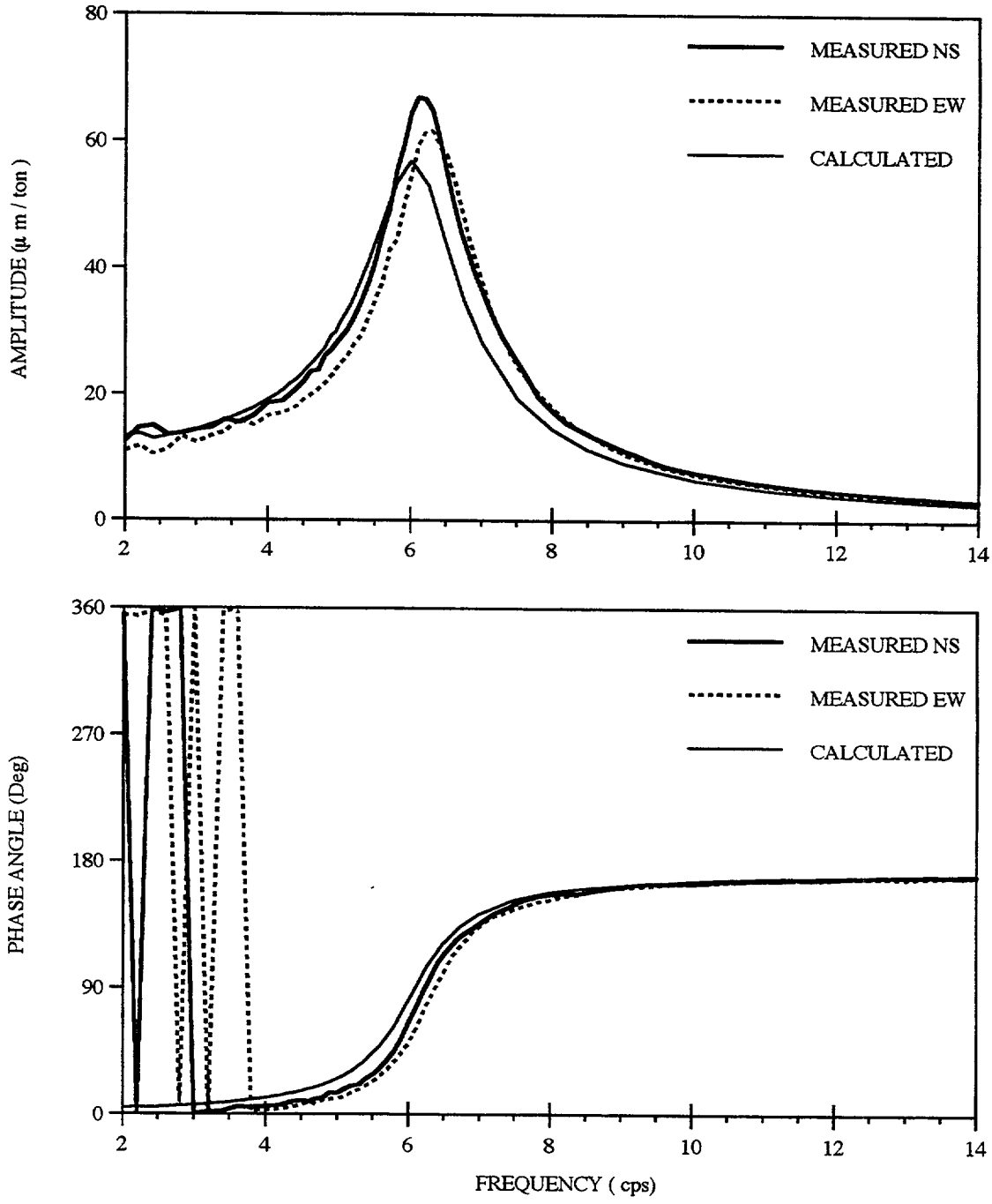

Fig. 4.1 Comparison of Predicted and Measured Horizontal Response at Roof Caused by Horizontal Shaker Load at Roof (FVT-2)

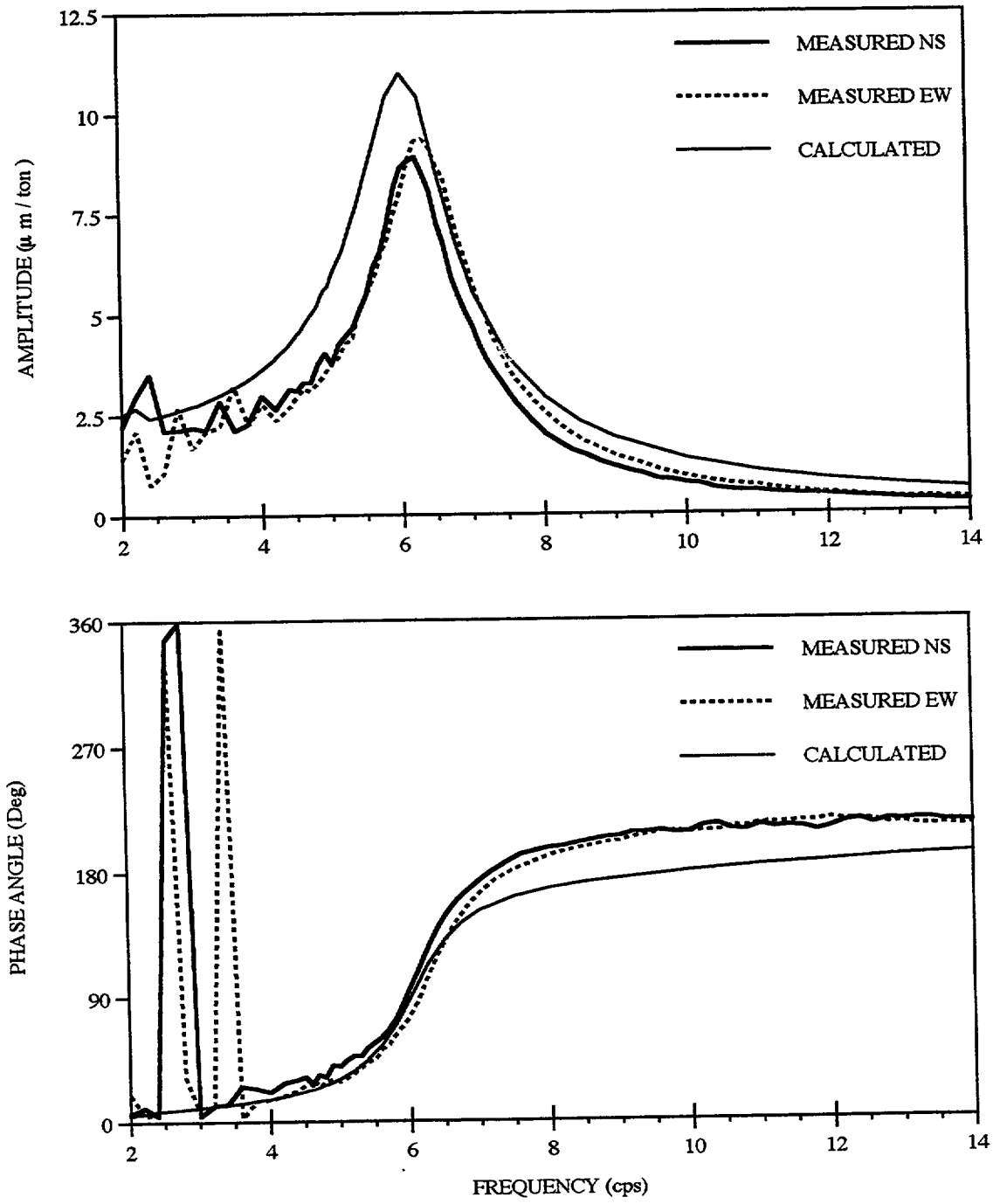

Fig. 4.2 Comparison of Predicted and Measured Horizontal Response at First Floor Caused by Horizontal Shaker Load at Roof (FVT-2)

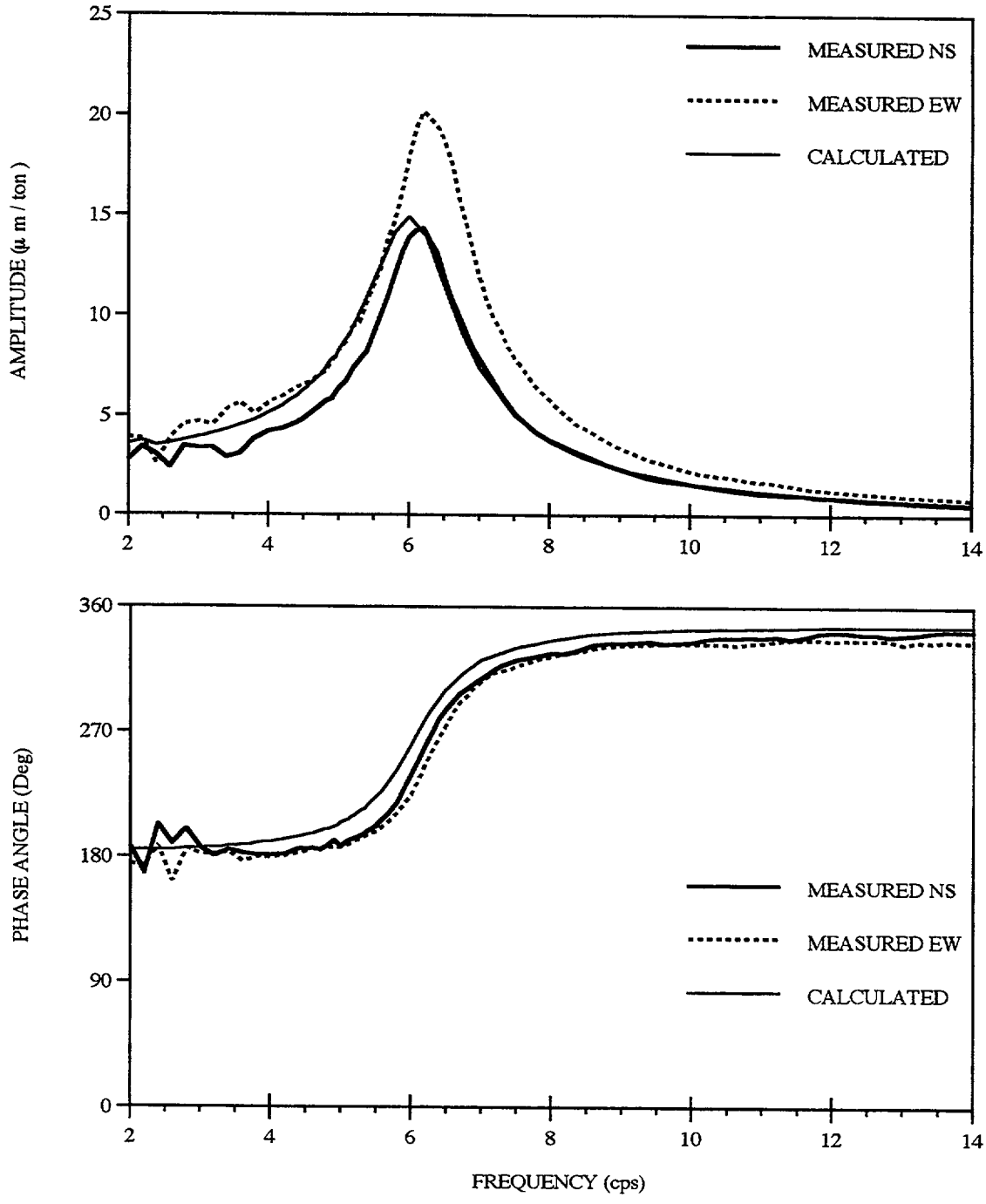

Fig. 4.3 Comparison of Predicted and Measured Vertical Response at Roof Caused by Horizontal Shaker Load at Roof (FVT-2)

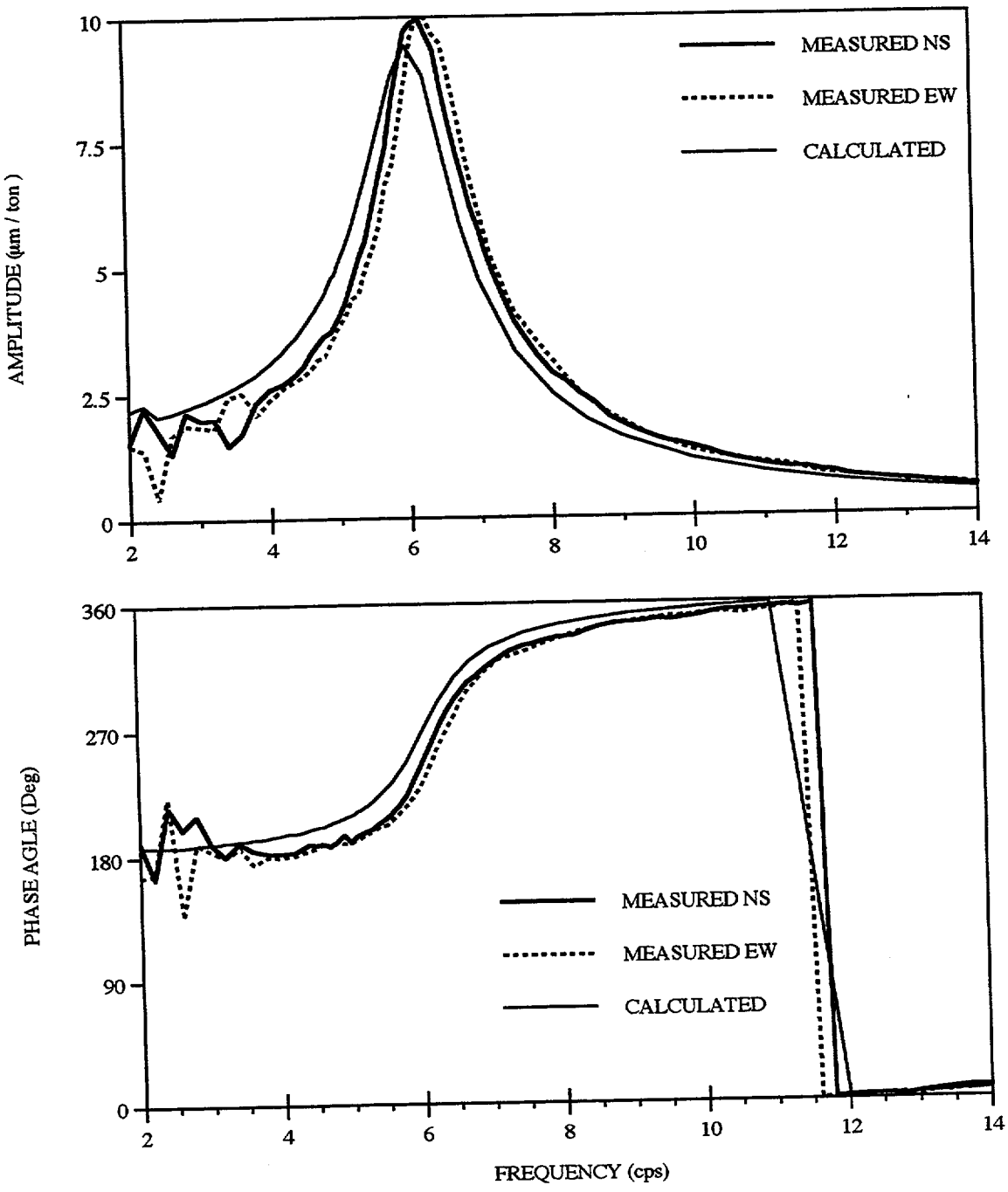

Fig. 4.4 Comparison of Predicted and Measured Vertical Response at First Floor Caused by Horizontal Shaker Load at Roof (FVT-2)

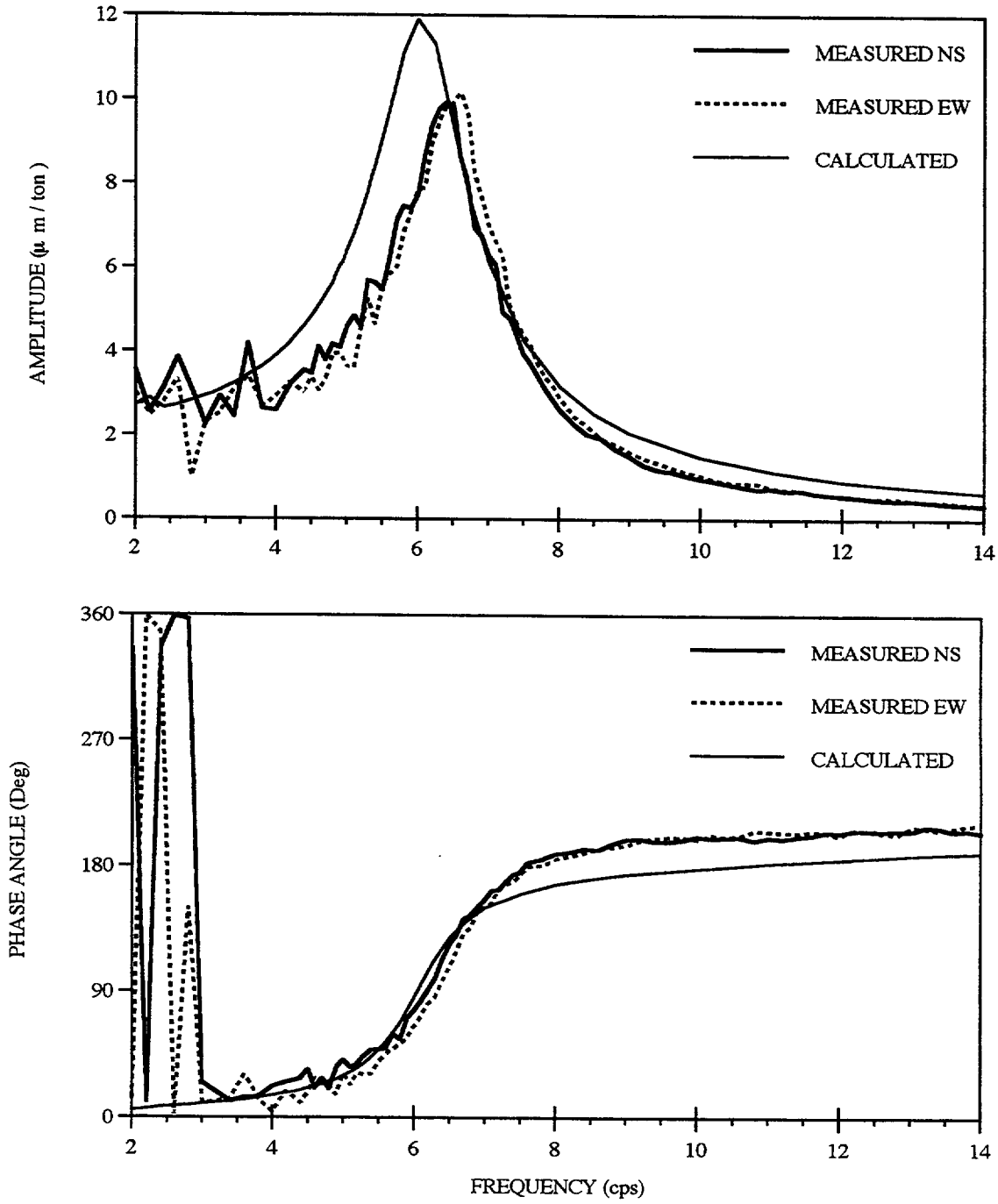

Fig. 4.5 Comparison of Predicted and Measured Horizontal Response at Roof Caused by Horizontal Shaker Load at First Floor (FVT-2)

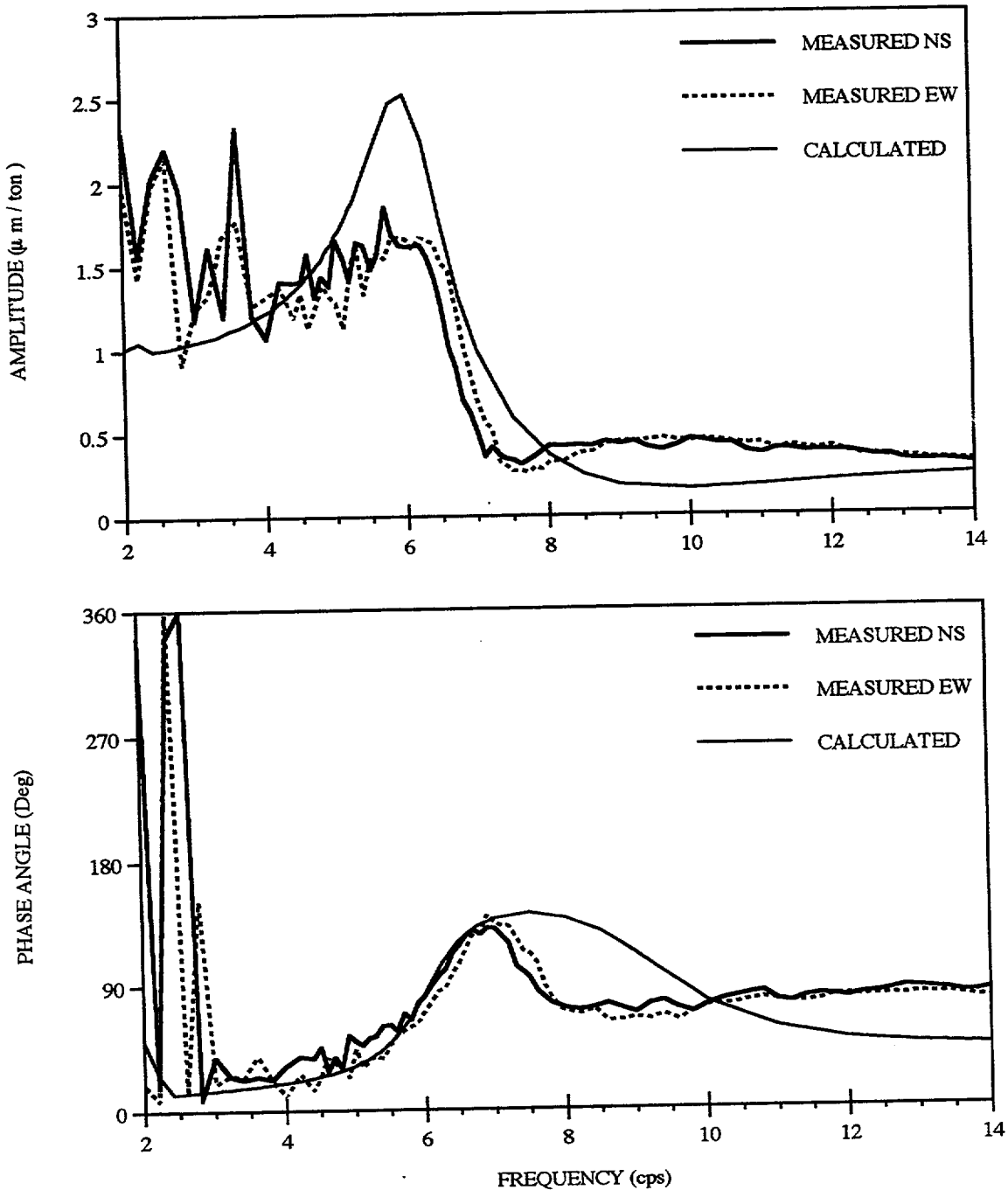

Fig. 4.6 Comparison of Predicted and Measured Horizontal Response at First Floor Caused by Horizontal Shaker Load at First Floor (FVT-2)

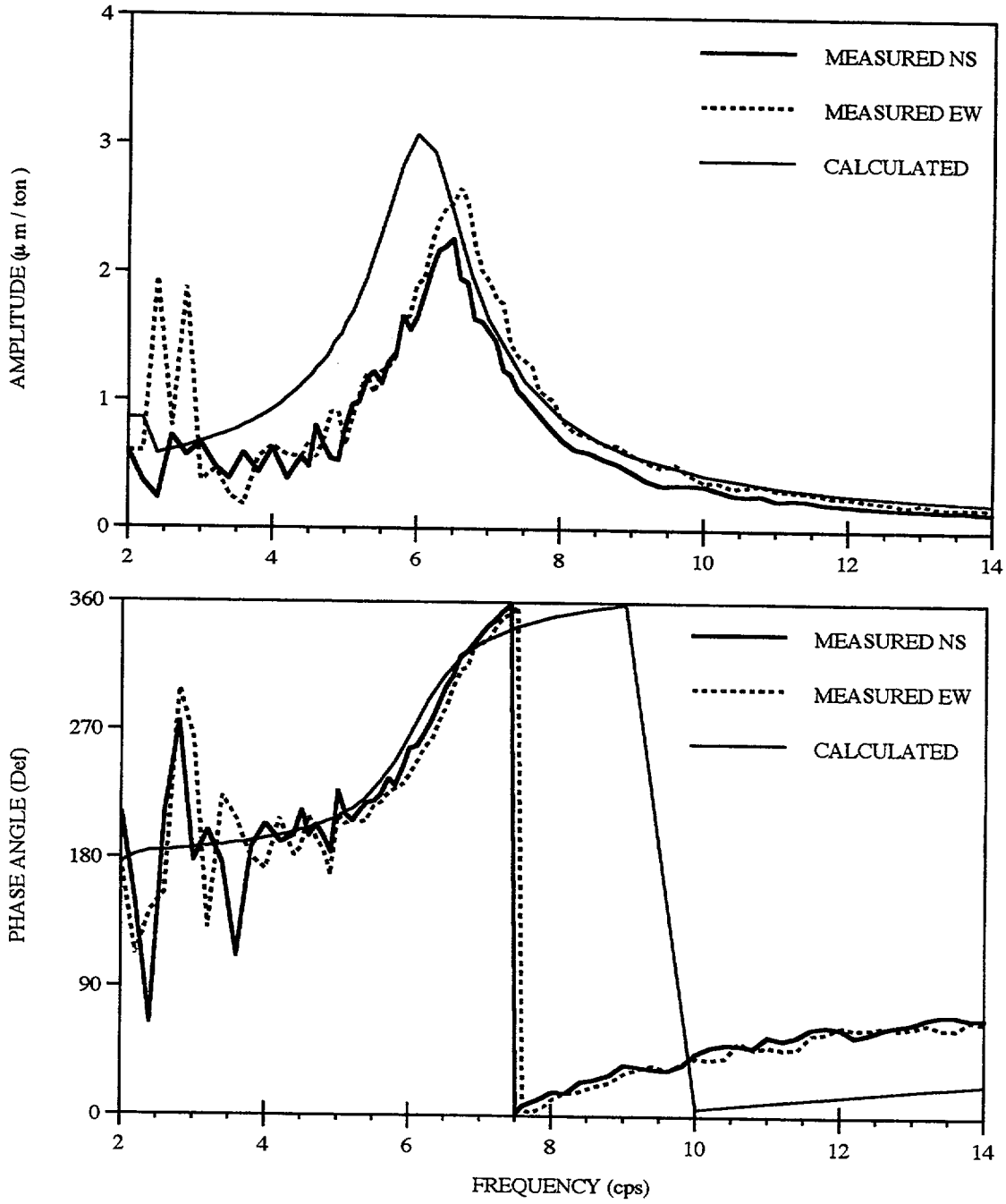

Fig. 4.7 Comparison of Predicted and Measured Vertical Response at Roof Caused by Horizontal Shaker Load at First Floor (FVT-2)

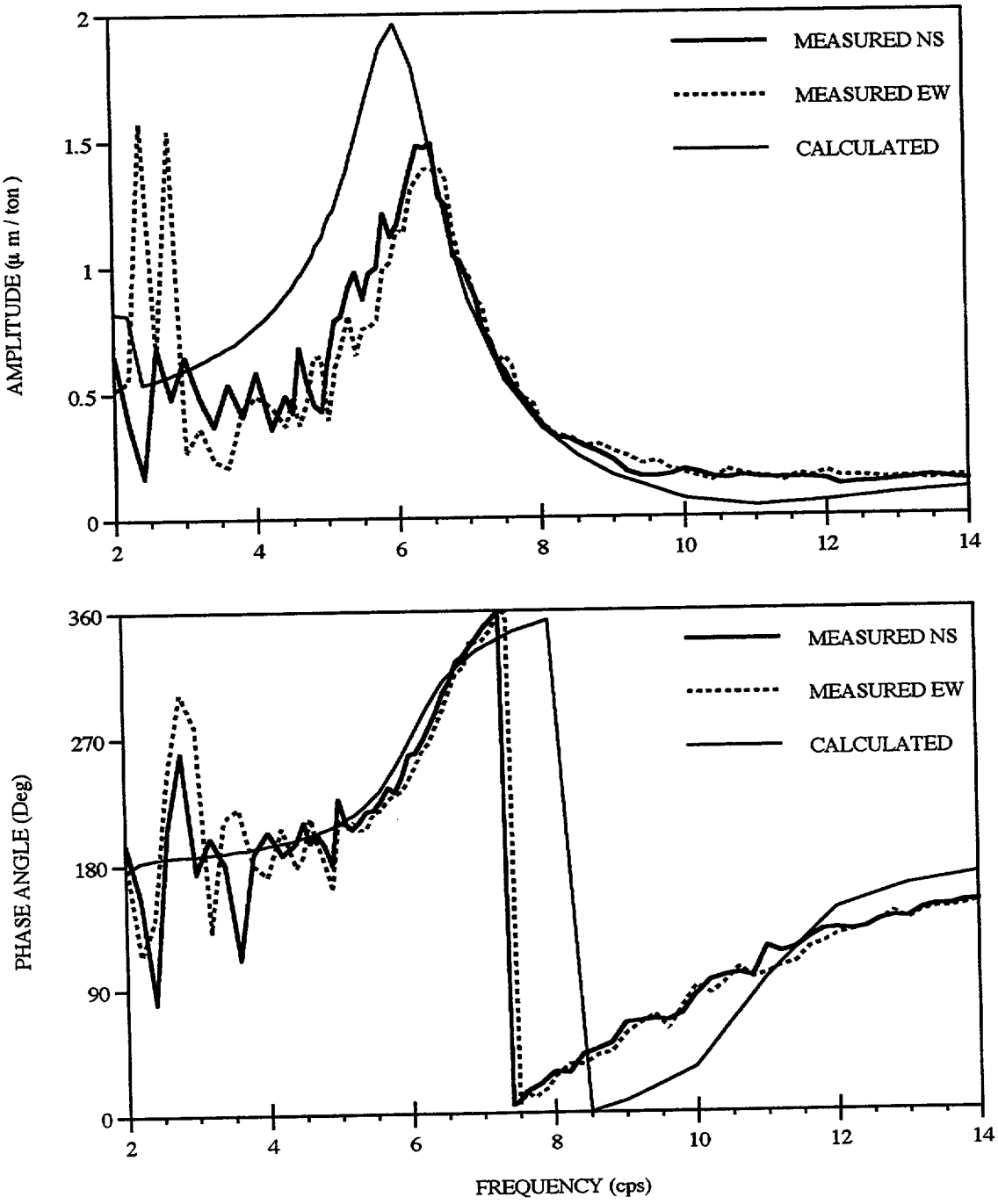

Fig. 4.8 Comparison of Predicted and Measured Vertical Response at First Floor Caused by Horizontal Shaker Load at First Floor (FVT-2)

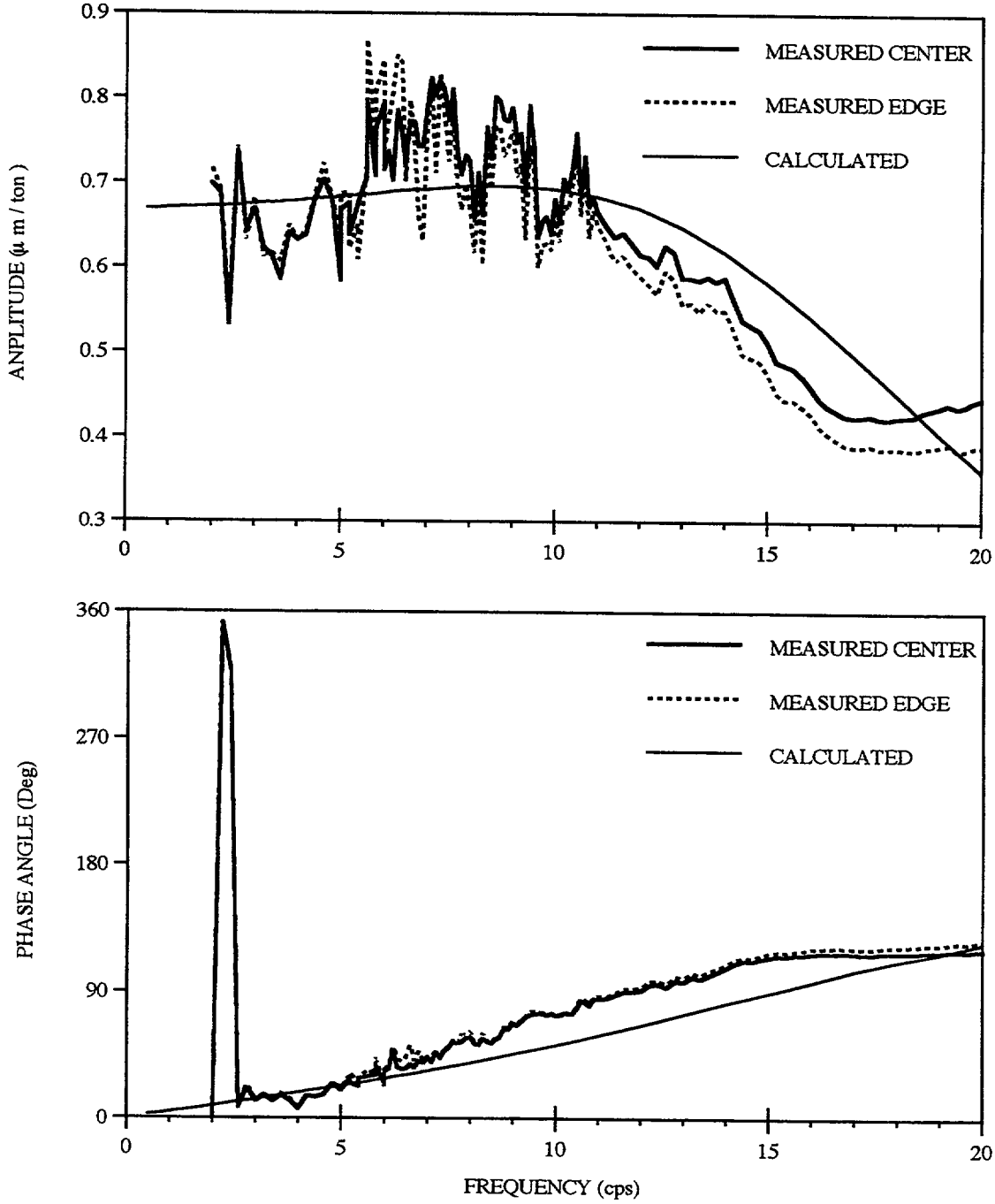

Fig. 4.9 Comparison of Predicted and Measured Vertical Response at Roof Caused by Vertical Shaker Load at First Floor (FVT-2)

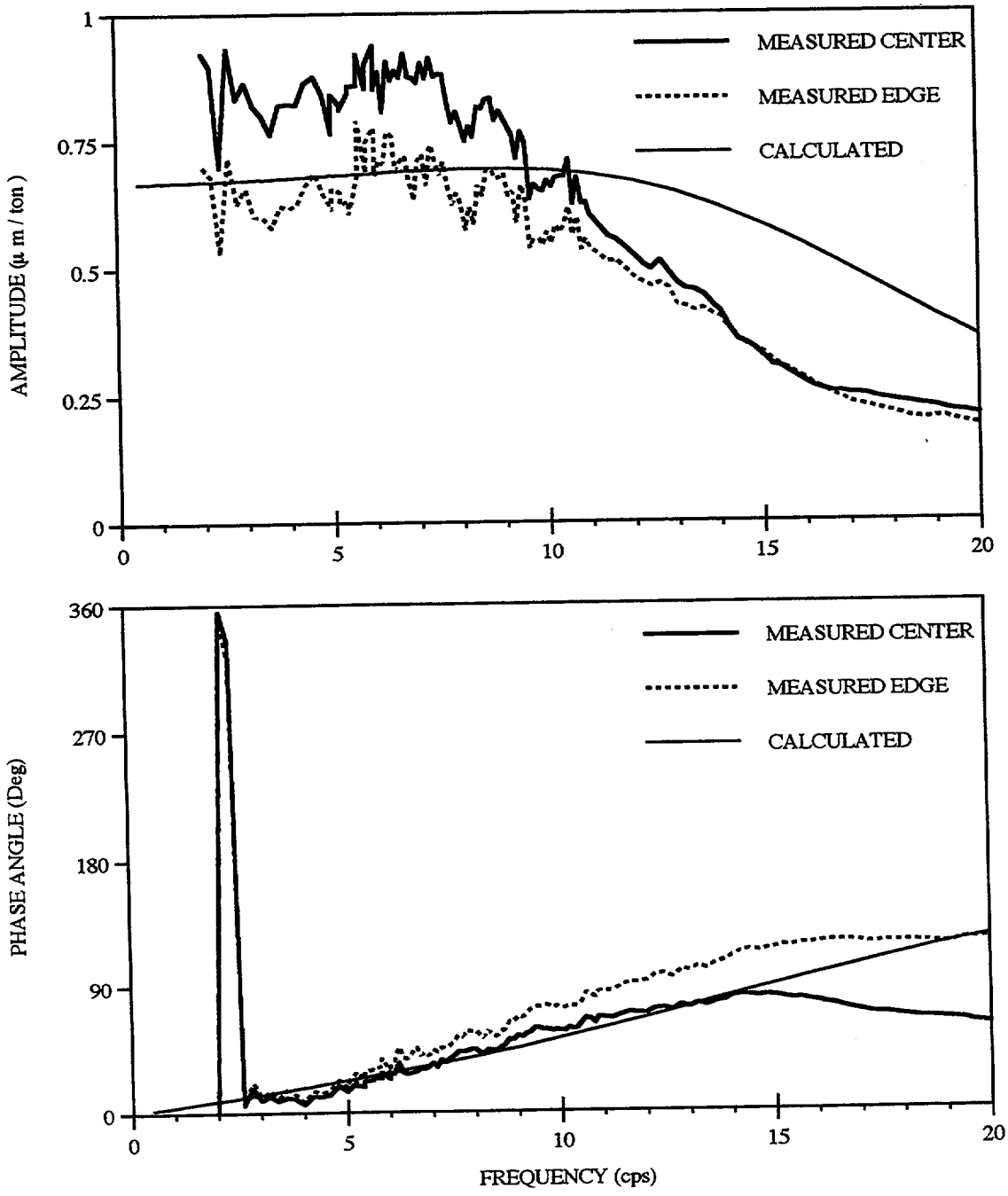

Fig. 4.10 Comparison of Predicted and Measured Vertical Response at First Floor Caused by Vertical Shaker Load at First Floor (FVT-2)

5.0 Correlation of Predictions with FVT-1 and FVT-2 Measured Data

The effect of the shear wave velocities of the side soil and underlying soil on the predicted responses are considered. Solutions are obtained (using the CARES program and Beredugo-Novak SSI model) for side soil shear wave velocities varying from 0 to 1640 fps (500 m/s) and underlying soil shear wave velocities varying from 820 fps (250 m/s) to 1640 fps (500 m/s). All other parameters for the soil and structure are assigned the values given in Table 4.1. Solutions are obtained for the horizontal roof excitation test and the horizontal roof response is used for the correlation studies. Amplification results are obtained for each case. The fundamental frequency (at which the peak response occurs and the phase angle equals 90^{o}) and the magnitude of the peak response are identified from the response curves.

The frequency at which the peak horizontal roof response occurs is plotted on the top portion of Fig. 5.1 as a function of the side soil shear wave velocity with the underlying soil shear wave velocity shown as a parameter. The variation of the peak roof response with the soil shear wave velocities is shown on the bottom portion of Fig. 5.1. The data shown on Fig. 5.1 show that the frequency of the structural system depends primarily on the underlying soil shear wave velocity with the side soil shear wave velocity only playing a significant role when the underlying soil shear wave velocity is less than 300 m/s. On the other hand it can be seen that the underlying soil shear wave velocity has little effect on the roof displacement except for very low values of the side soil shear wave velocity. It should also be noted that the roof displacement varies only slightly with the side soil stiffness for shear wave velocities greater than about 200 m/s.

Lines identifying the FVT measured results are also shown on Fig. 5.1. The average (EW and NS) FVT-1 measured frequency is 4.3 cps with a peak roof displacement equal to 194 μm/t. The best agreement can be seen to occur when an underlying shear wave velocity slightly less than 317 m/s is used (of course the side soil shear wave velocity is equal to zero for the FVT-1 tests). This is the unified soil model recommended by CRIEPI.

The fundamental frequencies of the measured FVT-2 data are 6.1 cps in the N-S test and 6.3 cps in the E-W test. The measured roof responses are 64 μm/t for the N-S test and 60 μm/t for the E-W test. It can be seen that good correlations of the predicted and measured roof displacements are obtained for any underlying soil shear wave velocity greater than 250 m/s and for side soil shear wave velocities between 300 m/s and 400 m/s. Good correlations of the fundamental frequency of the system is obtained for any side soil shear wave velocity if the underlying soil shear wave velocity is between 383 m/s and 500 m/s. In summary, the predictions will compare favorably with the measured data if an underlying soil shear wave velocity is specified to be

between 383 m/s and 500 m/s and the side soil shear wave velocity is taken between 300 m/s and 400 m/s. These ranges in shear wave velocity are consistent with the unified soil model.

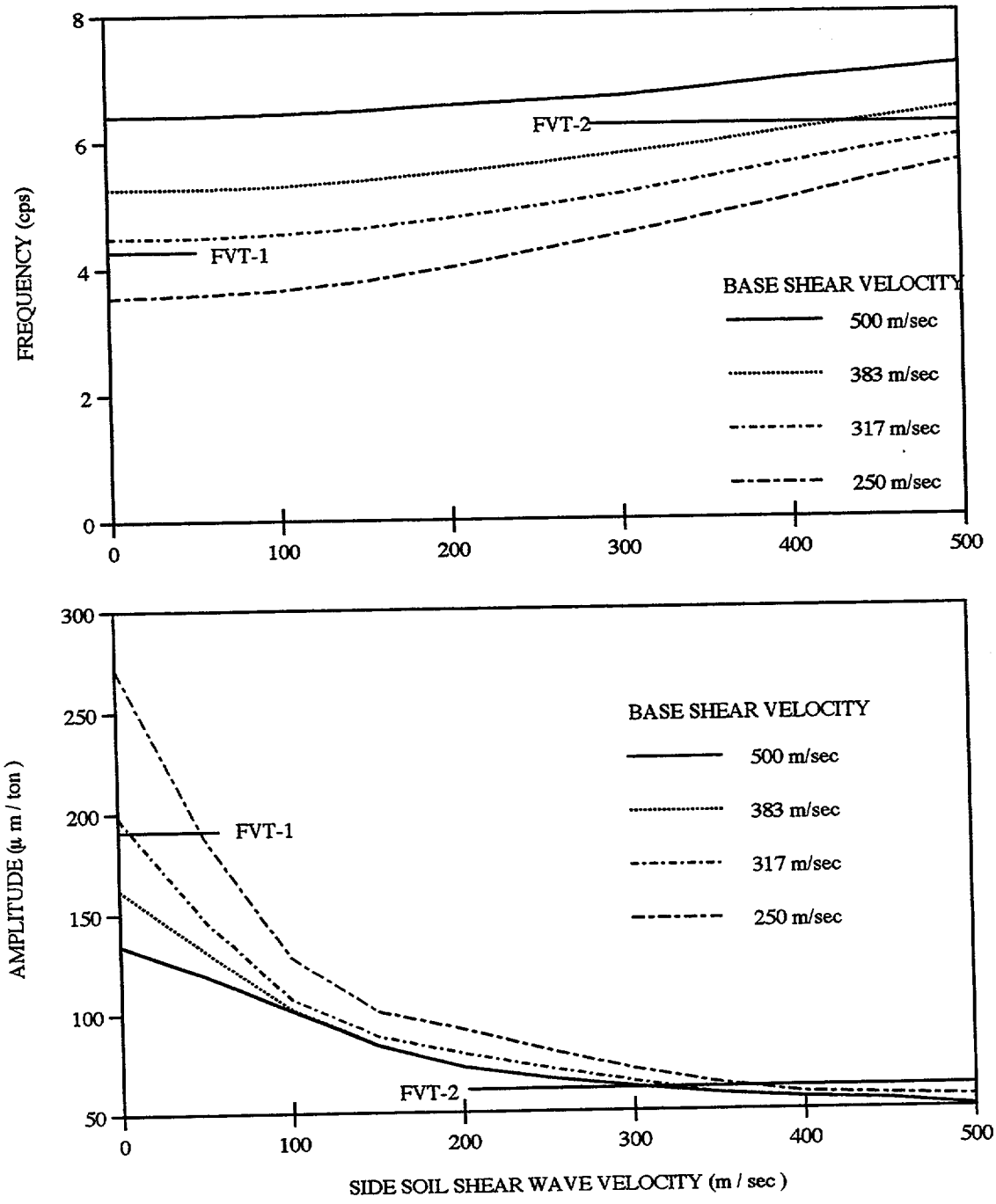

Fig. 5.1 Variation of Predictions With Soil Shear Wave Velocity

6.0 Summary

The FVT tests consisted of five shaker experiments performed on the Hualien quarter scale model. The shaker was placed on the roof with the excitation in the N-S and E-W directions for the first two tests, the third and fourth tests were conducted with the shaker placed on the basemat and the excitation applied again in the N-S and E-W directions, and the shaker excitation for the fifth test was in the vertical direction with the shaker located on the basemat. Two sets of such tests were performed, one before placement of the backfill and one after placement of the backfill.

The response characteristics as deduced from the FVT-1 measured data are discussed in Section 3 of the report. The measured data are also correlated with predictions made using the CARES (Ref.5) computer code. The following conclusions are drawn from the study:

1. The peak responses for the horizontal shaker tests (both with the shaker at the roof and basemat levels) occur at 4.1 cps when the excitation is in the N-S direction and 4.6 cps when the excitation is in the E-W direction. The contributions to the measured peak response at the roof level for the excitation placed at the roof is about 11-12 % rigid body translation, 66-69 % rigid body rocking about the base, and 19-23 % flexural deformation of the structure.

2. The difference in frequency for the N-S and E-W response is likely due to some non isotropic behavior in the soil. The "stiffer" behavior in the E-W direction is also demonstrated by the peak measured responses. The peak response in the N-S direction due to N-S excitation is 213 μm/t and the peak response in the E-W direction due to E-W excitation is 175 μm/t. The excitation in each of the horizontal directions also results in an out of plane response that is about 60 % and 35 % respectively for the N-S and E-W excitations. The soils exploration program did not uncover this non isotropic characteristic.

3. The amplifications of the horizontal displacements indicate that the effective damping in the system is about 7 %.

4. The measured results from the vertical excitation case indicate that the system is highly damped in this direction (greater that 50 %) and that the vertical system frequency is about 11 cps.

5. The correlation studies comparing the predicted and measured results show good agreement. The comparisons of the measured and predicted peak displacement and frequencies at which the peak displacements occur are shown on Table 3.3. Of course the models do not predict the out of plane response since the models are symmetric. There is no bases in the data describing the experiment to incorporate nonsymmetries.

The response characteristics as deduced from the FVT-2 measured data are discussed in the report. The measured data are also correlated with predictions made using the CARES (Ref.5) computer code. The following conclusions are drawn from the study:

1. The measured response of the structure caused by the horizontal shaker loads indicate that the system frequency is about 6.2 cps with peak response at the roof being about 62 μm/t. Comparison of these data with the FVT-1 results indicate that the backfill has increased the frequency by about 50 % and decreased the peak response by a factor of about 3 to 4. This is a modest increase in frequency and a significant reduction in response. It can be concluded that the principal effect of embedment is to increase the damping and thereby reduce the response.The embedment effects of the test structure would be expected to be more significant than found for most nuclear power plant structures since the depth of embedment is almost equal to the radius and the backfill material has a stiffness larger than the underlying material.

2. The out of plane response (N-S loading introduces E-W response) found in the FVT-1 results is also found for the FVT-2 results although the effect is much less. This would indicate that the backfill material results in responses in the same plane as the loading and thereby reduces the out of plane responses caused by the underlying material.

3. The horizontal loading introduces a small vertical rigid body deformation of the structure. This is not found in the FVT-1 results.

4. The total roof displacement caused by the roof shaker load is distributed so that about 55 % results from rigid body rocking of the structure, 5 % results from rigid body translation of the structure, and the remaining 40 % results from flexure.

5. The predictions are in excellent agreement with the measurements for the horizontal shaker experiments. For example the predicted fundamental frequency is 6 cps as compared with the measured 6.2 cps, and the predicted amplitude of the roof displacement is 58 μm/t as compared with the measured 62 μm/t. The predicted distribution of the roof displacement between the rigid body and flexural modes is very close to the measured data,

6. A correlation study of the effect of the soil shear wave velocities indicates that good correlations between the measured and computed results would be obtained if the underlying soil shear wave velocity is between 383 m/s and 500 m/s and for side soil shear wave velocities in the range of 300 m/s and 400 m/s.

7. The vertical shaker test resulted in a fundamental frequency of 10.8 cps and peak vertical responses of about 0.6 μm/t. This frequency is about the same as found for the FVT-1 test but surprisingly the displacements are about 60 % of those measured in the FVT-1 test. It is surprising that the backfill has a significant effect for the vertical excitation test.

8. The predicted vertical response is similar in magnitude and frequency with the measured data but the shape of the amplitude - frequency curve is quite different.

References

1. H. T. Tang, "Large Scale Soil Structure Interaction Report," Electric Power Research Institute, Report NP-5513-SR, 1987.

2. C.A. Miller, C.J. Costantino, and J. McClean, "Prediction of the Response of the Hualien Quarter Scale Model Containment Structure for the Forced Vibration Tests Before Backfill," The City College of New York for U.S. Nuclear Regulatory Commission on Contract No. NRC-04-92-049, April 1993.

3. C.A. Miller, C.J. Costantino, J. McClean, and C.J. Higgins,"Hualien Consortium EOC/TMC Meeting November 2-3, 1993," The City College of New York for U.S. Nuclear Regulatory Commission on Contract No. NRC-04-92-049, November 1993.

4. "Forced Vibration Test of Hualien Large Scale SSI Model ; Part I Before Backfill," TEPCO, January 1993.

5. "Status Report of the Forced Vibration Tests (Before Backfill & After Backfill)," TEPCO, November 1993.

6. "Concrete and Rebar Properties of Hualien Containment Model," Taiwan Power Company, December 31, 1992.

7. J.Xu, A.J. Philippacopoulas, C.A. Miller, and C.J. Costantino, "CARES (Computer Analysis for Rapid Evaluation of Structures) Version 1.0," NUREG/CR-52241, Brookhaven National Laboratory, July 1990.

8. "Seismic Analysis of Safety-Related Nuclear Structures and Commentary on Standard for Seismic Analysis of Safety-Related Nuclear Structures," Standard 4-86, American Society of Civil Engineers, September 1986.

9. E. Kausel, and R. Ushijima, "Vertical and Torsional Stiffness of Cylindrical Footings," Publication No. R79-6 MIT, February 1979.

10. Y.O. Beredugo, and M. Novak, "Coupled Horizontal and Rocking Vibration of Embedded Footings," Canadian Geotechnical Journal, 1972.

11. A. Veletsos, and B. Verbic, " Vibration of Viscoelastic Foundations," Rice University, April 1973.

Appendix A

MEASURED DATA

Page Numbers

MEASUREMENT LOCATION	SHAKER LOCATION AND DIRECTION				
	ROOF NS	ROOF EW	1st FLR NS	1st FLR EW	1st FLR U D
ROOF	A.2	A.5	A.8	A.11	A.14
MIDHEIGHT	A.3	A.6	A.9	A.12	A.14
FIRST FLOOR	A.4	A.7	A.10	A.13	A.14
SOIL	A.15	A.16	A.17	A.18	A.19

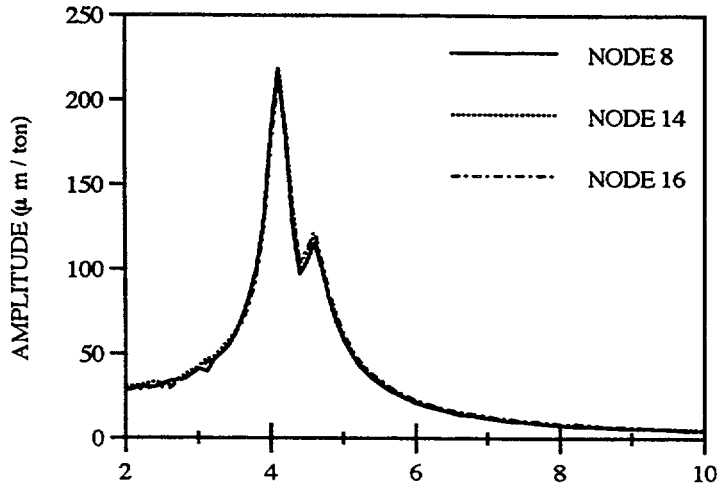

Fig. A.1
NS Measured Response At Roof
Due To NS Shaker Load At Roof

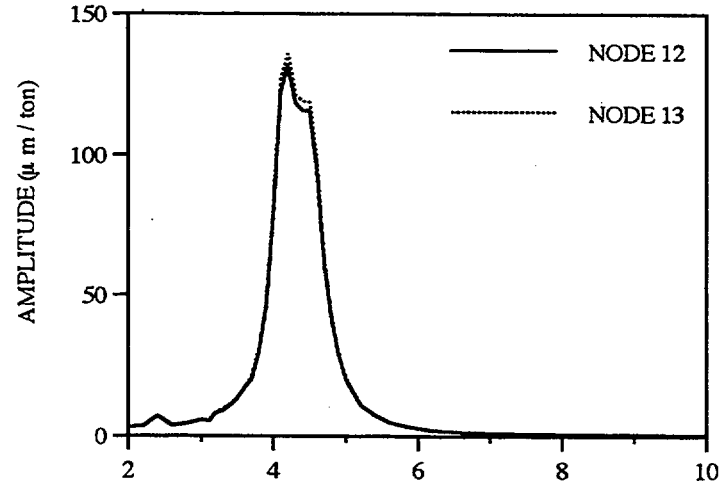

Fig. A.2
EW Measured Response At Roof
Due to NS Shaker Load At Roof

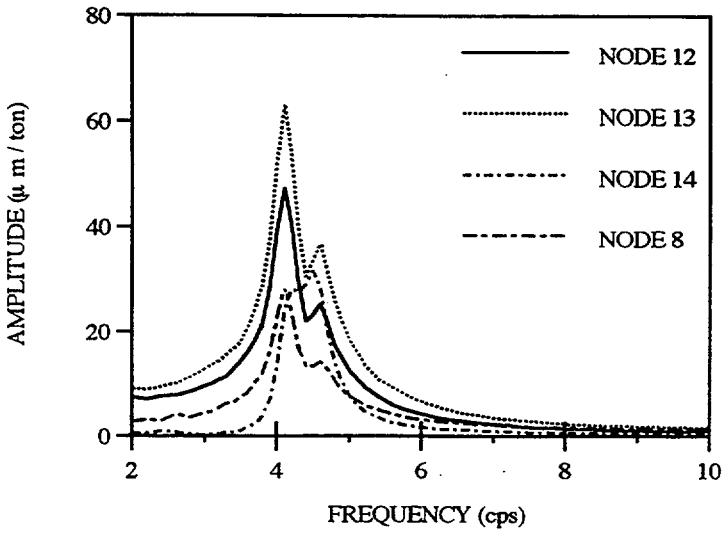

Fig. A.3
UD Measured Response At Roof
Due To NS Shaker Load At Roof

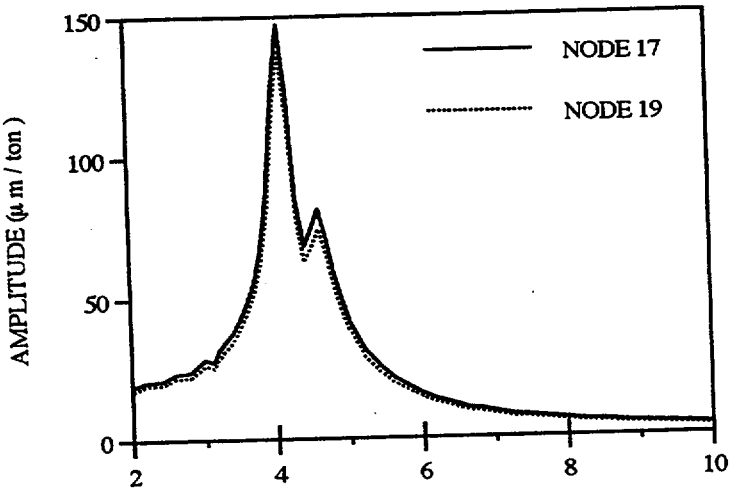

Fig. A.4
NS Measured Response At Midheight
Due TO NS Shaker Load At Roof

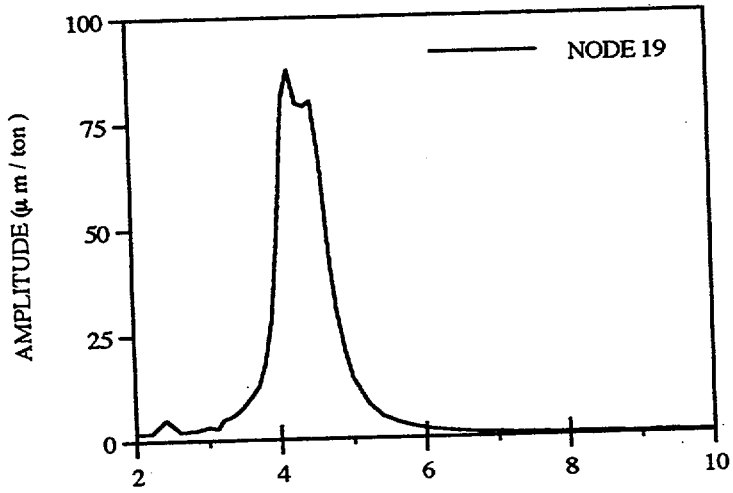

Fig. A.5
EW Measured Response At Midheight
Due To NS Shaker Load At Roof

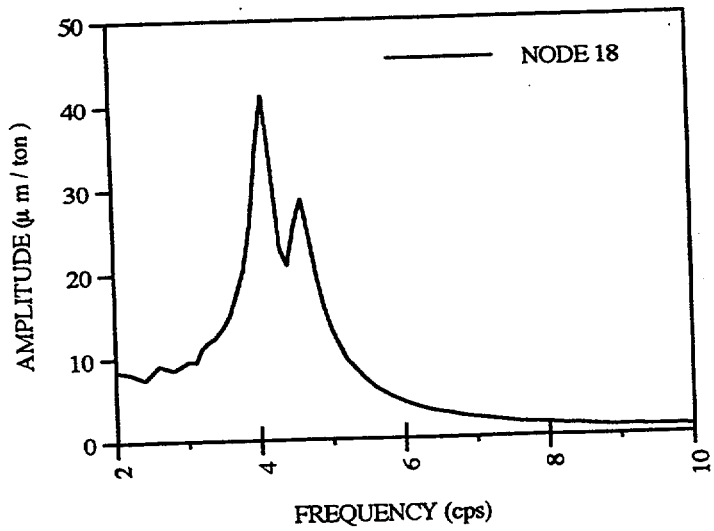

Fig. A.6
UD Measured Response At Midheight
Due To NS Shaker Load At Roof

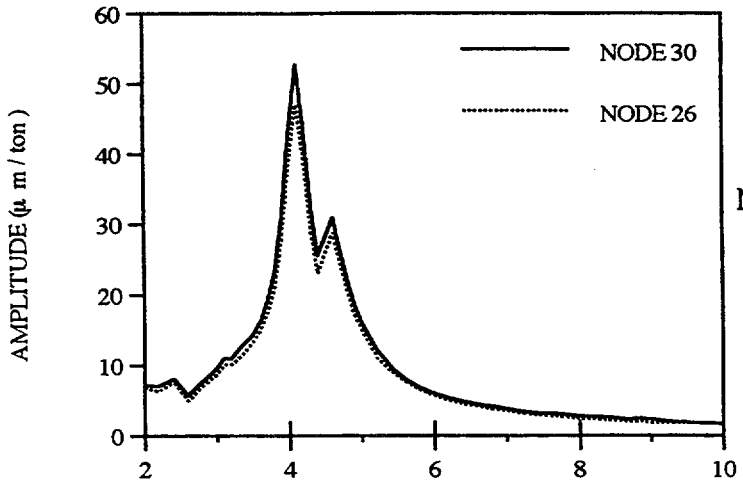

Fig. A.7
NS Measured Response At First Floor
Due To NS Shaker Load At Roof

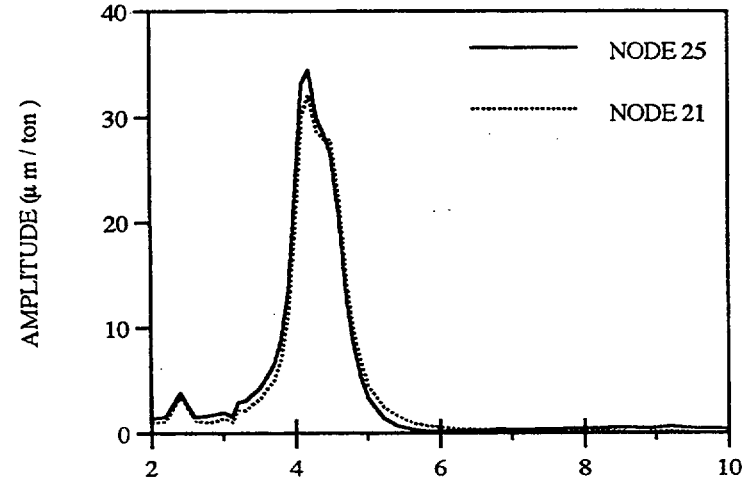

Fig. A.8
EW Measured Response At First Floor
Due To NS Shaker Load At Roof

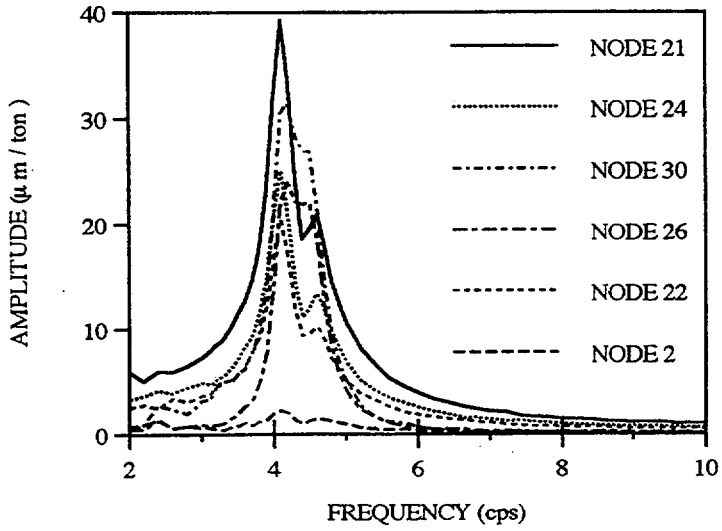

Fig. A. 9
UD Measured Response At First Floor
Due To NS Shaker Load At Roof

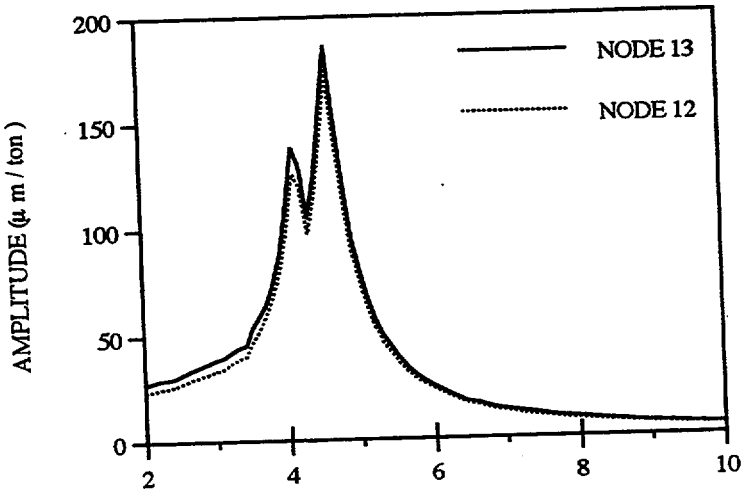

Fig. A.10
EW Measured Response At Roof
Due To EW Shaker Load At Roof

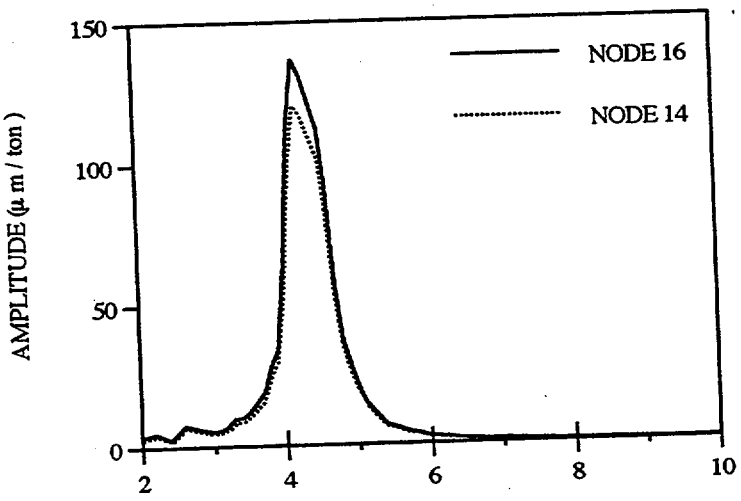

Fig. A.11
NS Measured Response At Roof
Due To EW Shaker Load At Roof

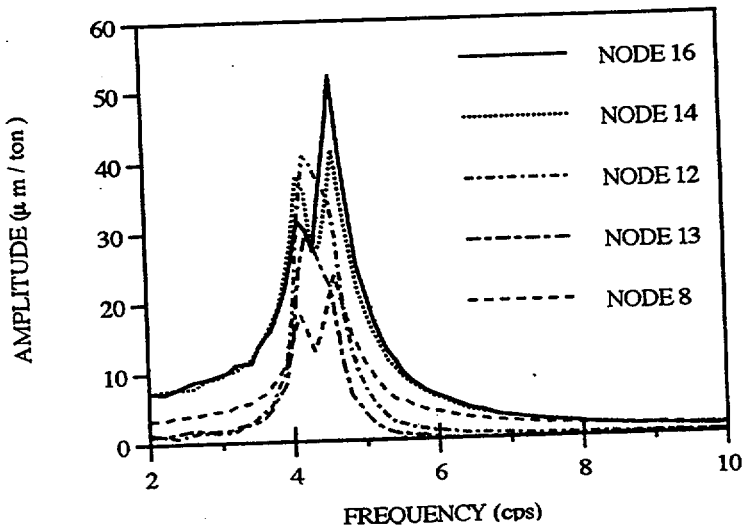

Fig. A.12
UD Measured Response At Roof
Due To EW Shaker Load At Roof

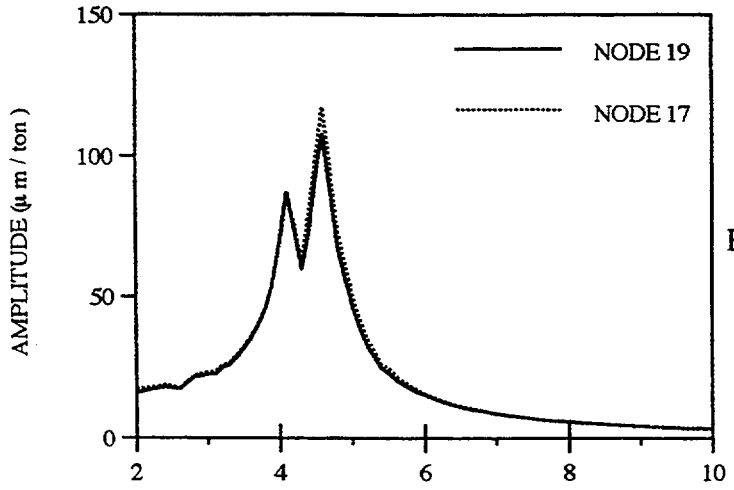

Fig. A.13
EW Measured Response At Midheight
Due To EW Shaker Load At Roof

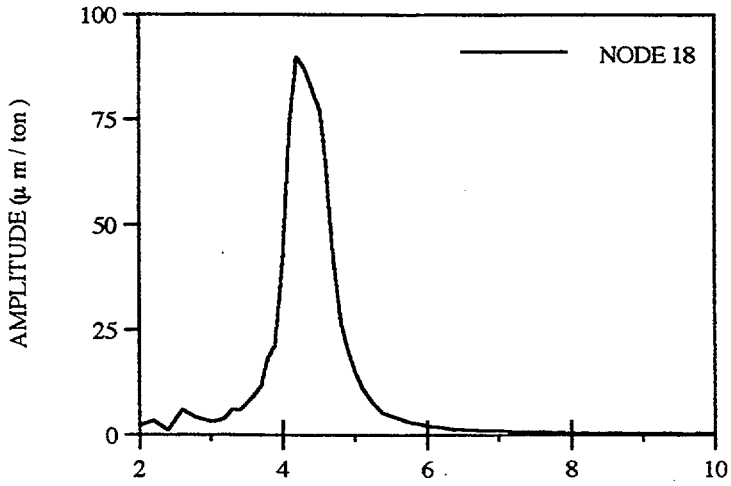

Fig. A.14
NS Measured Response At Midheight
Due To EW Shaker Load At Roof

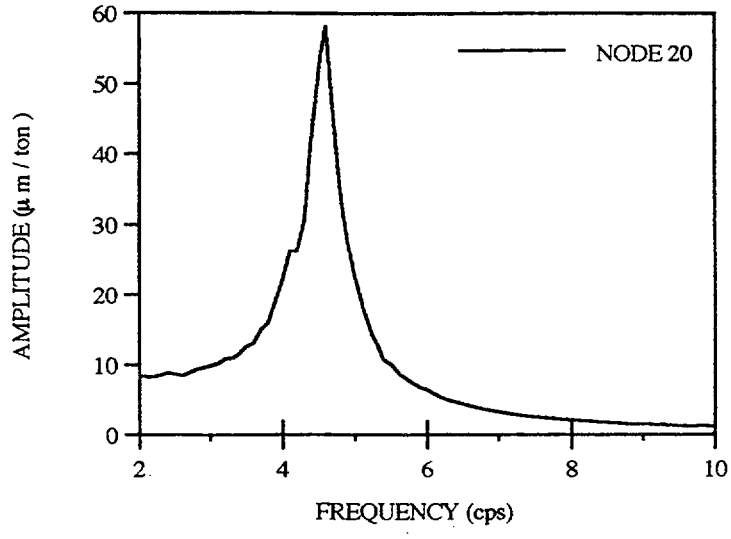

Fig. A.15
UD Measured Response At Midheight
Due To EW Shaker Load At Roof

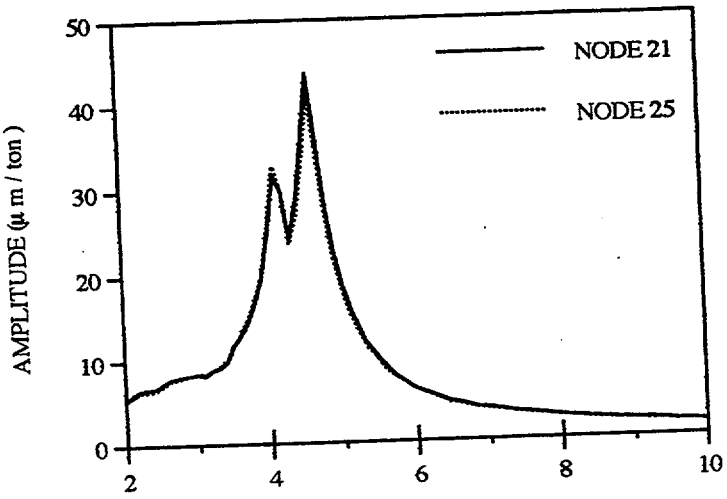

Fig. A.16
EW Measured Response At First Floor
Due To EW Shaker Load At Roof

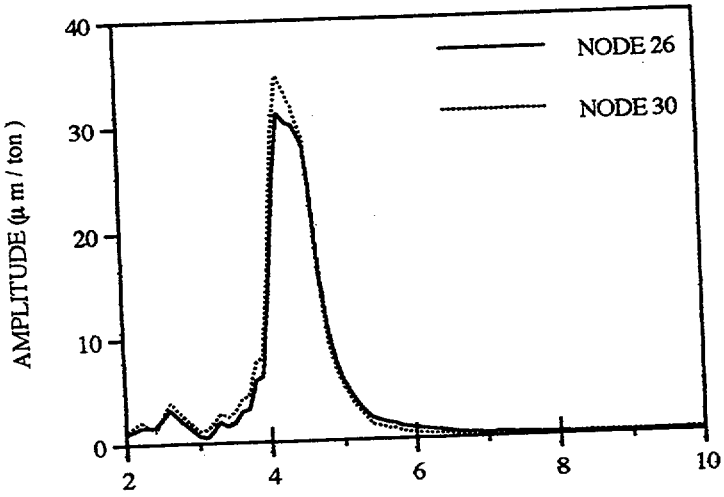

Fig. A.17
NS Measured Response At First Floor
Due To EW Shaker Load At Roof

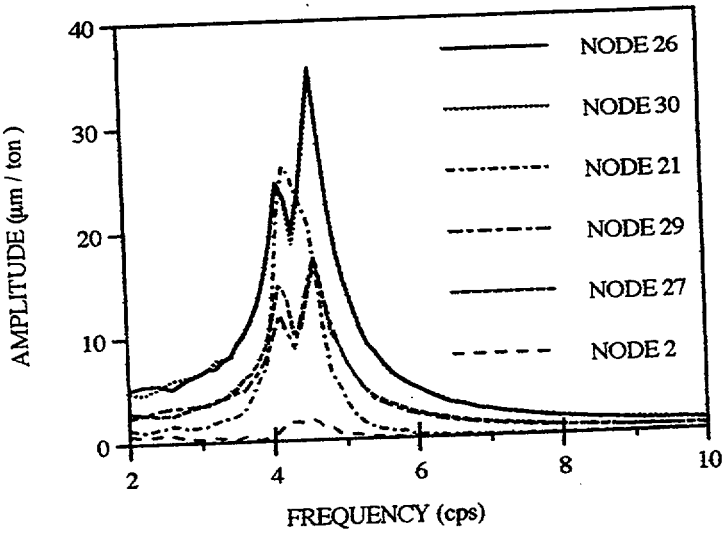

Fig. A.18
UD Measured Response At First Floor
Due To EW Shaker Load At Roof

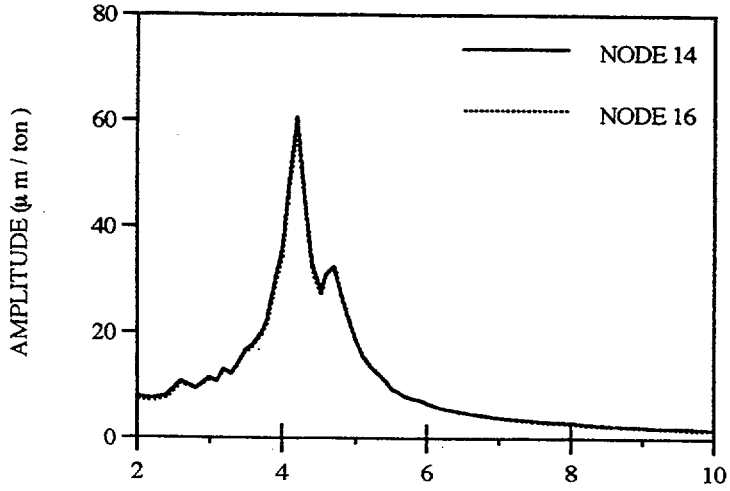

Fig. A.19
NS Measured Response At Roof
Due To NS Shaker Load At First Floor

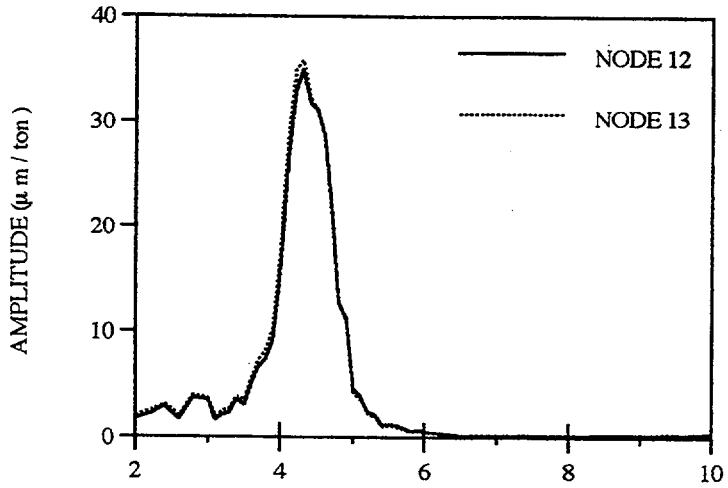

Fig. A.20
EW Measured Response At Roof
Due To NS Shaker Load At First Floor

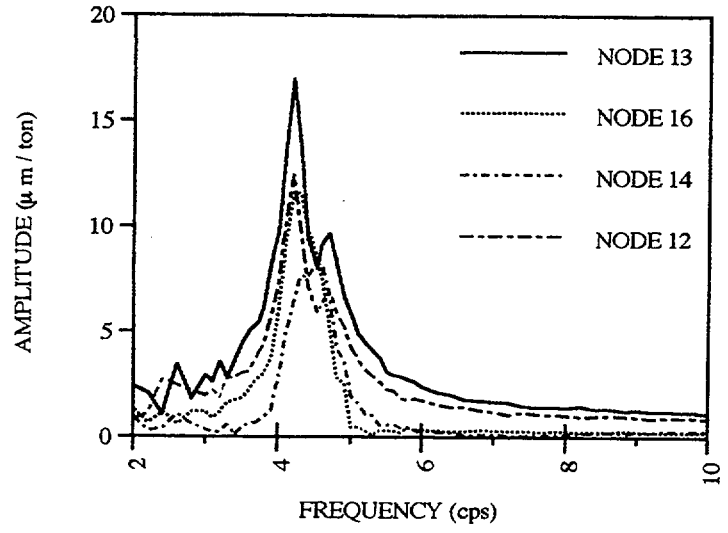

Fig. A.21
UD Measured Response At Roof
Due To NS Shaker Load At First Floor

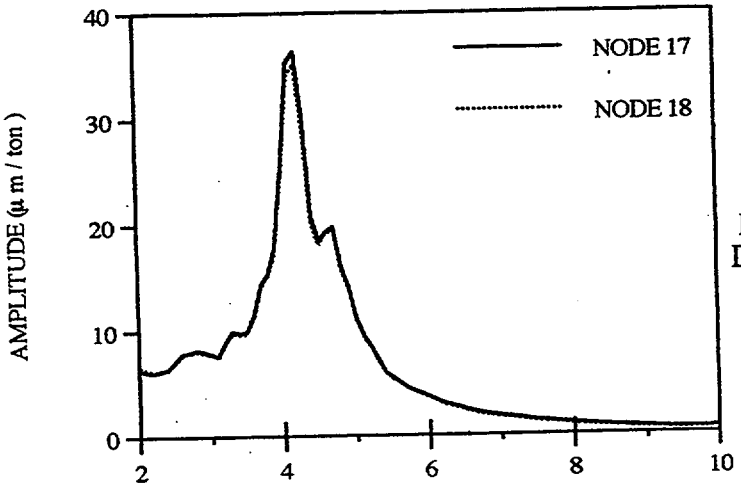

Fig. A.22
NS Measured Response At Midheight
Due To NS Shaker Load At First Floor

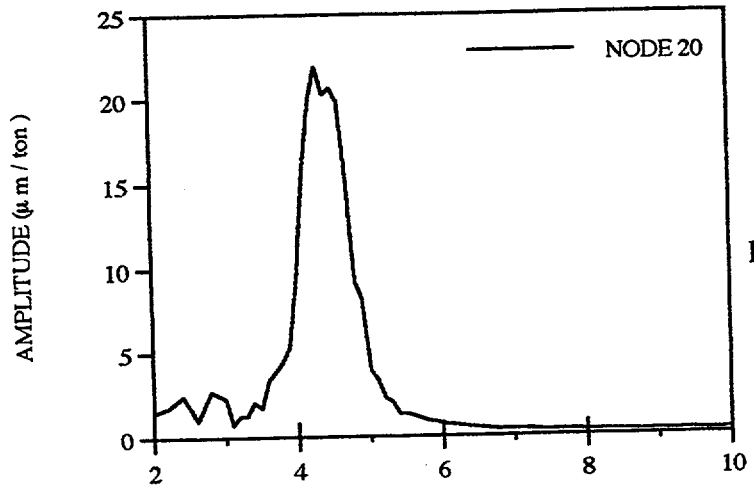

Fig. A.23
EW Measured Response At Midheight
Due To NS Shaker Load At First Floor

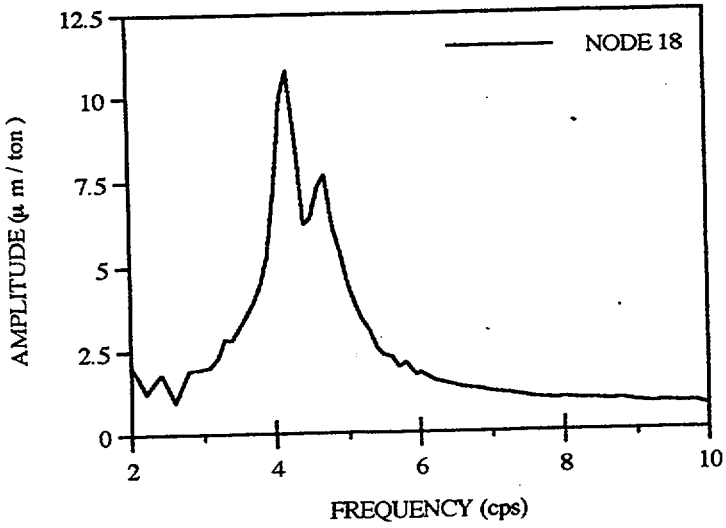

Fig. A.24
UD Measured Response At Midheight
Due To NS Shaker Load At First Floor

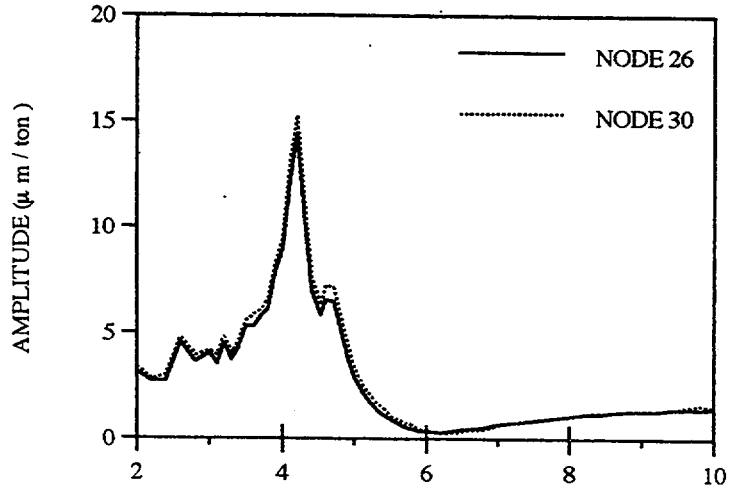

Fig. A.25
NS Measured Response At First Floor
Due To NS Shaker Load At First Floor

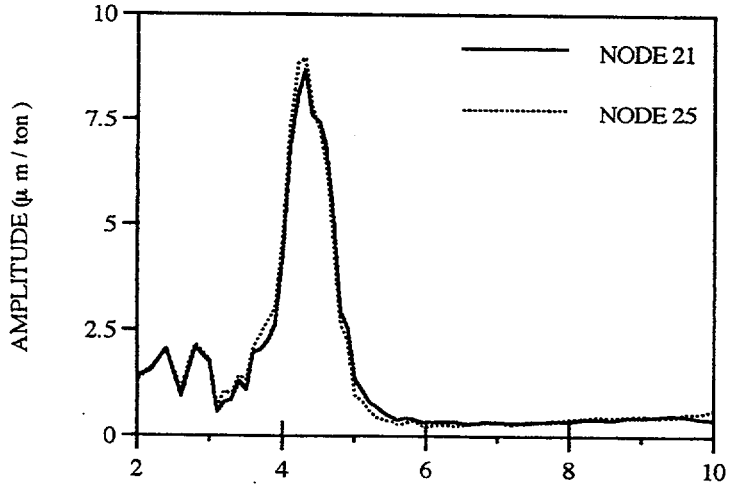

Fig. A.26
EW Measured Response At First Floor
Due To NS Shaker Load At First Floor

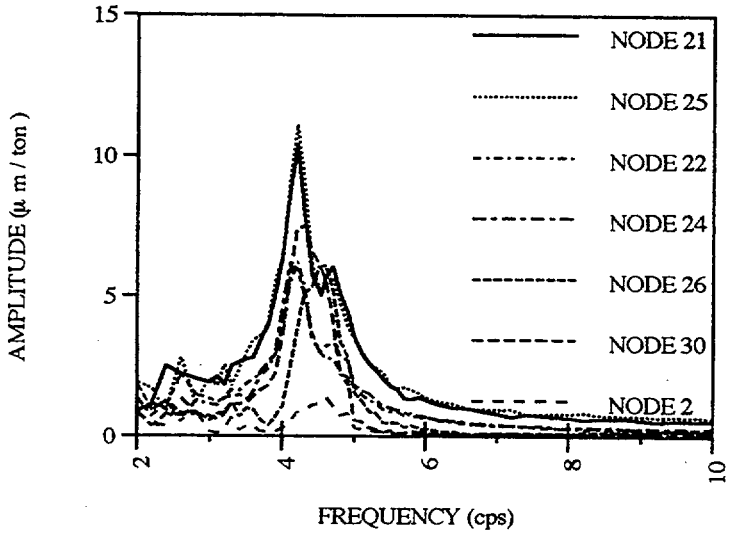

Fig. A.27
UD Measured Response At First Floor
Due To NS Shaker Load At First Floor

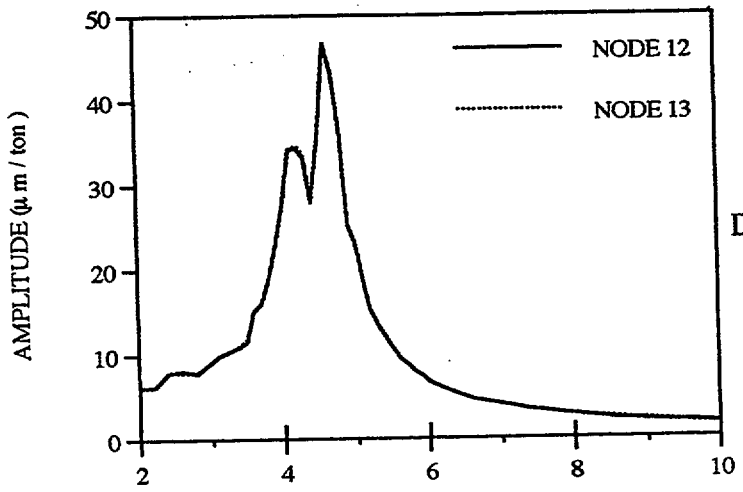

Fig. A.28
EW Measured Response At Roof
Due To EW Shaker Load At First Floor

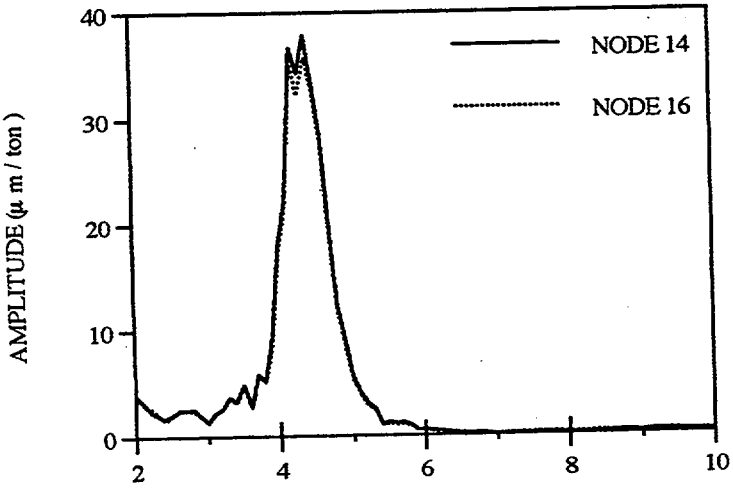

Fig. A.29
NS Measured Response At Roof
Due To EW Shaker Load At First Floor

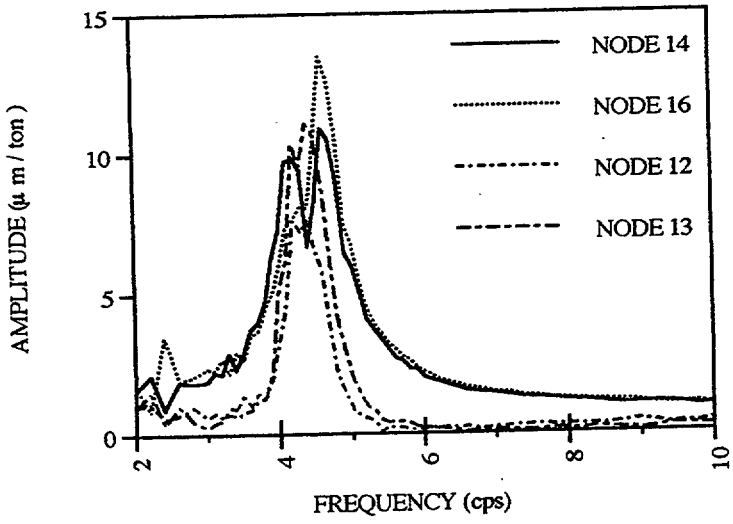

Fig. A.30
UD Measured Response At Roof
Due To EW Shaker Load At First Floor

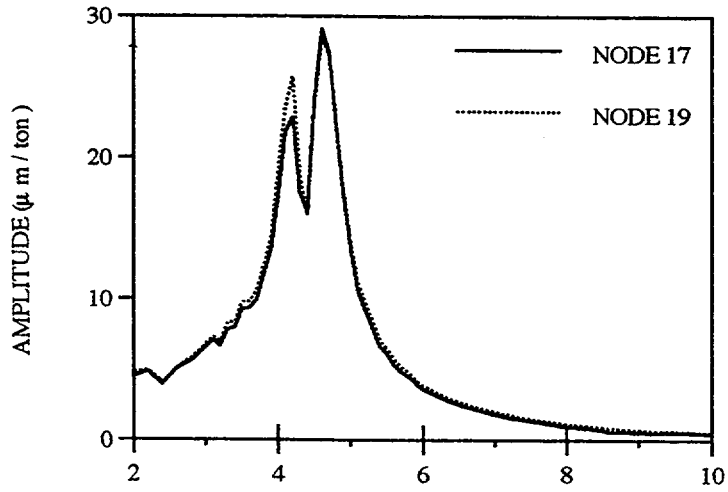

Fig. A.31
EW Measured Response At Midheight
Due To EW Shaker Load At First Floor

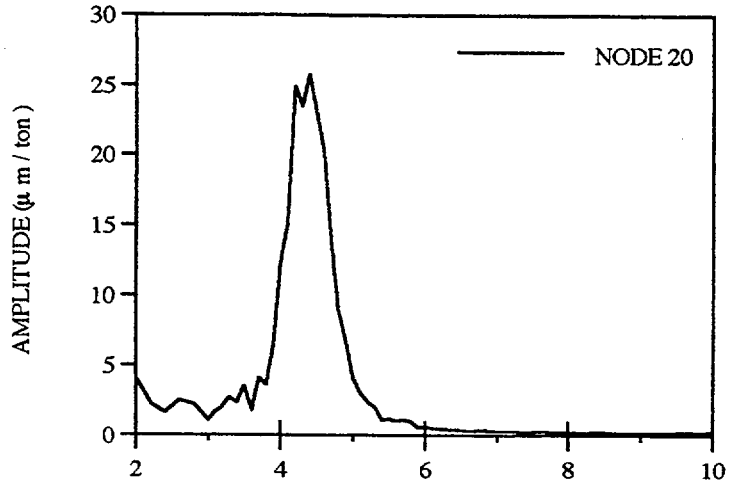

Fig. A.32
NS Measured response At Midheight
Due To EW Shaker Load At First Floor

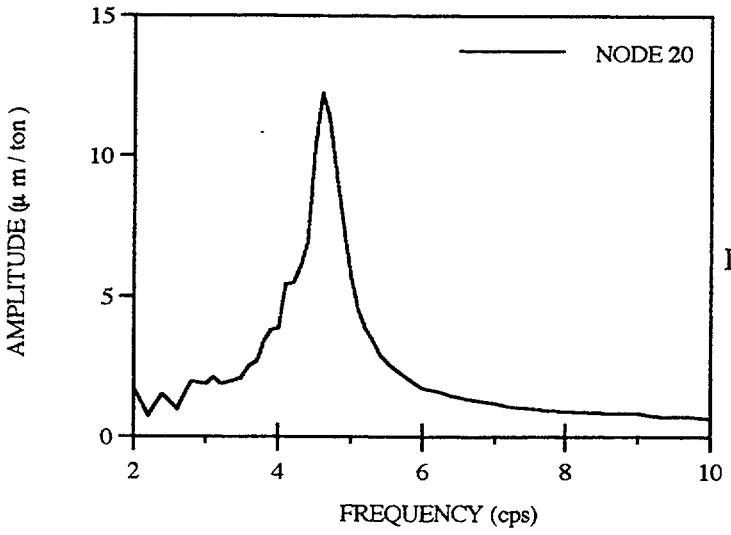

Fig. A.33
UD Measured Response At Midheight
Due To EW Shaker Load At First Floor

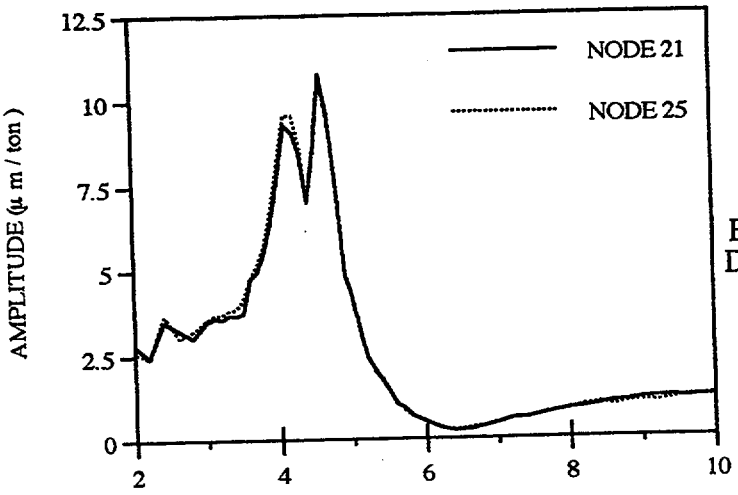

Fig. A.34
EW Measured Response At First Floor
Due To EW Shaker Load At First Floor

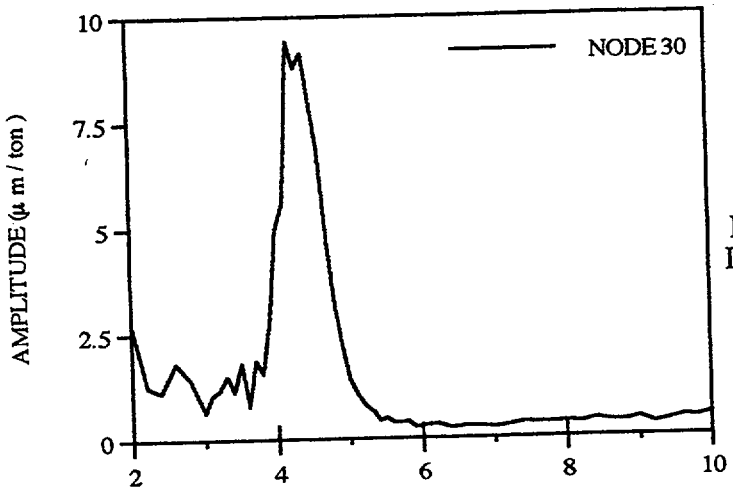

Fig. A.35
NS Measured Response At First Floor
Due To EW Shaker Load At First Floor

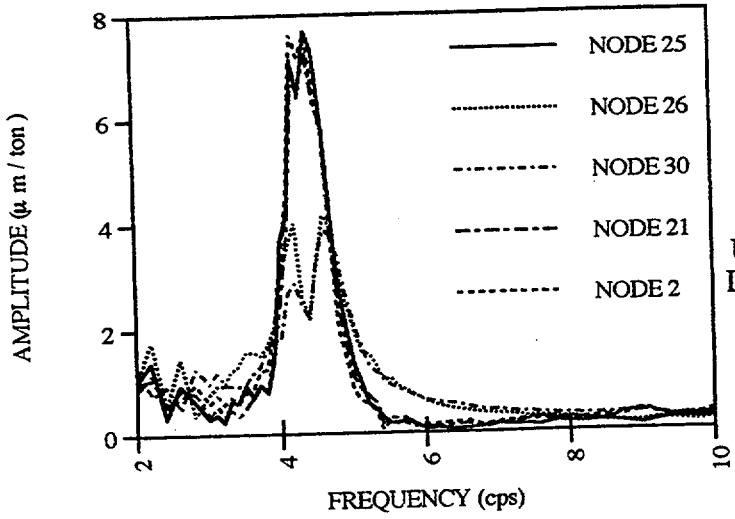

Fig. A.36
UD Measured Response At First Floor
Due To EW Shaker Load At First Floor

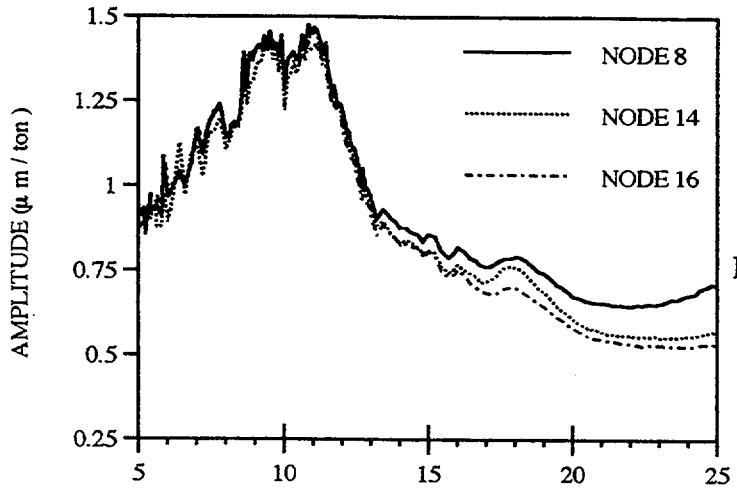

Fig. A.37
UD Measured Response At Roof
Due To UD Shaker Load At First Floor

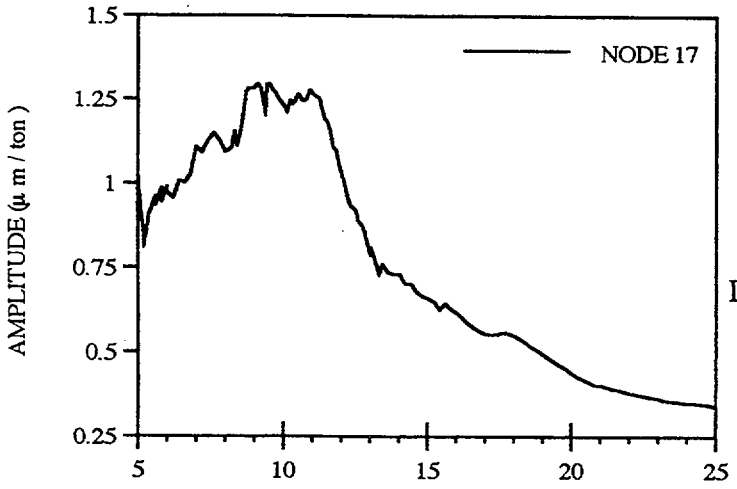

Fig. A.38
UD Measured Response At Midheight
Due To UD Shaker Load At First Floor

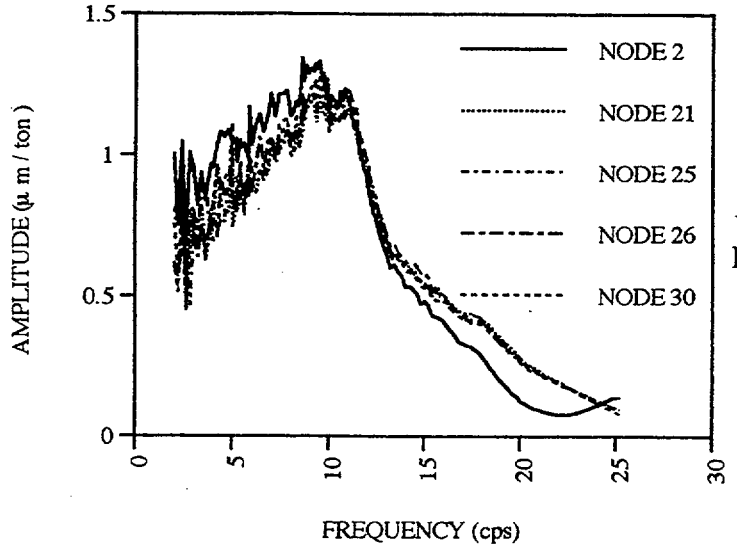

Fig. A.39
UD Measured Response At First Floor
Due To UD Shaker Load At First Floor

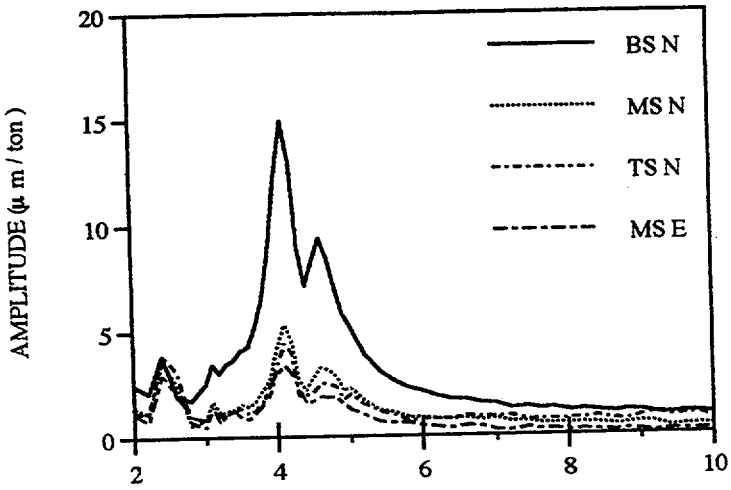

Fig. A.40
NS Measured Response In Soil
Due To NS Shaker Load At Roof

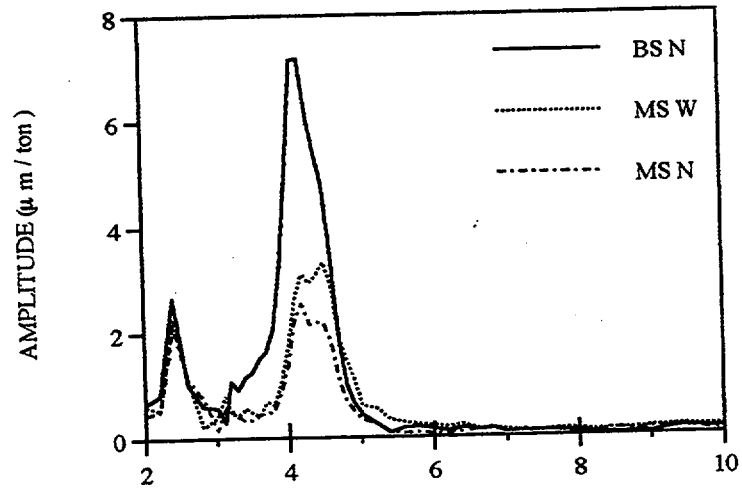

Fig. A.41
EW Measured Response In Soil
Due To NS Shaker Load At Roof

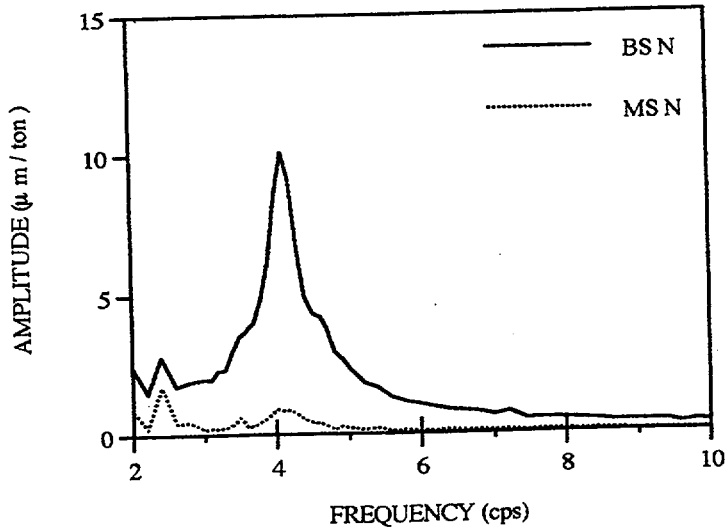

Fig. A.42
UD Measured Response in Soil
Due To NS Shaker Load At Roof

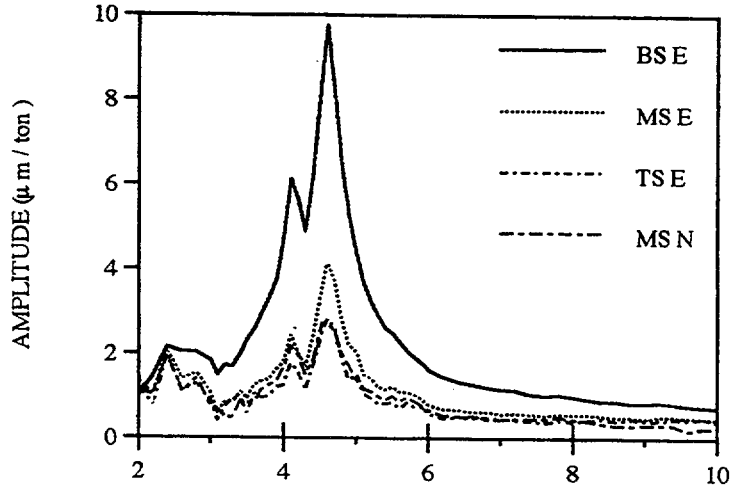

Fig. A.43
EW Measured Response In Soil
Due To EW Shaker Load At Roof

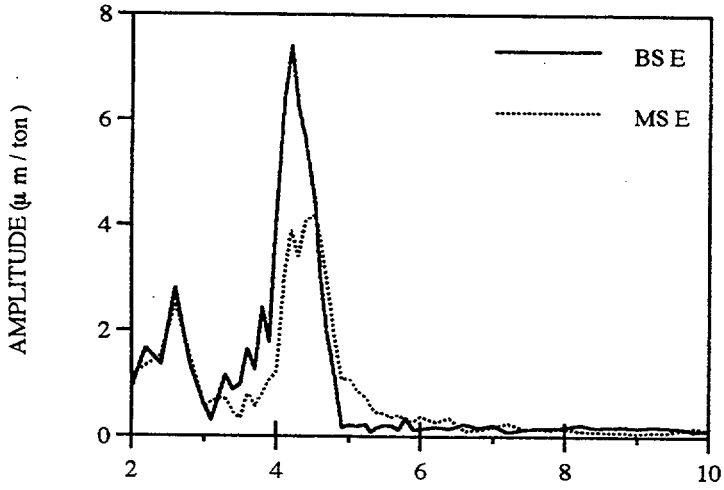

Fig. A.44
NS Measured Response In Soil
Due To EW Shaker Load At Roof

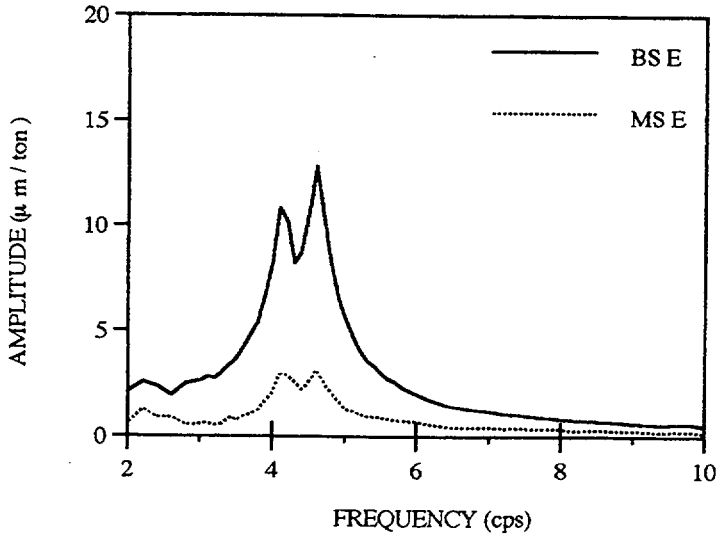

Fig. A.45
UD Measured Response In Soil
Due To EW Shaker Load At Roof

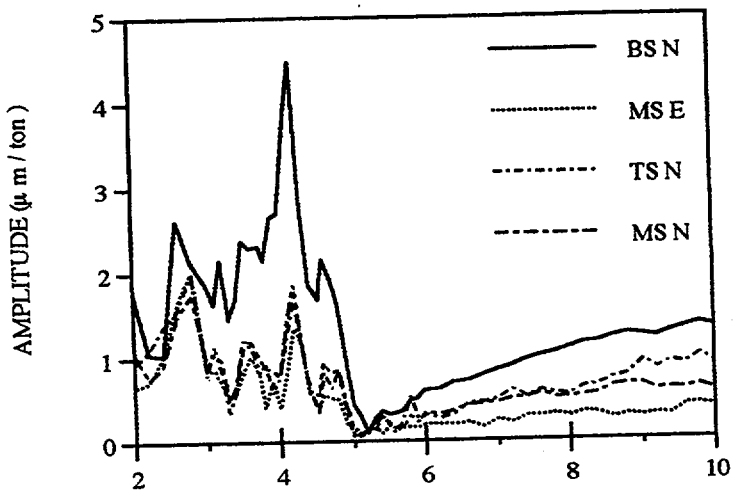

Fig. A.46
NS Measured Response In Soil
Due To NS Shaker Load At First Floor

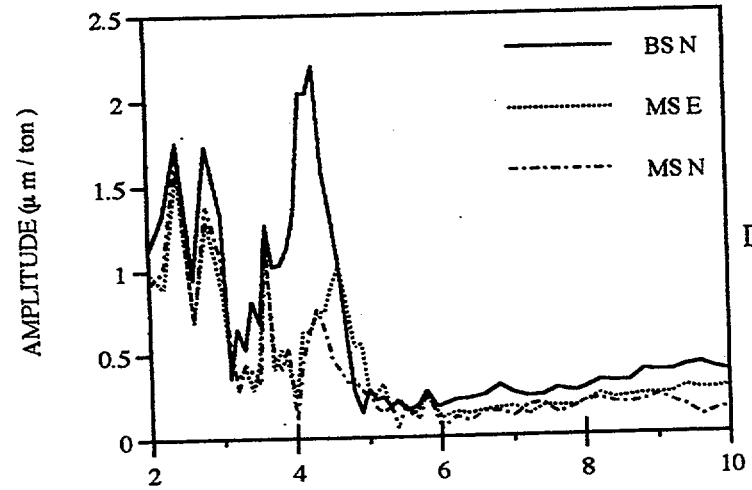

Fig. A.47
EW Measured Response In Soil
Due To NS Shaker Load At First Floor

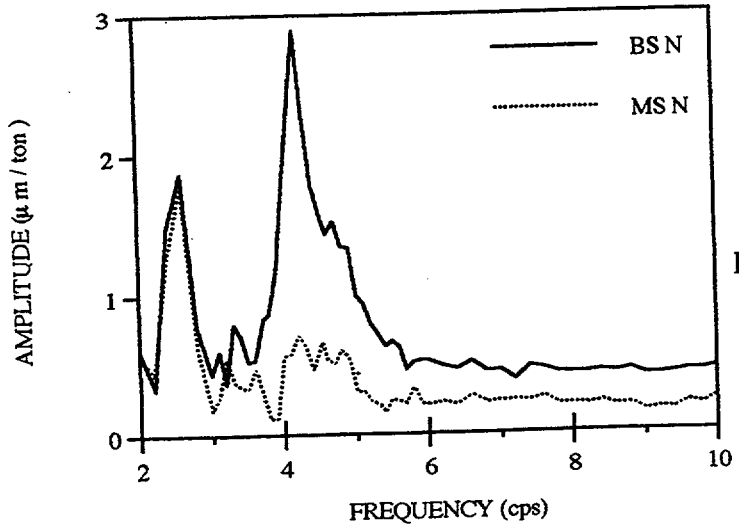

Fig. A.48
UD Measured Response In Soil
Due To NS Shaker Load At First Floor

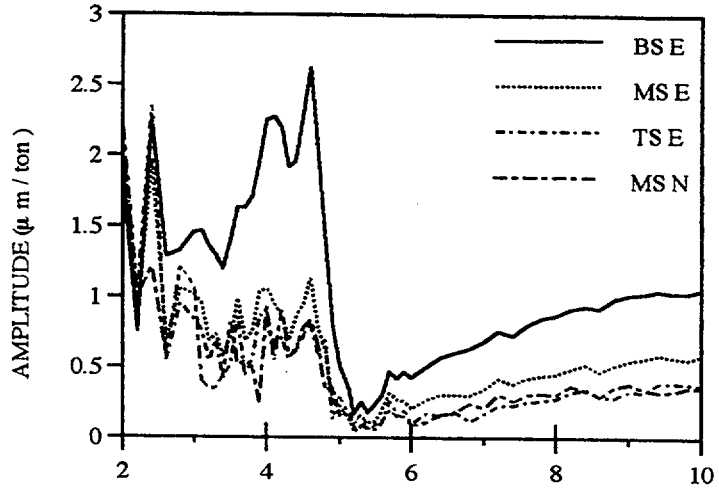

Fig. 49
EW Measured Response In Soil
Due To EW Shaker Load At First Floor

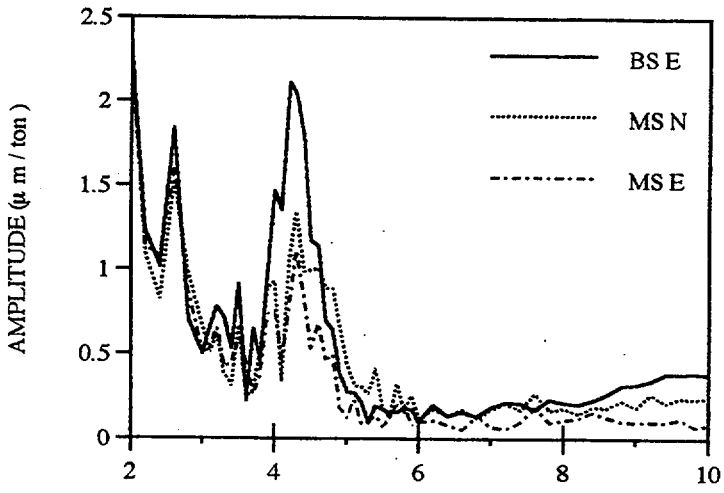

Fig. A.50
NS Measured Response In Soil
Due To EW Shaker Load At First Floor

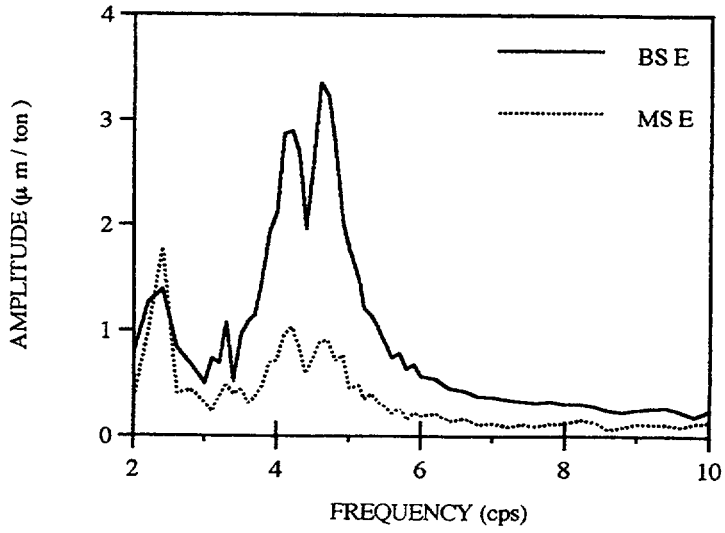

Fig. A.51
UD Measured Response In Soil
Due To EW Shaker Load At First Floor

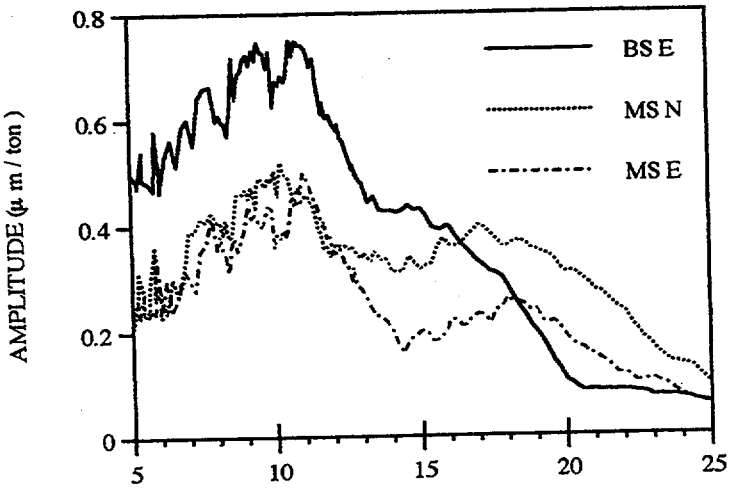

Fig. A.52
UD Measured Response In Soil
Due To UD Shaker Load At First Floor

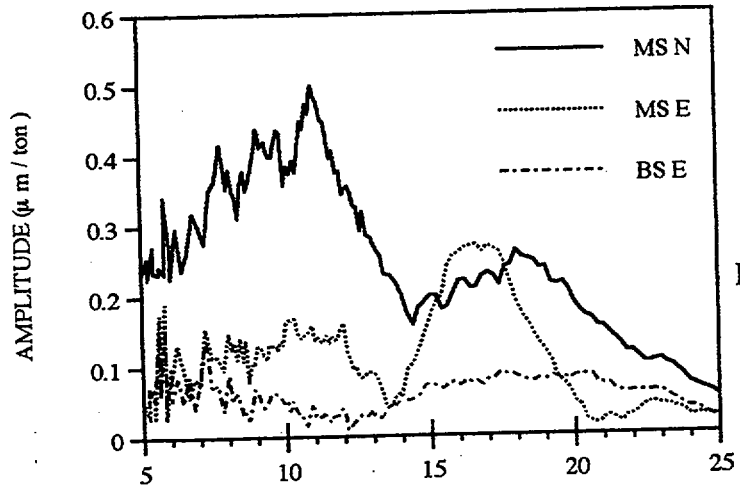

Fig. A.53
NS Measured Response In Soil
Due To UD Shaker Load At First Floor

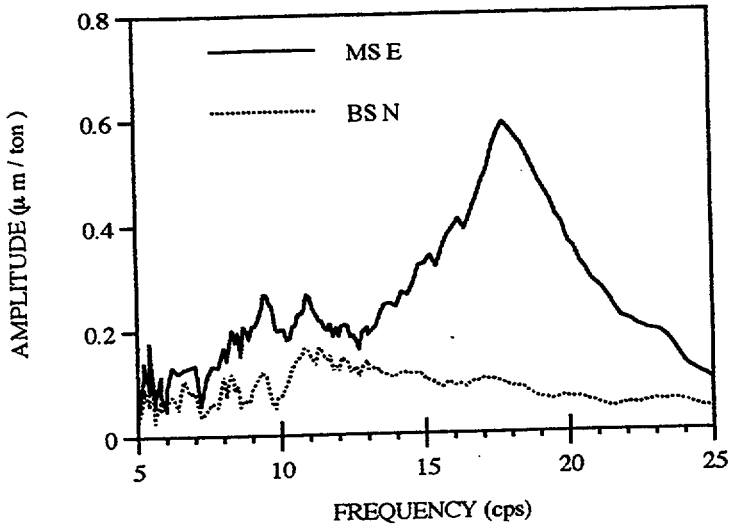

Fig. A.54
EW Measured Response In Soil
Due To UD Shaker Load At First Floor

Appendix B

MEASURED DATA

Page Numbers

MEASUREMENT LOCATION	SHAKER LOCATION AND DIRECTION				
	ROOF NS	ROOF EW	1st FLR NS	1st FLR EW	1st FLR U D
ROOF	B.2	B.5	B.8	B.11	B.14
MIDHEIGHT	B.3	B.6	B.9	B.12	B.14
FIRST FLOOR	B.4	B.7	B.10	B.13	B.14
SOIL	B.15	B.16	B.17	B.18	B.19

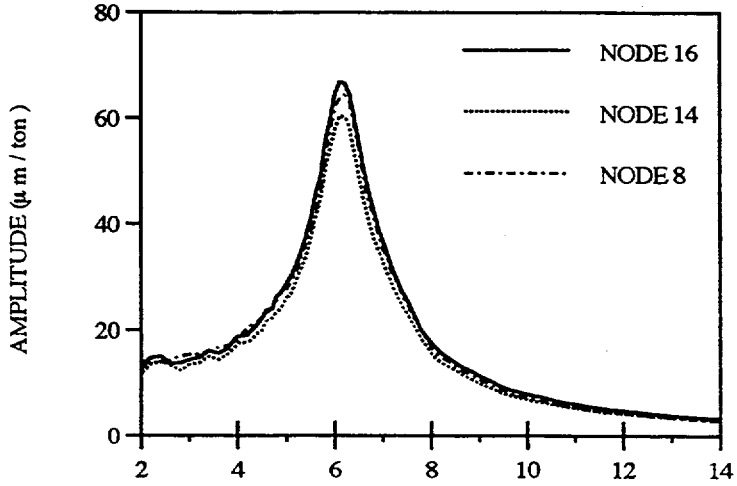

Fig. B.1
NS Measured Response At Roof
Due To NS Shaker Load At Roof

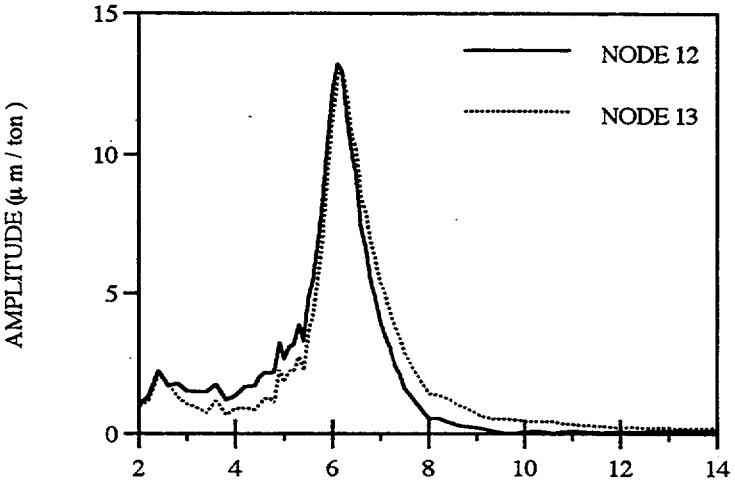

Fig. B.2
EW Measured Response At Roof
Due To NS Shaker Load At Roof

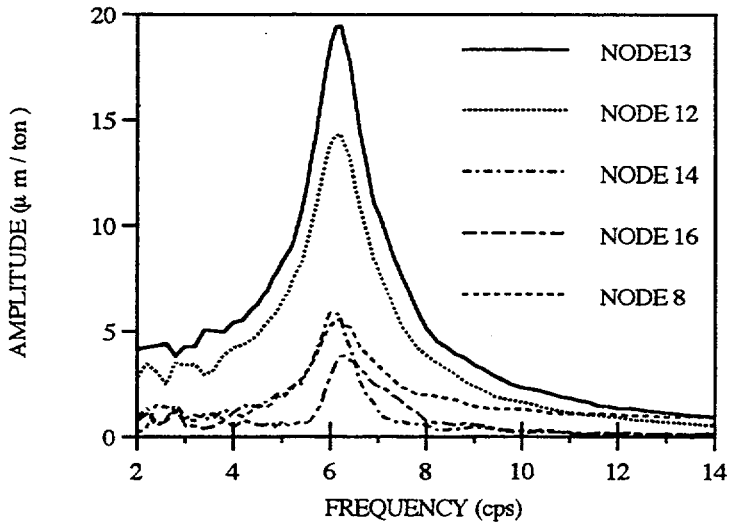

Fig. B.3
UD Measured Response At Roof
Due To NS Shaker Load At Roof

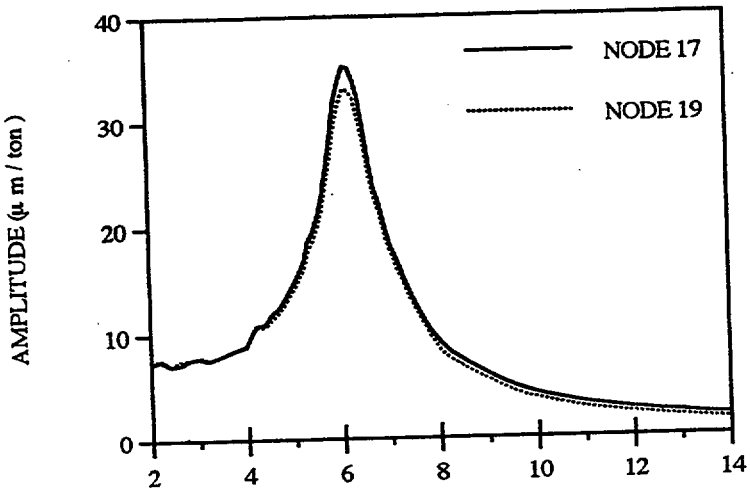

Fig. B.4
NS Measured Response At Midheight
Due To NS Shaker Load At Roof

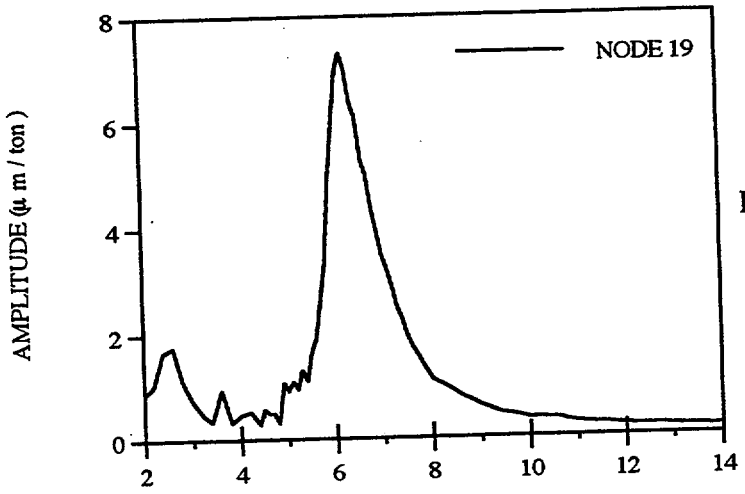

Fig. B.5
EW Measured Response At Midheight
Due To NS Shaker Load At Roof

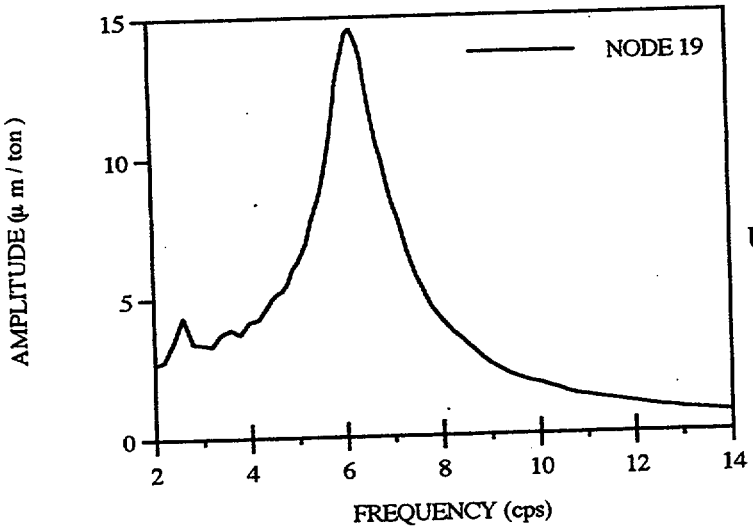

Fig. B.6
UD Measured Response At Midheight
Due To NS Shaker Load At Roof

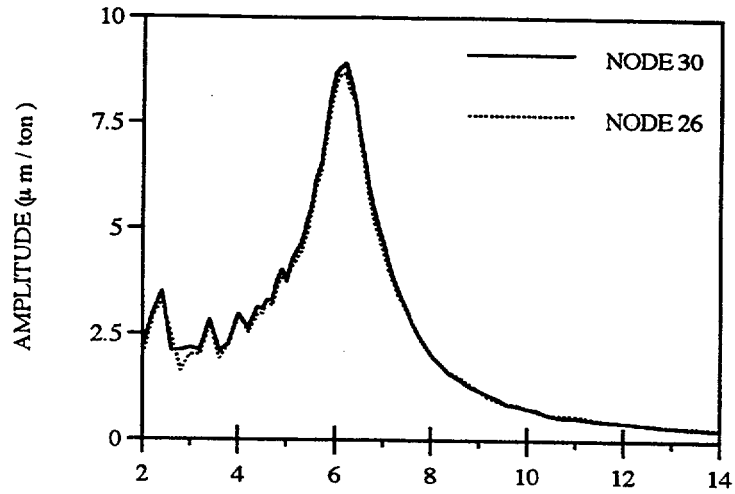

Fig. B.7
NS Measured Response At First Floor
Due To NS Shaker Load At Roof

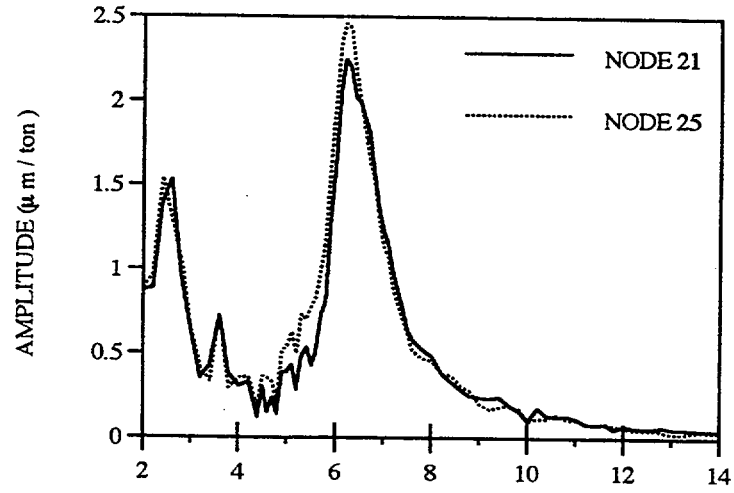

Fig. B.8
EW Measured Response At First Floor
Due To Shaker Load At Roof

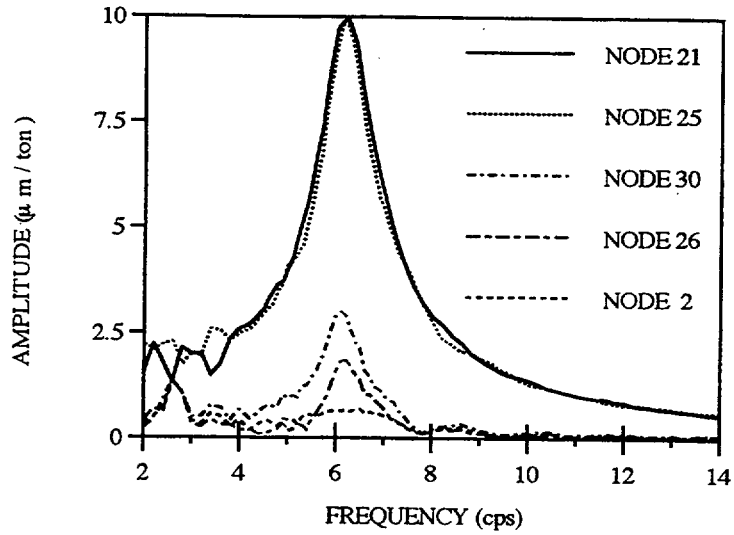

Fig. B.9
UD Measured Response At First Floor
Due To NS Shaker Load At Roof

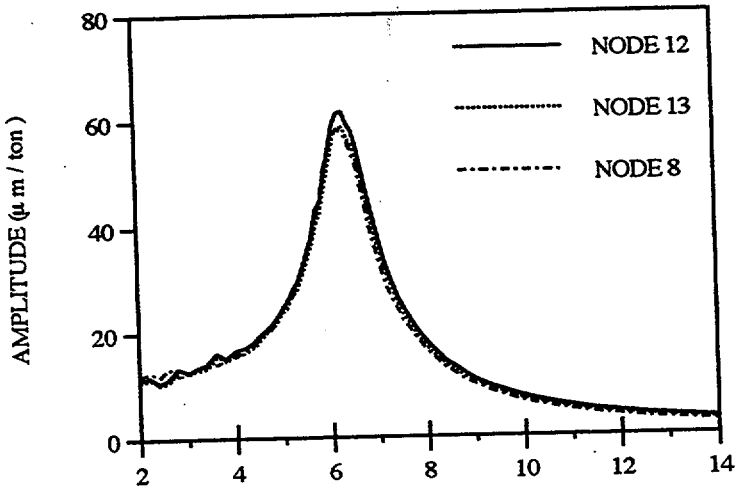

Fig. B.10
EW Measured Response At Roof
Due To EW Shaker Load At Roof

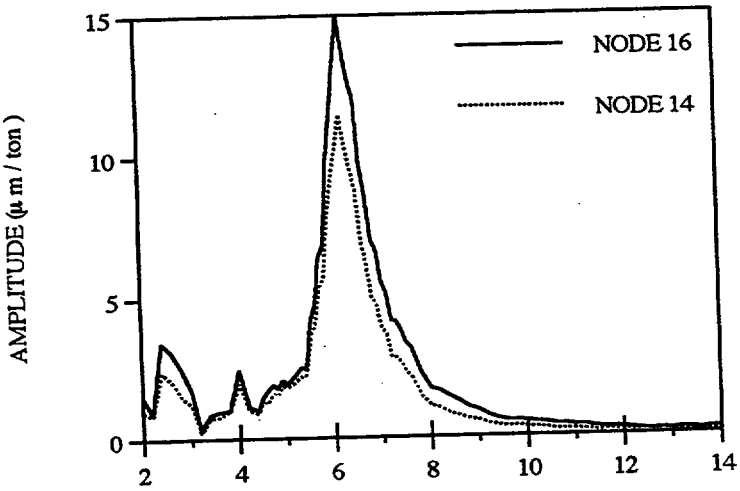

Fig. B.11
NS Measured Response At Roof
Due To EW Shaker Load At Roof

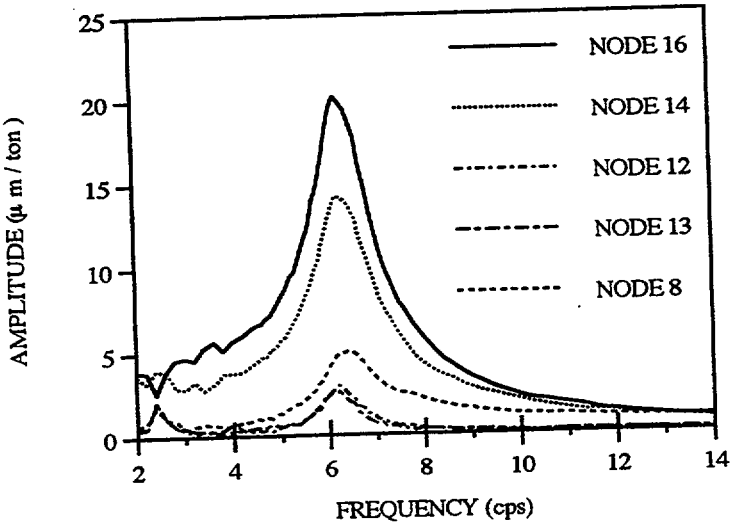

Fig. B.12
UD Measured Response At Roof
Due To EW Shaker Load At Roof

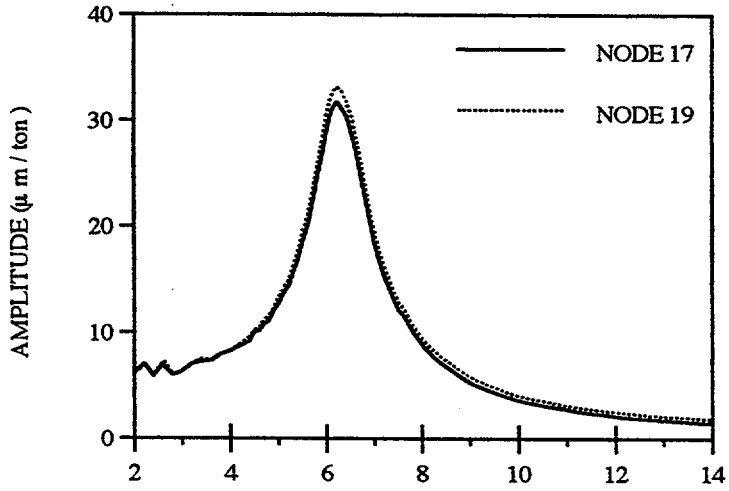

Fig. B.13
EW Measured Response At Midheight
Due To EW Shaker Load At Roof

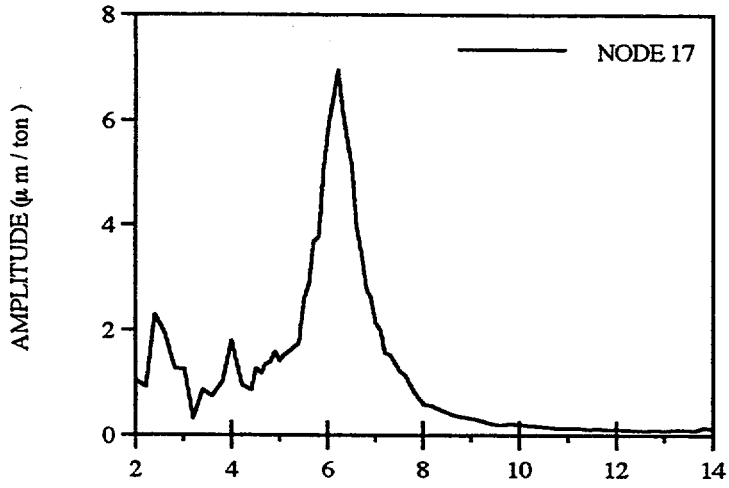

Fig. B.14
NS Measured Response At Midheight
Due To EW Shaker Load At Roof

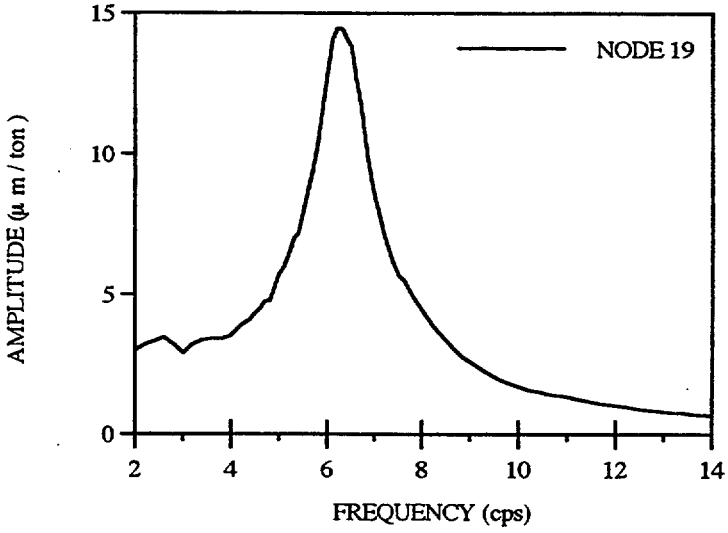

Fig. B.15
UD Measured Response At Midheight
Due To EW Shaker Load At Roof

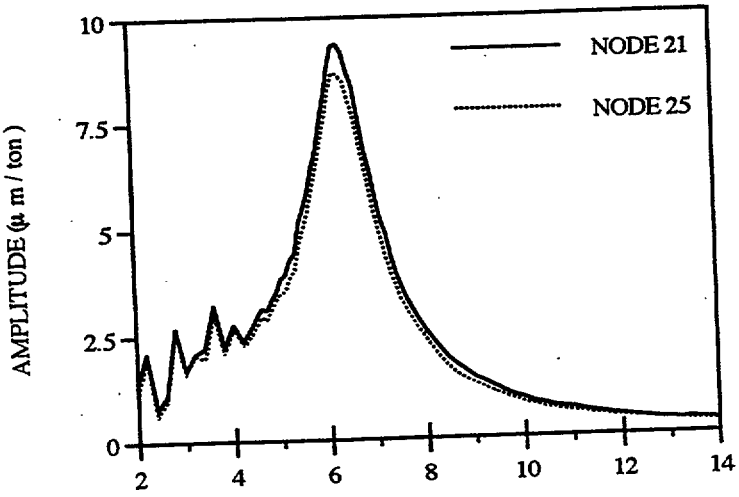

Fig. B.16
EW Measured Response At First Floor
Due To EW Shaker Load At Roof

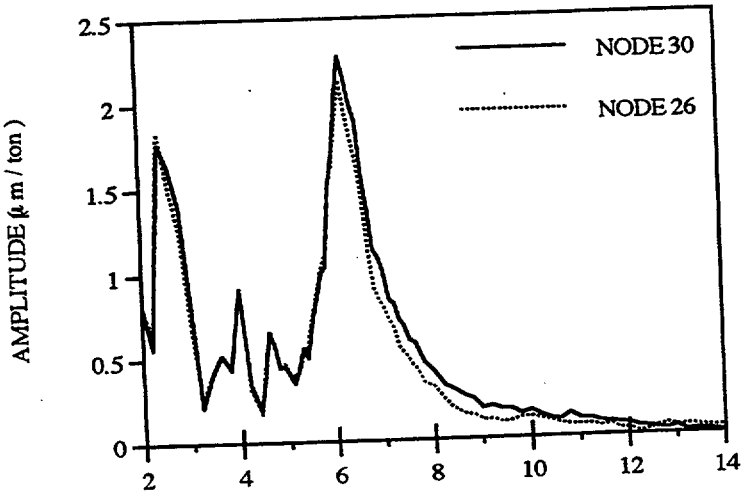

Fig. B.17
NS Measured Response At First Floor
Due To EW Shaker Load At Roof

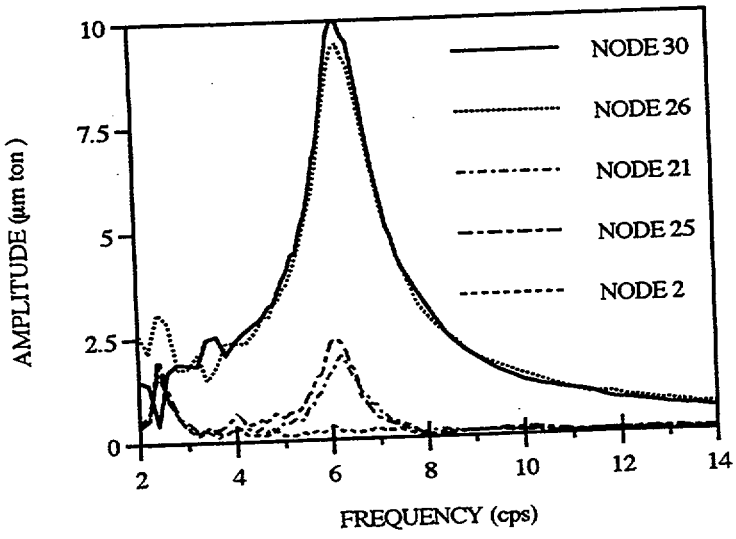

Fig. B.18
UD Measured Response At First Floor
Due To EW Shaker Load At Roof

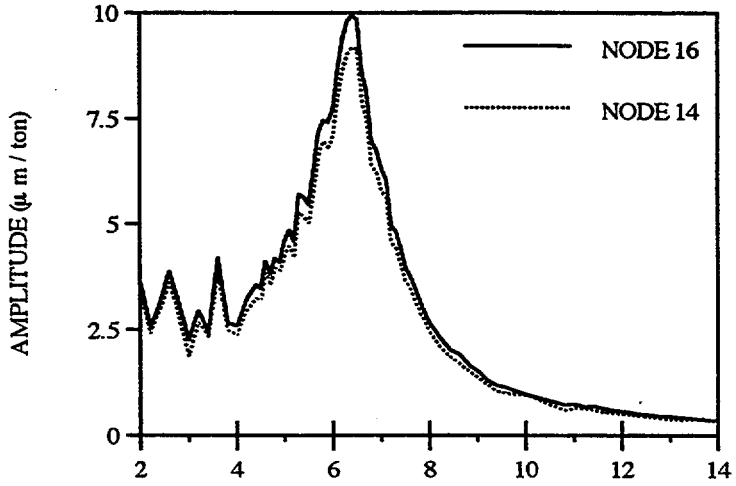

Fig. B.19
NS Measured Response At Roof
Due To NS Shaker Load At First Floor

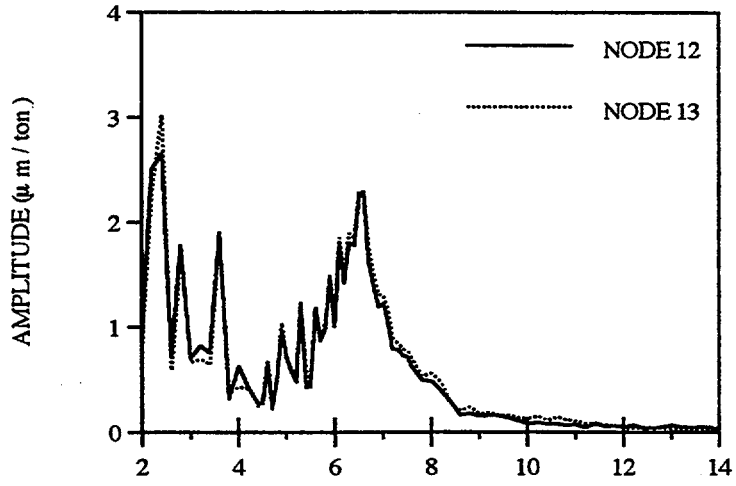

Fig. B.20
EW Measured Response At Roof
Due To NS Shaker Load At First Floor

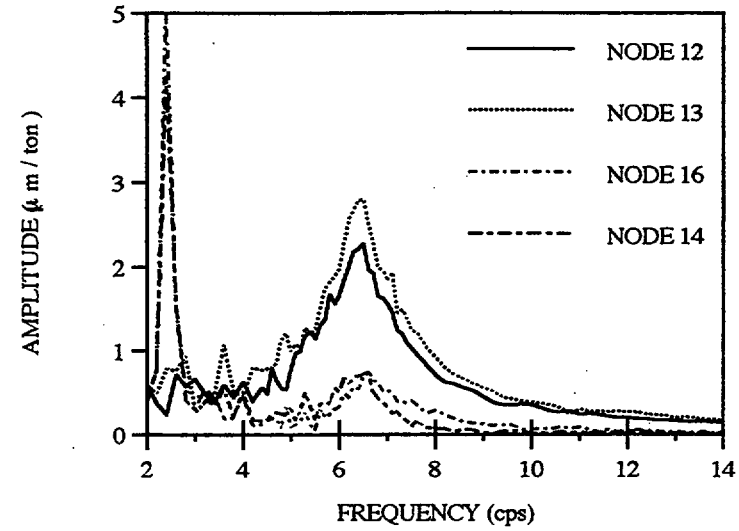

Fig. B.21
UD Measured Response At Roof
Due To NS Shaker Load At First Floor

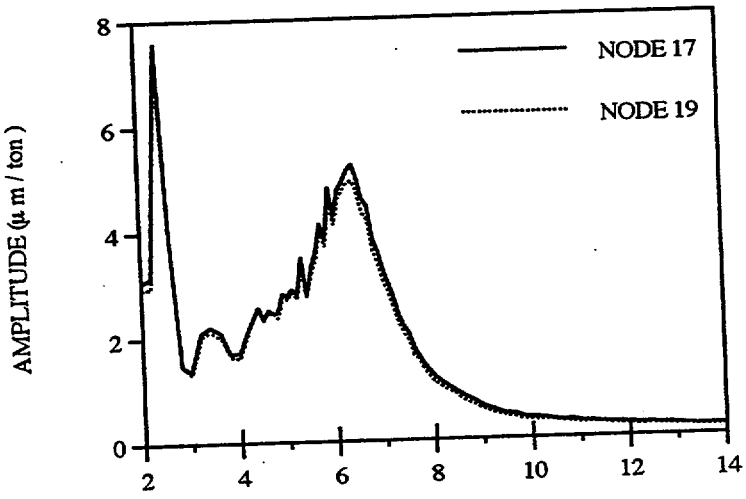

Fig. B.22
NS Measured Response At Midheight
Due To NS Shaker Load At First Floor

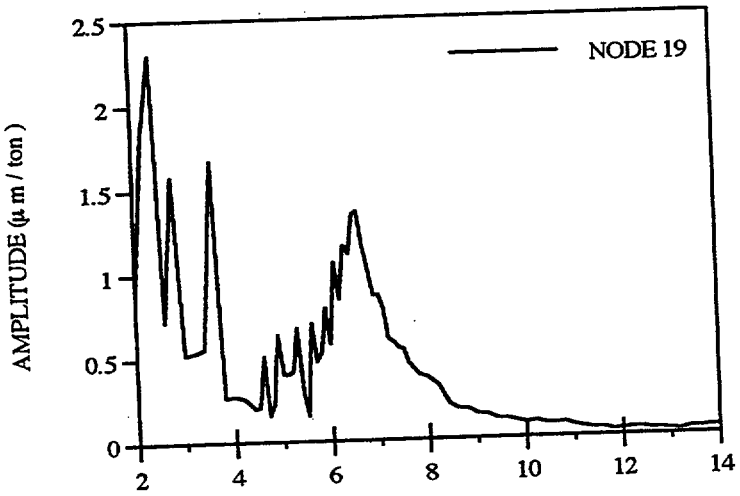

Fig. B.23
EW Measured Response At Midheight
Due To NS Shaker Load At First Floor

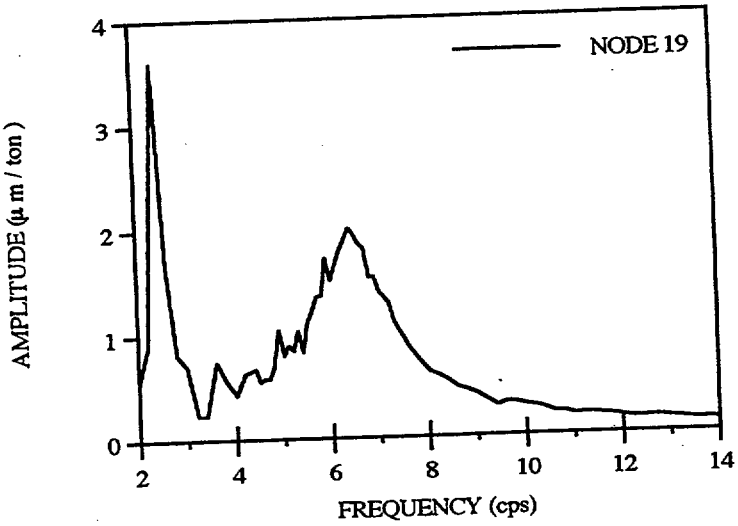

Fig. B.24
UD Measured Response At Midheight
Due To NS Shaker Load At First Floor

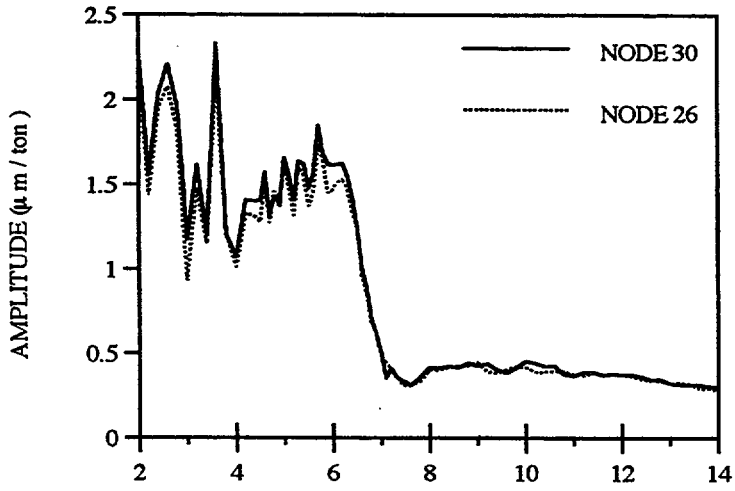

Fig. B.25
NS Measured Response At First Floor
Due To NS Shaker Load At First Floor

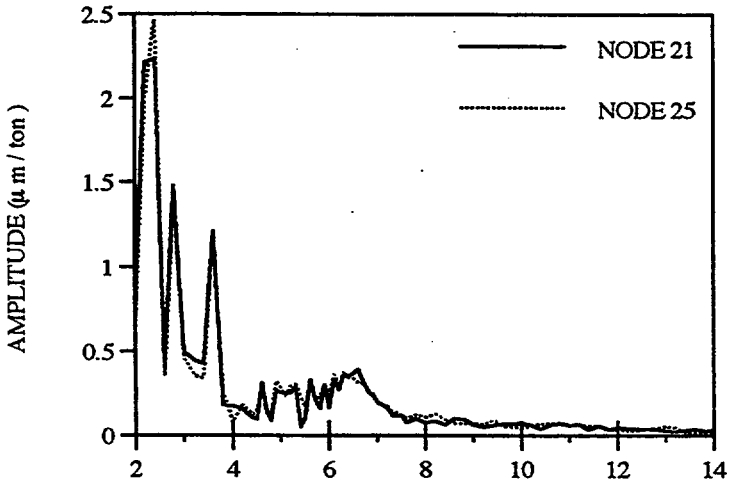

Fig. B.26
EW Measured Response At First Floor
Due To NS Shaker Load At First Floor

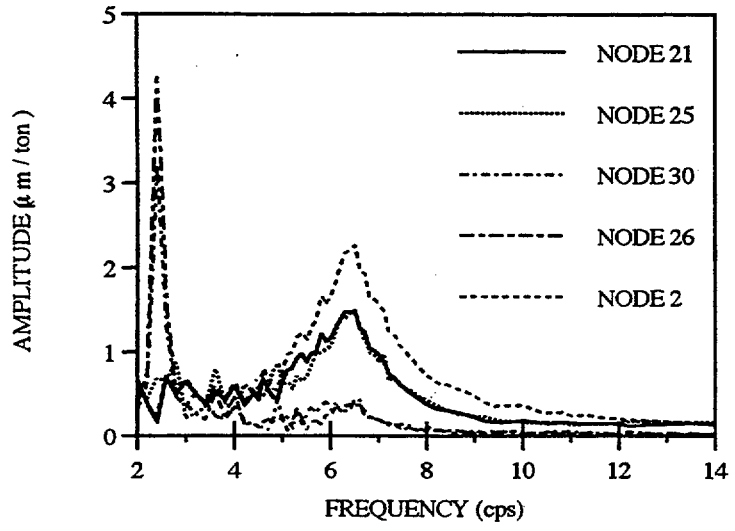

Fig. B.27
UD Measured Response At First Floor
Due To NS Shaker Load At First Floor

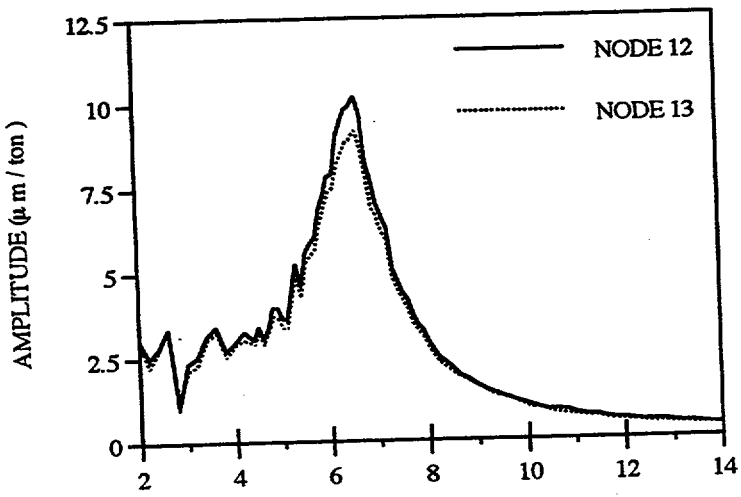

Fig. B.28
EW Measured Response At Roof
Due To EW Shaker Load At First Floor

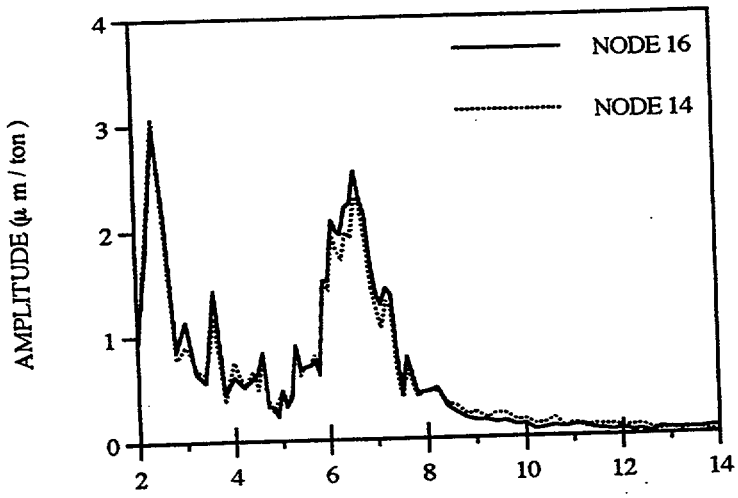

Fig. B.29
NS Measured Response At Roof
Due To EW Shaker Load At First Floor

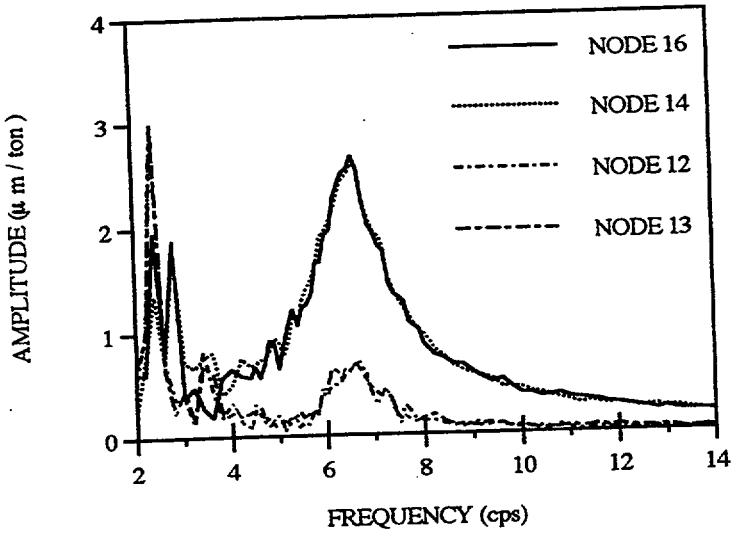

Fig. B.30
UD Measured Response At Roof
Due To EW Shaker Load At First Floor

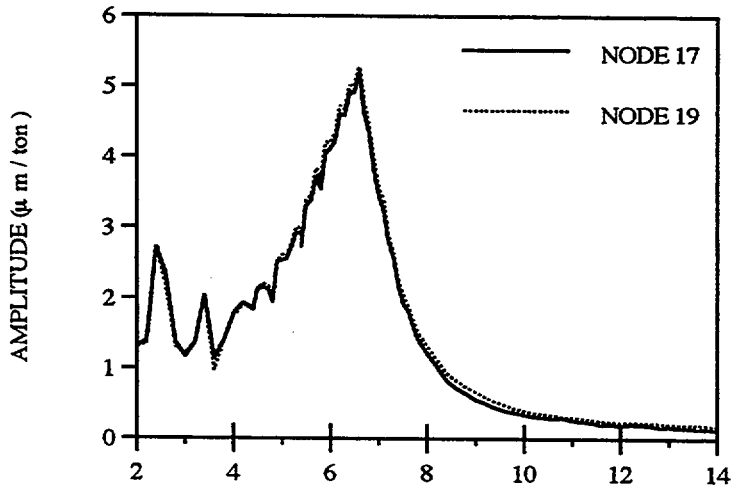

Fig. B.31
EW measured Response At Midheight
Due To EW Shaker Load At First Floor

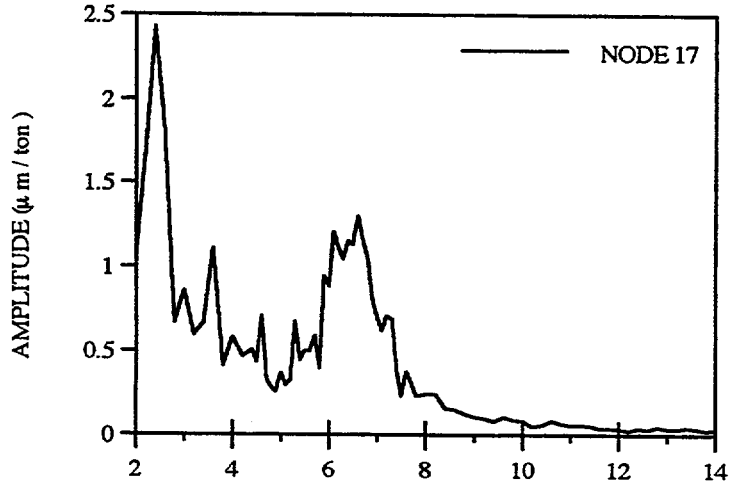

Fig. B.32
NS Measured Response At Midheight
Due To EW Shaker Load At First Floor

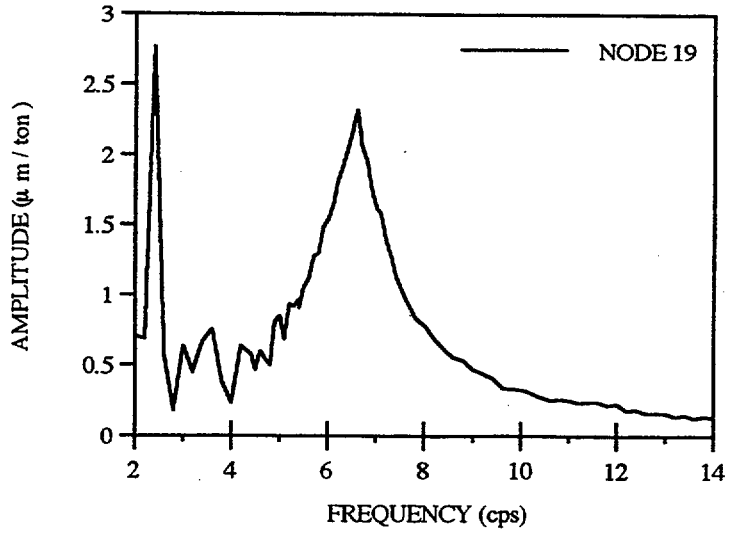

Fig. B.33
UD Measured Response At Midheight
Due To EW Shaker Load At First Floor

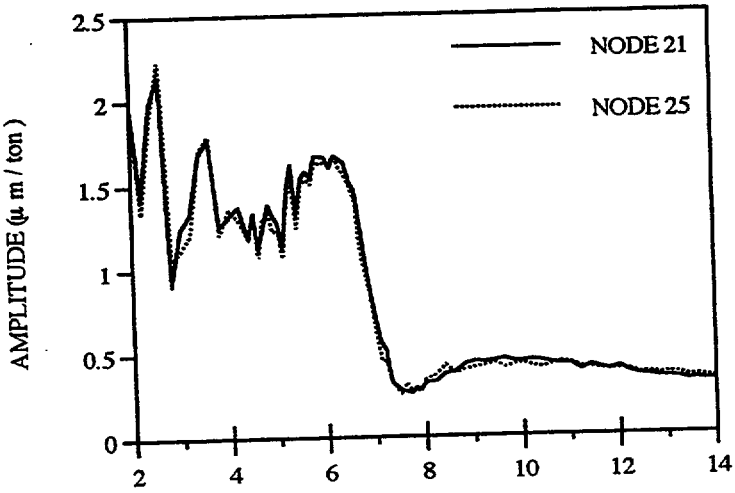

Fig. B.34
EW Measured Response At First Floor
Due To EW Shaker Load At First Floor

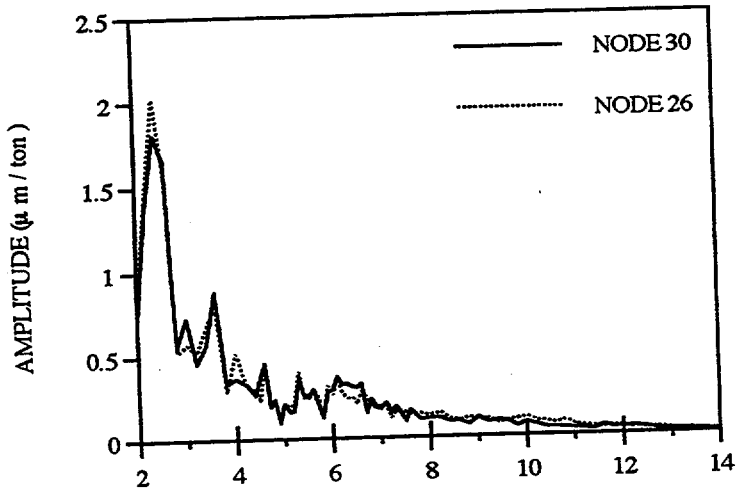

Fig. B.35
NS Measured Response At First Floor
Due To EW Shaker Load At First Floor

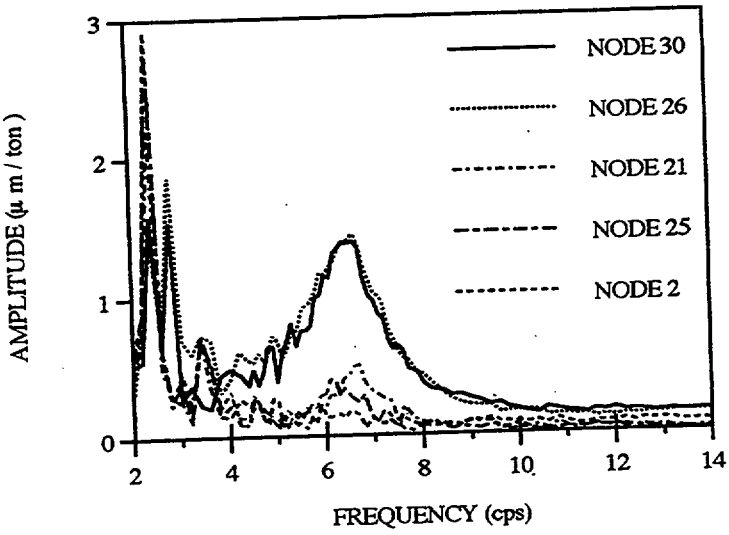

Fig. B.36
UD Measured Response At First Floor
Due To EW Shaker Load At First Floor

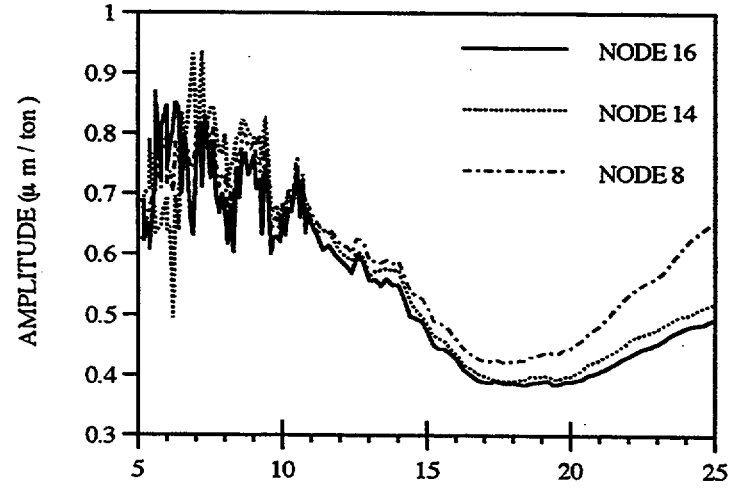

Fig. B.37
UD Measured Response At Roof
Due To UD Shaker Load At First Floor

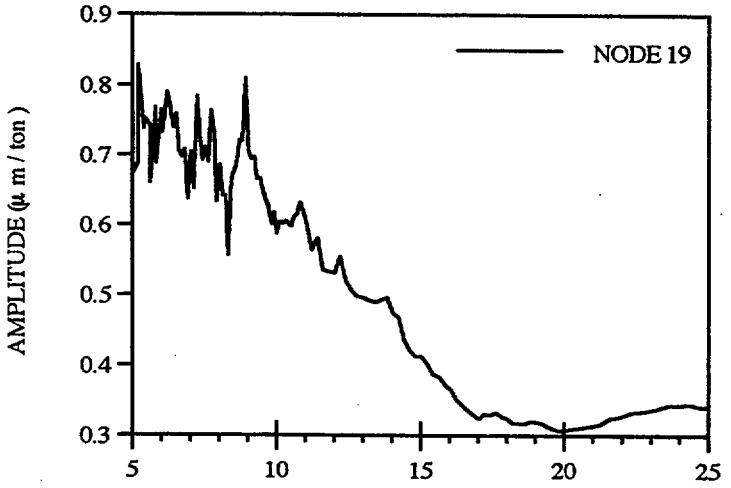

Fig. B.38
UD Measured Response At Midheight
Due To UD Shaker Load At First Floor

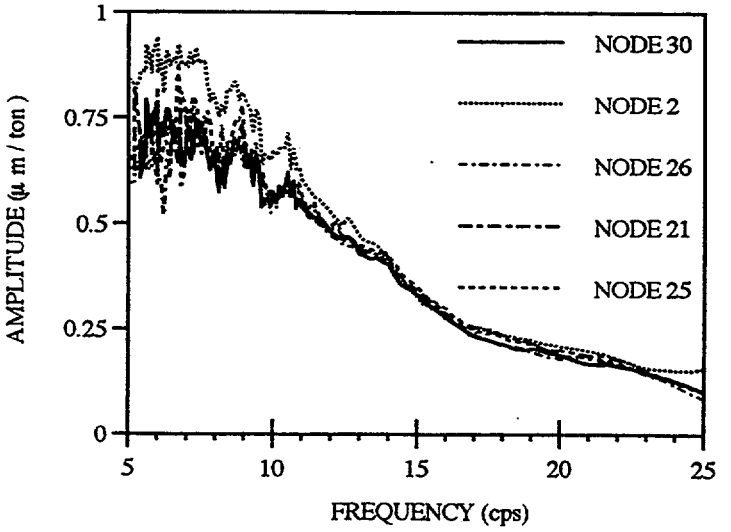

Fig. B.39
UD Measured Response At First Floor
Due To UD Shaker Load At First Floor

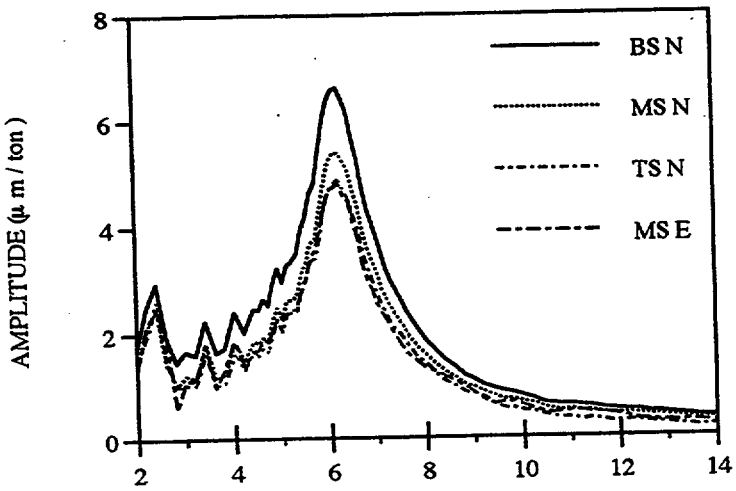

Fig. B.40
NS Measured Response In Soil
Due To NS Shaker Load At Roof

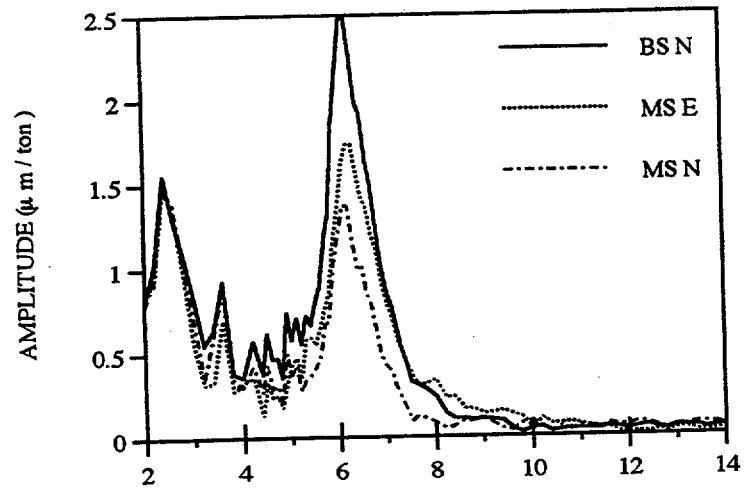

Fig. B.41
EW Measured Response In Soil
Due To NS Shaker Load At Roof

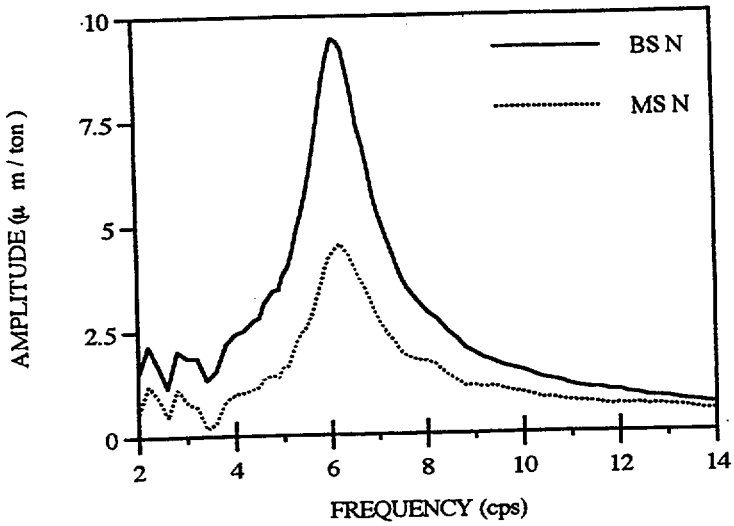

Fig. B.42
UD Measured Response In Soil
Due To NS Shaker Load At Roof

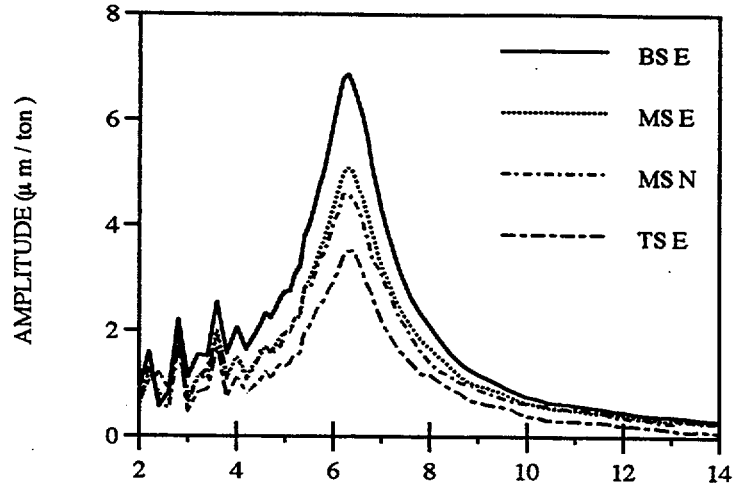

Fig. B.43
EW Measured Response In Soil
Due To EW Shaker Load At Roof

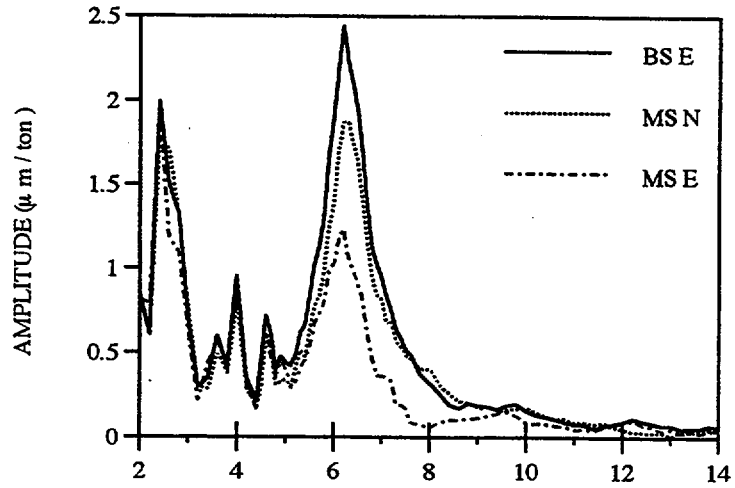

Fig. B.44
NS Measured Response In Soil
Due To EW Shaker Load At Roof

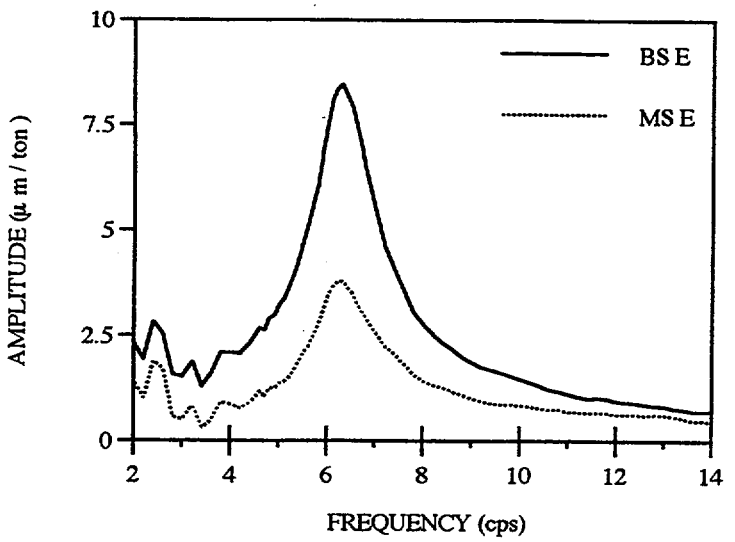

Fig. B.45
UD Measured Response In Soil
Due To EW Shaker Load At Roof

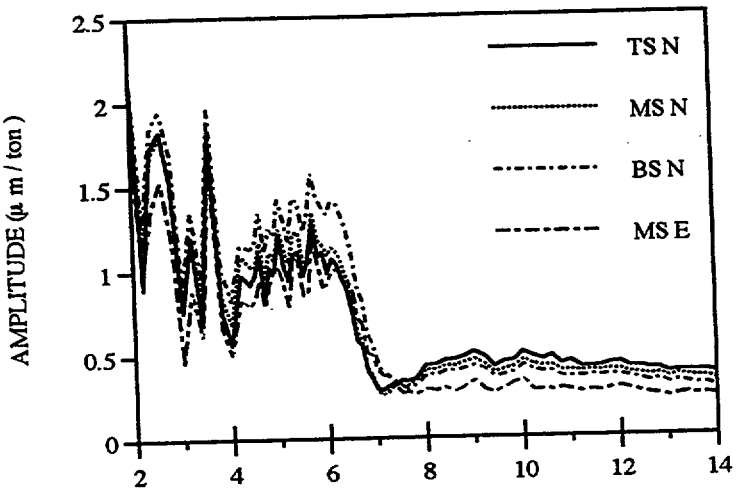

Fig. B.46
NS Measured Response In Soil
Due To NS Shaker Load At First Floor

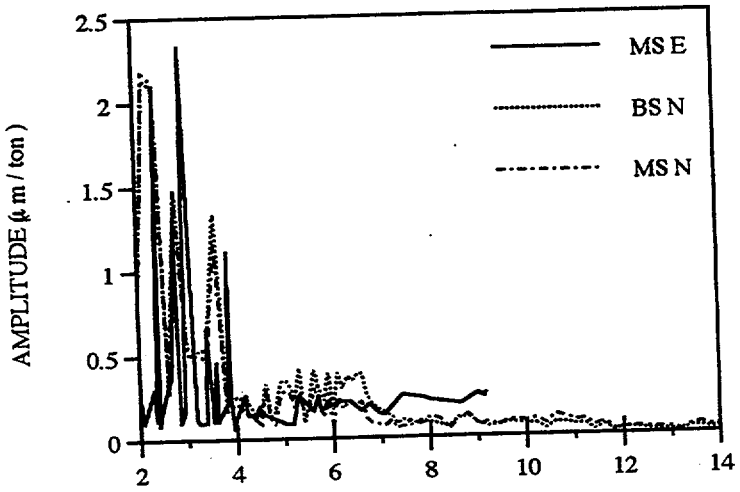

Fig. B.47
EW Measured Response In Soil
Due To NS Shaker Load At First Floor

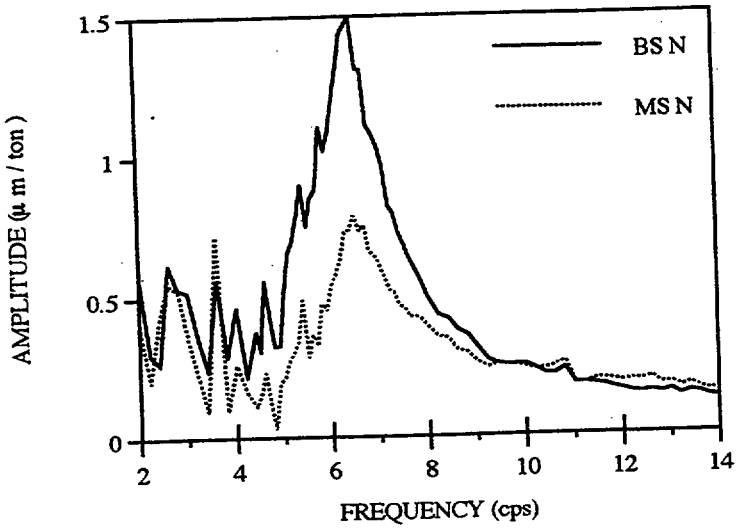

Fig. B.48
UD Measured Response In soil
Due To NS Shaker Load At First Floor

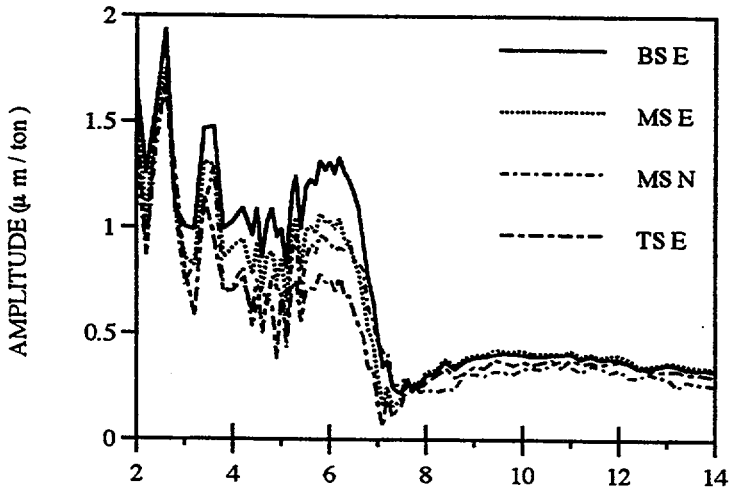

Fig. B.49
EW Measured Response In Soil
Due To EW Shaker Load At First Floor

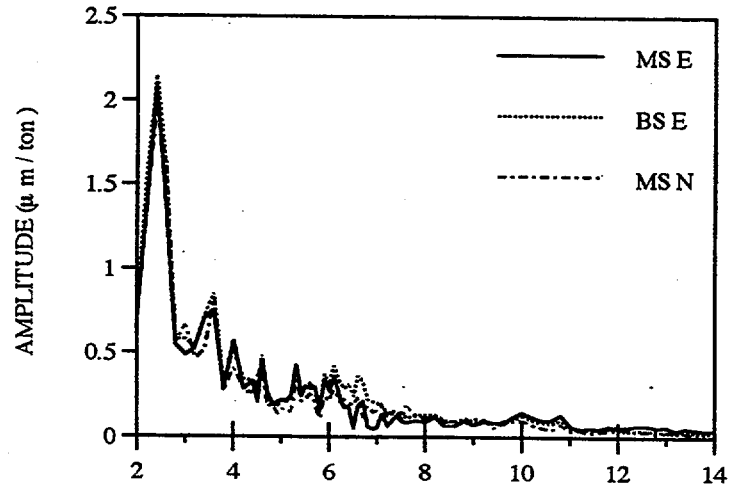

Fig. B.50
NS Measured Response In Soil
Due To EW Shaker Load At First Floor

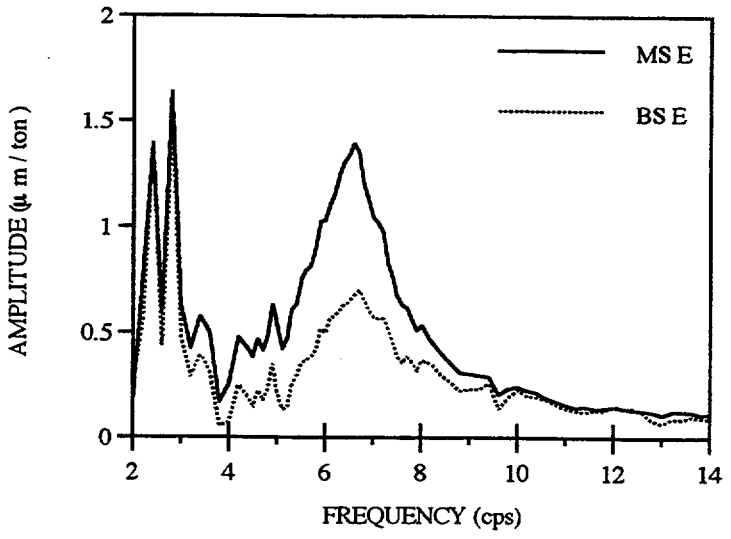

Fig. B.51
UD Measured Response In Soil
Due To EW Shaker Load At First Floor

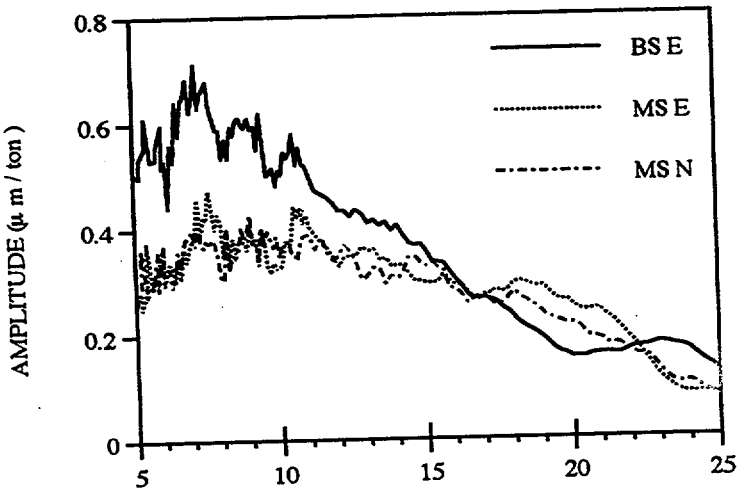

Fig. B.52
UD Measured Response In Soil
Due To UD Shaker Load At First Floor

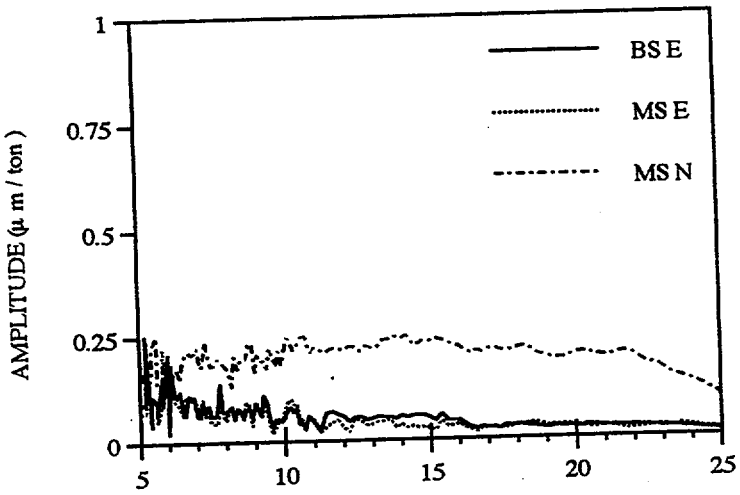

Fig. B.53
NS Measured Response In Soil
Due To UD Shaker Load At First Floor

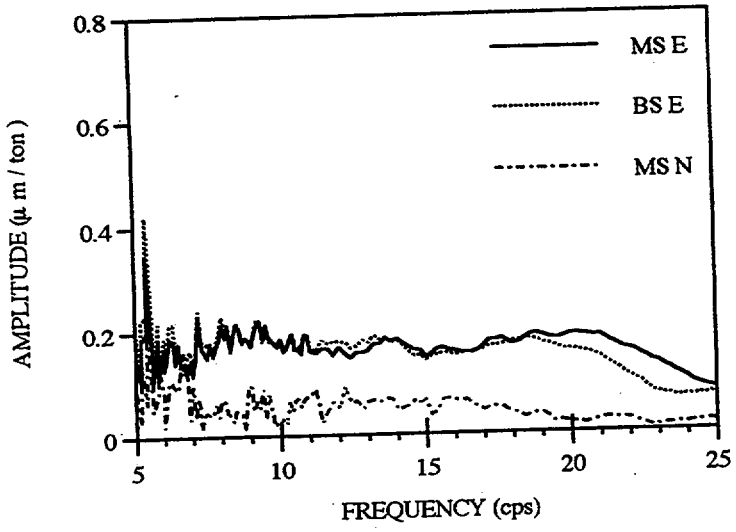

Fig. B.54
EW Measured Response In Soil
Due To UD Shaker Load At First Floor

NRC FORM 335 (2-89) NRCM 1102, 3201, 3202

U.S. NUCLEAR REGULATORY COMMISSION

BIBLIOGRAPHIC DATA SHEET

(See instructions on the reverse)

1. REPORT NUMBER (Assigned by NRC, Add Vol., Supp., Rev., and Addendum Numbers, if any.)

NUREG/CR-6584

2. TITLE AND SUBTITLE

Evaluation of the Hualien Quarter Scale Model Seismic Experiment
Volume 3

3. DATE REPORT PUBLISHED

MONTH	YEAR
March	2001

4. FIN OR GRANT NUMBER

W6769

5. AUTHOR(S)

C. A. Miller, C. J. Costantino

6. TYPE OF REPORT

Final

7. PERIOD COVERED *(Inclusive Dates)*

3/92 to 10/99

8. PERFORMING ORGANIZATION - NAME AND ADDRESS *(If NRC, provide Division, Office or Region, U.S. Nuclear Regulatory Commission, and mailing address; if contractor, provide name and mailing address.)*

The City College of New York
Department of Civil Engineering
New York, NY 10031

9. SPONSORING ORGANIZATION - NAME AND ADDRESS *(If NRC, type "Same as above"; if contractor, provide NRC Division, Office or Region, U.S. Nuclear Regulatory Commission, and mailing address.)*

Division of Engineering Technology
Office of Nuclear Regulatory Research
U. S. Nuclear Regulatory Commission
Washington, DC 20555-0001

10. SUPPLEMENTARY NOTES

Herman L. Graves, Project Manager

11. ABSTRACT *(200 words or less)*

A quarter scale model of a containment structure was constructed in Hualien, a seismically active region in Taiwan. Forced vibration tests were performed both before and after placement of the backfill. The structure and surrounding free field were then instrumented with accelerometers, pressure gages, and displacement gages. Recordings were taken when significant seismic events occurred at the site. This report describes analytical studies that were performed to correlate the measured response with predictions. Soil - structure interaction effects were represented with a lumped parameter model.

The work is summarized in Volume 1 of the 4 volume report. The site characteristics are described in Volume 2. This includes a discussion of the field program used to determine the characteristics. The predictions for the forced vibration tests are compared with the measured data in Volume 3. The correlation is found to be quite good except that the measured data indicated that the site is anisotropic. This is not found from the site exploration phase of the work. Comparisons between the predictions and measured data for the earthquake responses are made in Volume 4. The soil responses compare reasonably well but the in structure responses do not compare very well. This is attributed to the anisotropic site characteristics.

12. KEY WORDS/DESCRIPTORS *(List words or phrases that will assist researchers in locating the report.)*

Hualien, soil-structure interaction, shear wave velocity, forced vibration

13. AVAILABILITY STATEMENT

unlimited

14. SECURITY CLASSIFICATION

(This Page) unclassified

(This Report) unclassified

15. NUMBER OF PAGES

16. PRICE

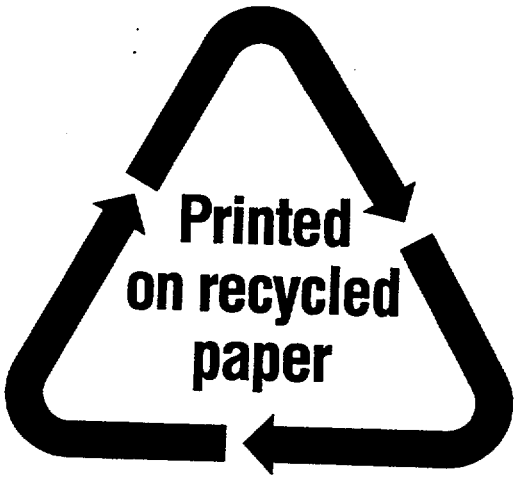

Federal Recycling Program